Supporting Information

Cofacial Organic Click Cage to Intercalate Polycyclic Aromatic Hydrocarbons

Jayanta Samanta,[†,‡] Ramalingam Natarajan[*,†,‡]

[†]Organic and Medicinal Chemistry Division, CSIR-Indian Institute of Chemical Biology, 4, Raja S. C. Mullick Road, Kolkata 700032, India.

[‡]Academy of Scientific and Innovative Research (AcSIR), 4, Raja S. C. Mullick Road, Kolkata 700032, India

Table of Contents

1. Materials and general methods:

General: All the chemicals were purchased from commercial suppliers and used as received. All the solvents were distilled prior to use. Dry solvents were obtained according to literature procedure. Both the starting materials were synthesized according to literature procedure.[1] Column chromatography was performed with silica gel (230-400). UV-VIS spectra were recorded on a Cary 60 UV-Vis spectrophotometer from Agilent technologies. Fluorescence spectra were recorded on a Quanta Master 40 spectrophotometer from Photon Technology International at a slit width of 2.0 nm. NMR spectra were recorded on a Bruker Advance 300 with operating frequency of 300 MHz (^{1}H NMR) and 75 MHz (^{13}C NMR) and Bruker Advance 600 with operating frequency of 600MHz (^{1}H NMR) and 150 MHz (^{13}C NMR). Chemical shifts are reported in ppm values relative to residual solvent peak ($CDCl_3$: δ_H = 7.27 ppm, δ_C =77.00, DMSO-D6: δ_H = 2.5, acetone-D6: δ_C= 206.68, 29.92). High resolution ESI mass spectra (HRMS) was recorded in a Q-TOF micro mass from Waters. X-ray data were collected on a Bruker APEX2 CCD diffractometer at 100K (±0.2K).

2. Synthesis:

Scheme 1. Synthesis of compound **1**

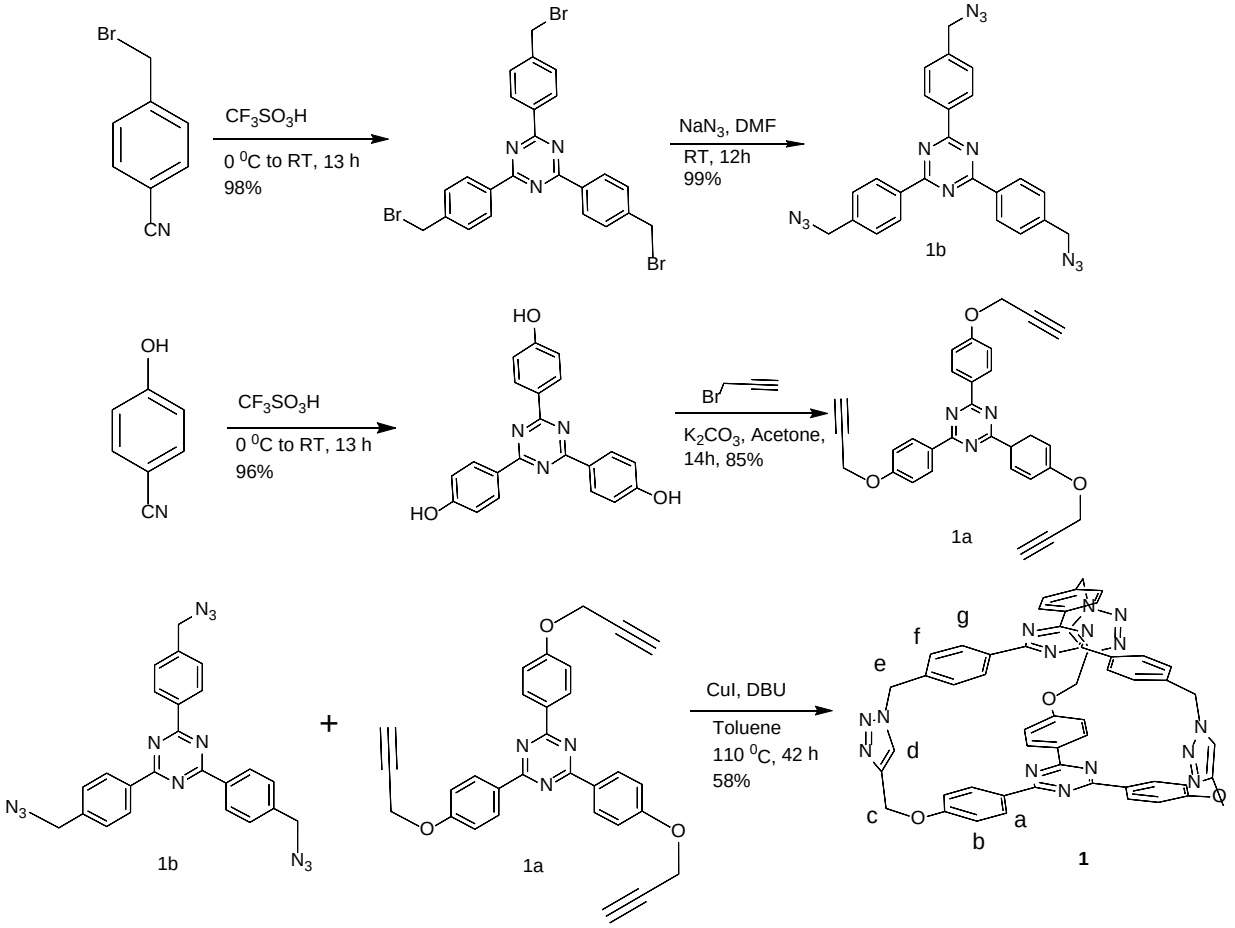

2,4,6-Triazinetriphenol: Trifluoromethanesulfonic acid (1.07 mL, 12.18 mmol) was slowly added to a stirred solution of 4-cyanophenol (0.5 g, 4.2 mmol) in DCM at 0 ^{0}C under a N_2 atmosphere. Then it was allowed to come to room temperature. After stirring for next 12 h, solvent was evaporated and ice-cold water was poured into it to obtain white precipitate. Then it was neutralized by adding ammonia solution. The precipitate was filtered, washed with water and dried to obtain the product as white powder (0.48 g, 96%). ^{1}H NMR (DMSO-d_6, 300 MHz): δ= 8.55 (d, *J* = 8.8 Hz, 2H), 6.97 (d, *J* = 8.8 Hz, 2H) ppm.

Compound 1a: To a stirred solution of triazinetriphenol obtained above (0.15 g, 0.42 mmol) and K_2CO_3 (0.869 g, 6.3 mmol) in acetone (10 mL), propargyl bromide (0.15 mL, 1.68 mmol) were added under a N_2 atmosphere, and the reaction mixture was allowed to reflux for 14 h. Then it

was cooled down to room temperature, the solvent was removed under vacuum and the residue was extracted with ethyl acetate, washed with water and dried with sodium sulfate. Finally the compound was purified by column chromatography (eluent EtOAc : hexane 1:4) to obtain the pure product (**1a**) as white fluffy solid (0.17 g, 85%). ^{1}H NMR ($CDCl_3$, 300 MHz): δ= 8.72 (d, *J* = 9.0 Hz, 2H), 7.13 (d, *J* = 9.0 Hz, 2H), 4.81 (d, *J* = 2.6 Hz, 2H), 2.60 - 2.54 (t, *J* = 2.3 1H) ppm. ^{13}C NMR (75 MHz, Acetone-d_6): δ= 171.6, 162.4, 131.5, 130.3, 115.8, 79.4, 77.6, 56.6 ppm. ESI MS: m/z = 472.11 $[m+H]^+$.

2,4,6-Triazinetribenzyl bromide: Trifluoromethanesulfonic acid (1.35 mL, 15.3 mmol) was slowly added to 4-cyanobenzyl bromide (1 g, 5.1 mmol) at 0 ^{0}C under a N_2 atmosphere. Then it was allowed to come to room temperature. After stirring for next 12 h, the mixture was poured into ice-cooled water to result in a white precipitate. The aqueous solution was then neutralized by adding ammonia solution. The precipitate was filtered, washed with acetone and dried to get the product as white powder (0.985 g, 98.5%). ^{1}H NMR ($CDCl_3$, 300 MHz): δ = 8.70 (d, *J* = 8.4 Hz, 2H), 7.58 (d, *J* = 8.4 Hz, 2H), 4.58 (s, 2H) ppm.

Compound 1b: To a suspension of triazinetribenzyl bromide (2.5 g, 4.25 mmol) in DMF (20 mL), sodium azide (1.105 g, 17 mmol) was added and stirred for 12 h at room temperature. Then DMF was removed under rotary evaporation and the residue was extracted with ethyl acetate followed by washing with water and brine. The organic portion is then dried with sodium sulfate and removed to obtained the product (**1b**) as crystalline solid (2.01 g, 99%). ^{1}H NMR ($CDCl_3$, 300 MHz): δ = 8.74(d, *J* = 8.4 Hz 2H), 7.52 (d, *J* = 8.4 Hz, 2H), 4.01 (s, 2H) ppm. ^{13}C NMR (75 MHz, $CDCl_3$): δ = 171.1, 139.9, 135.9, 129.4, 128.3, 54.4 ppm. ESI MS: m/z = 475.20 $[m+H]^+$.

Compound 1: CuI (0.02 g, 0.105 mmol) and DBU (1 mL) was added to degassed toluene (300 mL) and heated to 75 ^{0}C under N_2 atmosphere for 15 min. A mixture of azide **1a** (0.1 g, 0.21 mmol) and alkyne **1a** (0.1 g, 0.21 mmol) dissolved in degassed toluene (15 mL) and THF (5 mL) in a round bottom flask and transferred into a glass syringe (25 mL) and the mixture was then added slowly over 18 h at a flow rate of 0.02 mL/min using a syringe pump. The reaction mixture was stirred for further 24 h at 110 ^{0}C. The solvent was removed under reduced pressure, and the residue was taken in $CHCl_3$, washed with water and brine. Removal of solvent resulted the product which was purified by column chromatography (eluent- 2% MeOH in $CHCl_3$) to

obtain the pure product (**1**) as white solid (0.116 g, 58%). ^{1}H NMR ($CDCl_3$, 300 MHz) : δ = 8.57 (d, *J* = 8.4 Hz, 2H, C*H*$_g$), 8.29 (d, *J* = 8.8 Hz, 2H, C*H*$_a$), 7.41 (d, *J* = 8.4 Hz, 2H, C*H*$_f$), 7.11 (s, 1H C*H*$_d$), 6.86 (d, *J* = 8.8 Hz, 2H, C*H*$_b$), 5.53 (s, 2H, C*H*$_e$), 5.47 (s, 2H, C*H*$_c$) ppm. ^{13}C NMR (75 MHz, $CDCl_3$) δ = 170.8, 170.5, 160.3, 144.9, 138.4, 136.3, 130.5, 129.8, 129.0, 128.7, 121.4, 114.6, 61.3, 54.2 ppm, HRMS (ESI, positive mode, $CHCl_3$/MeOH 1:5) m/z: Calculated for $C_{54}H_{39}N_{15}O_3$: 968.3258 $[M+Na]^+$, found: 968.3237.

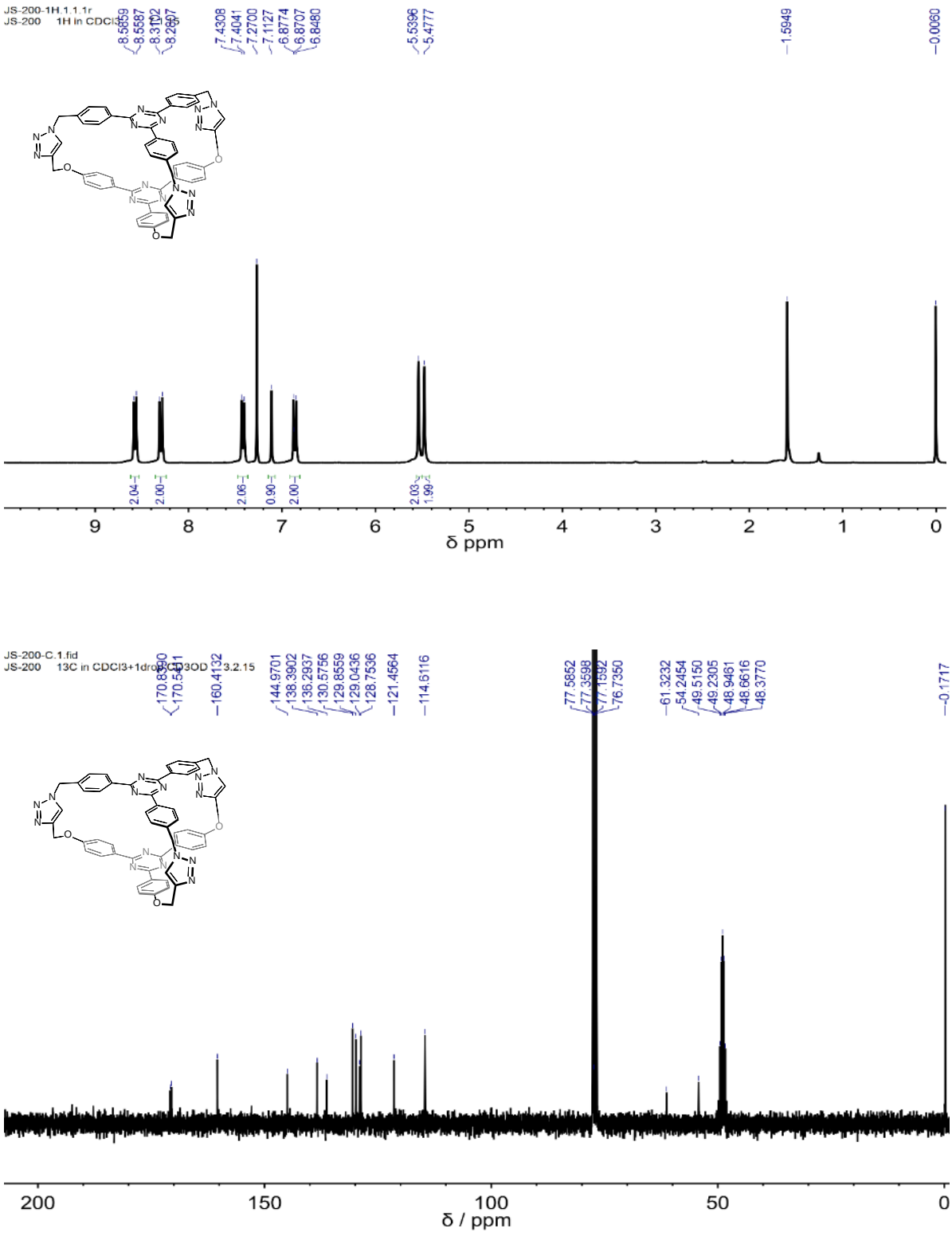

Figure S1. ^{1}H NMR (300 MHz, $CDCl_3$) and ^{13}C NMR (75 MHz, $CDCl_3$ + 5% MeOD) of **1.**

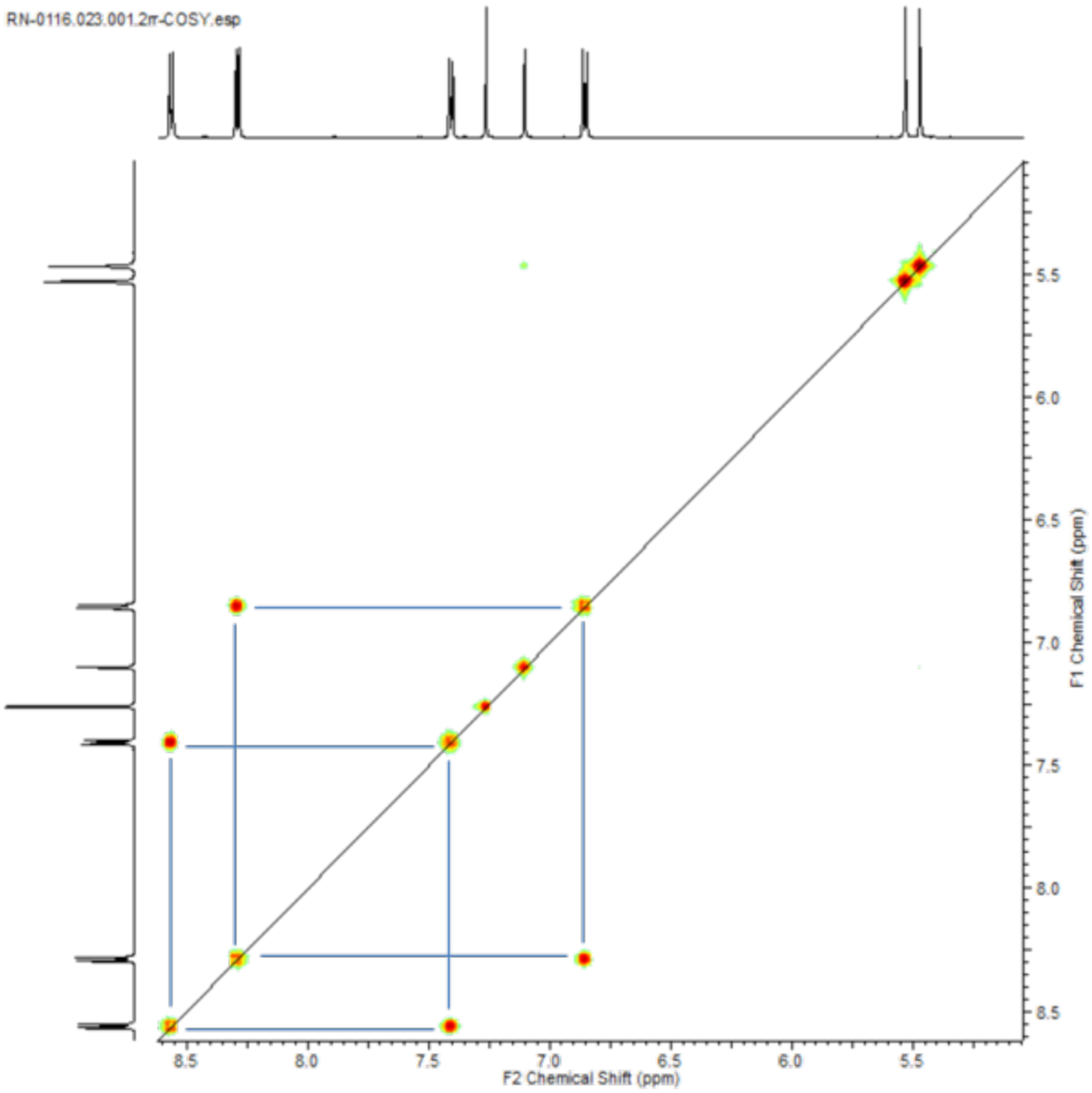

Figure S2. COSY NMR spectra of **1.**

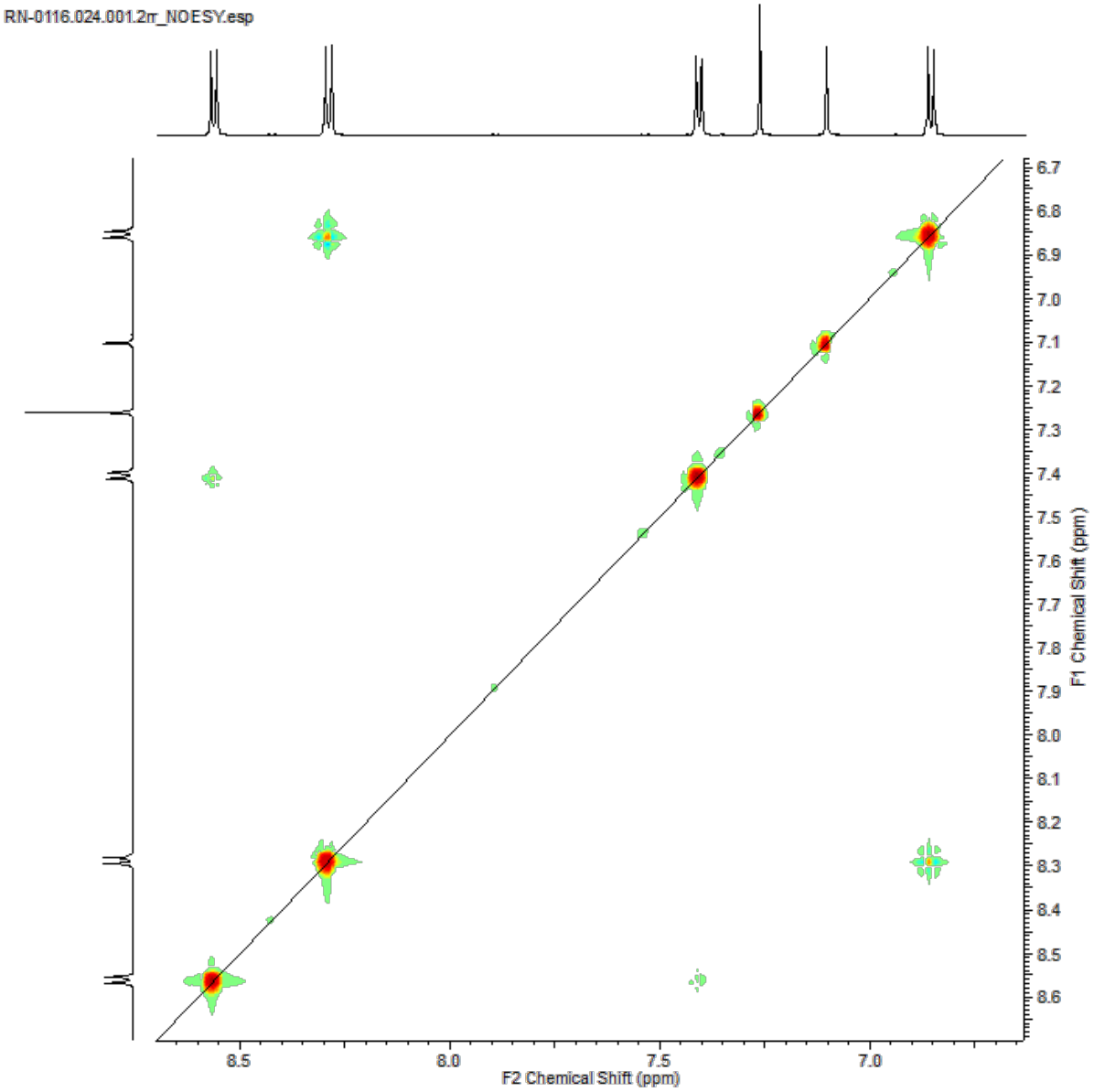

Figure S3. NOESY NMR spectra of **1** not showing any through-space cross peaks for the aromatic protons of top and bottom platforms.

3. NMR Spectroscopy of host-guest complexes:

For 1:1 NMR binding study in $CDCl_3$, stock solution of **1** and stock solution of guests were prepared in $CDCl_3$ and mixed in such a way so that **1**:guest ratio becomes 1:1. Then the mixture was allowed to stand for 1h and data were collected. For binding study in THF-d_8/$CDCl_3$ mixture, first all the stock solutions were prepared in $CDCl_3$, and mixed in such a way so that **1**:guest ratio becomes 1:1, then THF-d_8 was added to make 2:1 ratio of THF-d_8/$CDCl_3$ mixture. Then the mixture was allowed to equilibrate for 3 h and data were collected. The molecular structure of the guest molecules are listed below:

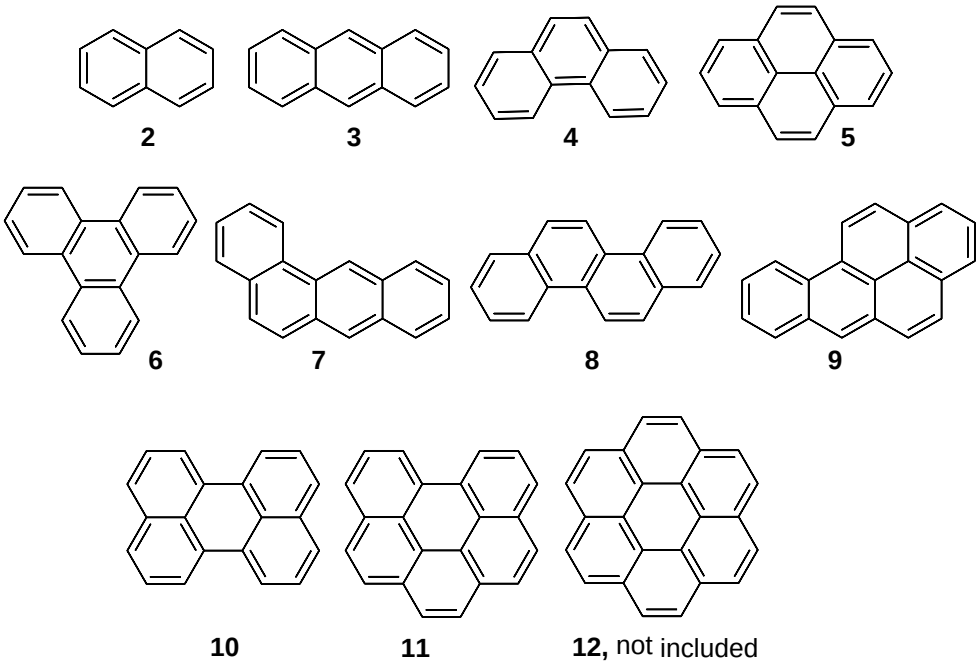

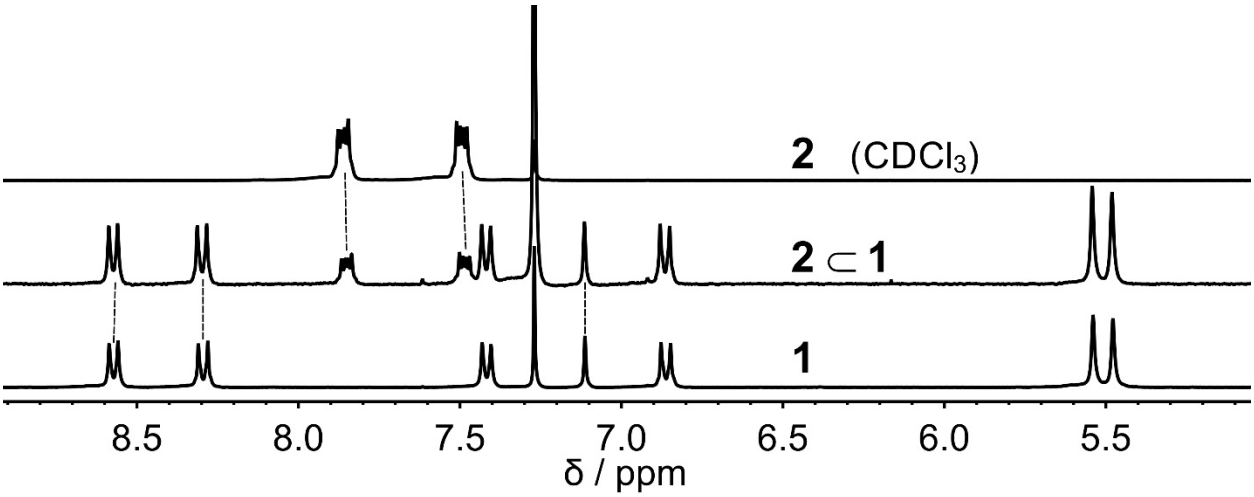

Figure S4. ^{1}H NMR of naphthalene ⊂ **1** in $CDCl_3$ showing no shift in naphthalene (**2**) protons (at 7.84, 7.47 ppm) and host (**1**) protons (at 8.55, 8.28, 7.11 ppm).

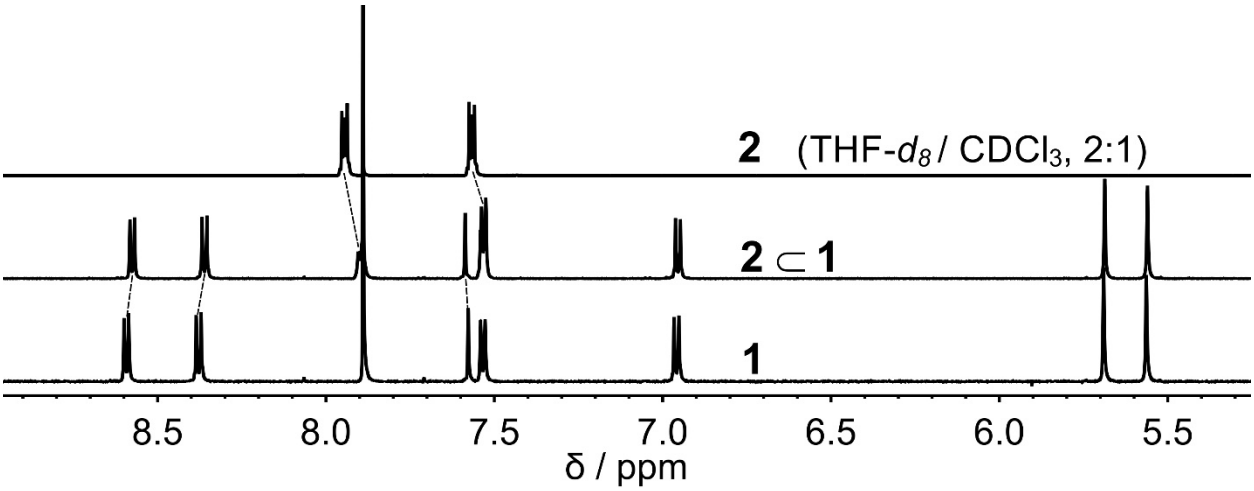

Figure S5. ^{1}H NMR of naphthalene ⊂ **1** in THF-d_8/$CDCl_3$ (2:1) showing mild upfield shift in naphthalene (**2**) protons (at 7.95, 7.57 ppm, Δδ= 0.05, 0.03 ppm) as well as in host (**1**) protons (at 8.58, 8.37 ppm, Δδ= 0.02, 0.02), and downfield shift in host proton (at 7.57 ppm, Δδ= 0.01ppm).

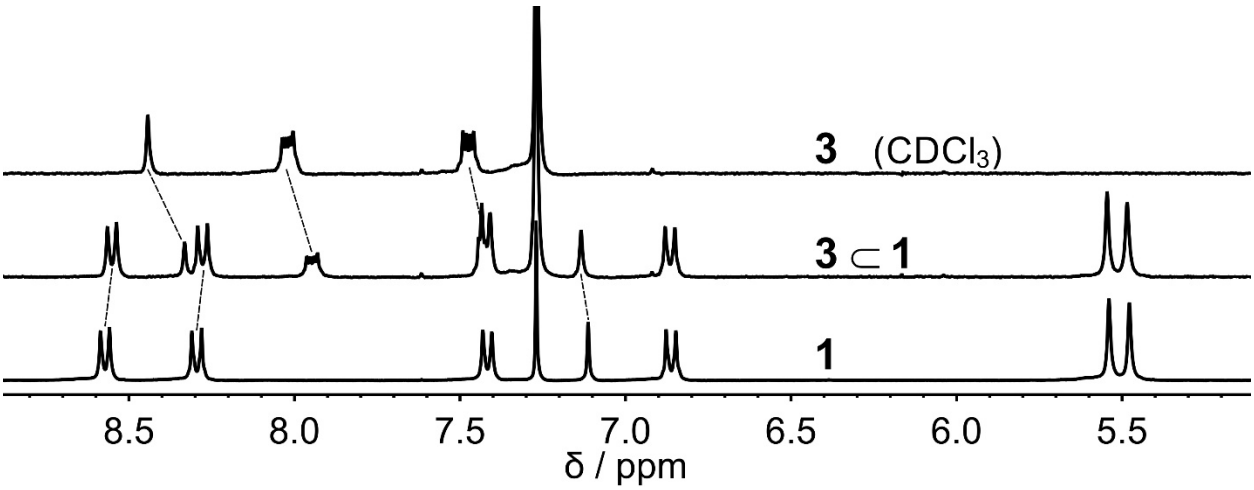

Figure S6. ^{1}H NMR of anthracene ⊂ **1** in $CDCl_3$ showing upfield shift in anthracene (**3**) protons (at 8.44, 8.0, 7.45 ppm, Δδ= 0.11, 0.07, 0.05 ppm) as well as in host (**1**) protons (at 8.55, 8.28, ppm, Δδ= 0.02, 0.02 ppm) and downfield shift in host proton (at 7.11 ppm, Δδ= 0.02 ppm).

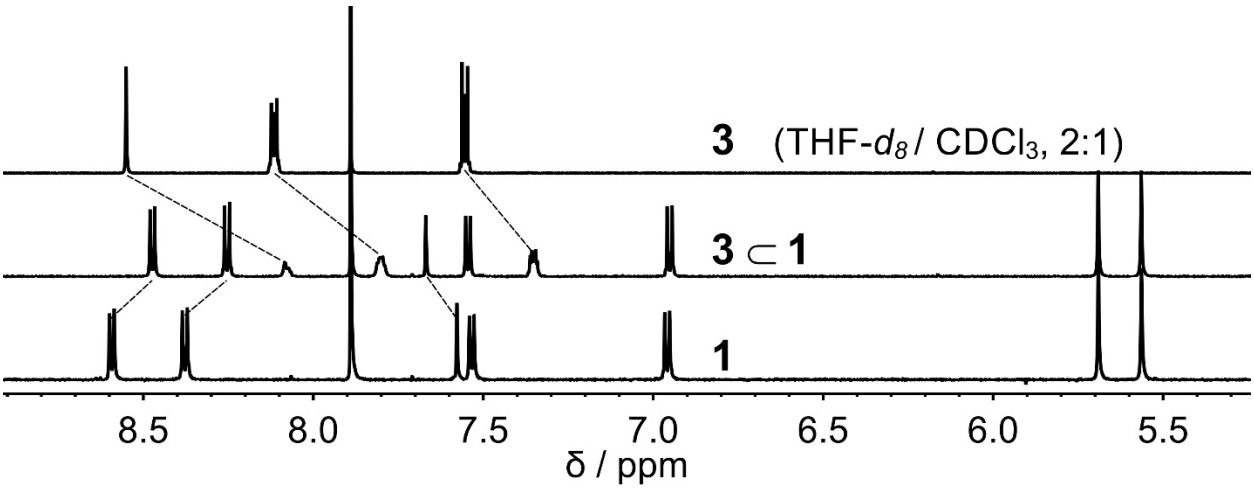

Figure S7. ^{1}H NMR of anthracene ⊂ **1** in THF-d_8/$CDCl_3$ (2:1) showing upfield shift in anthracene (**3**) protons (at 8.55, 8.1, 7.54 ppm, Δδ= 0.47, 0.31, 0.2 ppm) as well as in host (**1**) protons (at 8.58, 8.37 ppm, Δδ= 0.12, 0.13 ppm) and downfield shift in host proton (at 7.57 ppm, Δδ= 0.09 ppm).

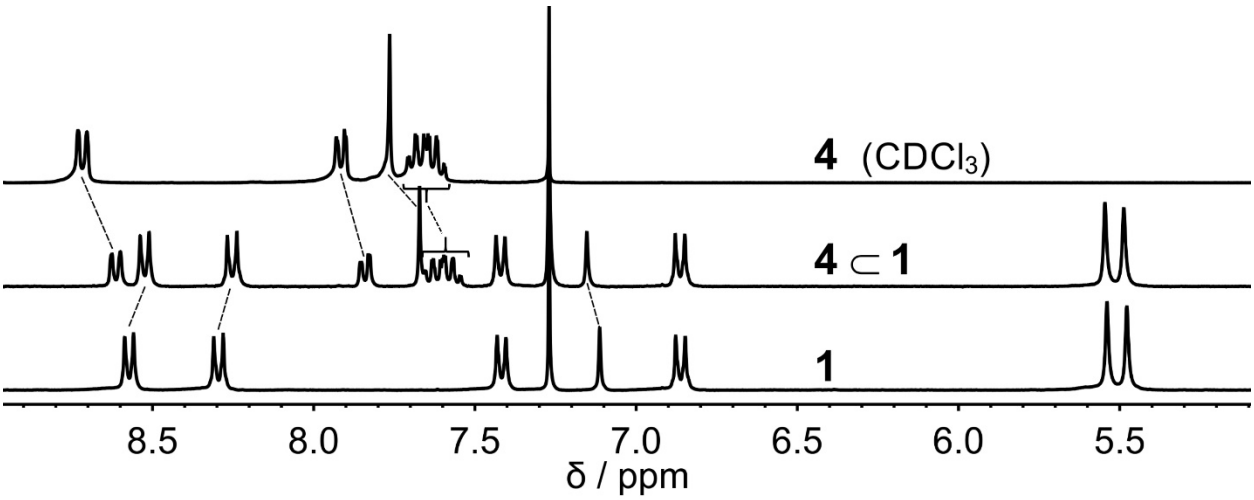

Figure S8. ^{1}H NMR of phenanthrene ⊂ **1** in $CDCl_3$ showing upfield shift in phenanthrene (**4**) proton (at 8.7, 7.9, 7.76 ppm, Δδ= 0.1, 0.08, 0.09 ppm) as well as in host (**1**) protons (at 8.55, 8.28 ppm Δδ= 0.04, 0.05 ppm) and downfield shift in host proton (at 7.11 ppm, Δδ= 0.04 ppm).

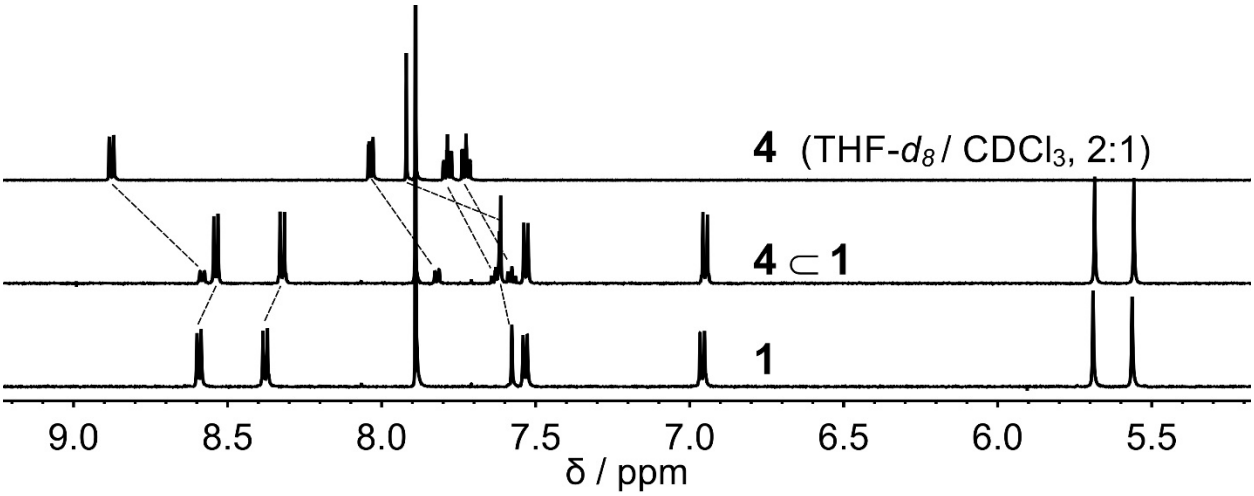

Figure S9. ^{1}H NMR of phenanthrene ⊂ **1** in THF-d_8/$CDCl_3$ (2:1) showing upfield shift in phenanthrene (**4**) protons (at 8.87, 8.03, 7.92 ppm, Δδ= 0.3, 0.22, 0.31 ppm) resonances as well as inn host (**1**) protons (at 8.58, 8.37 ppm, Δδ= 0.05, 0.06 ppm) and downfield shift in host proton (at 7.57 ppm, Δδ= 0.04 ppm).

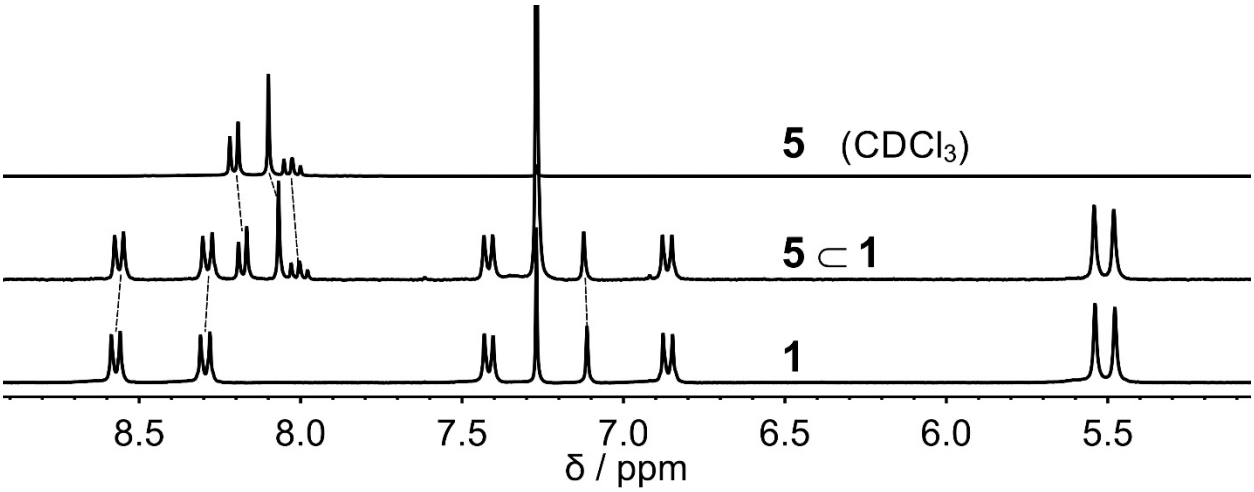

Figure S10. ^{1}H NMR of pyrene ⊂ **1** in $CDCl_3$ showing negligible shift in pyrene (**5**) protons (at 8.19, 8.09 ppm, Δδ= 0.03, 0.03 ppm) as well as in host (**1**) protons (at 8.55, 8.28 ppm Δδ= 0.01, 0.01 ppm) and downfield shift in host proton (at 7.11 ppm, Δδ= 0.01 ppm).

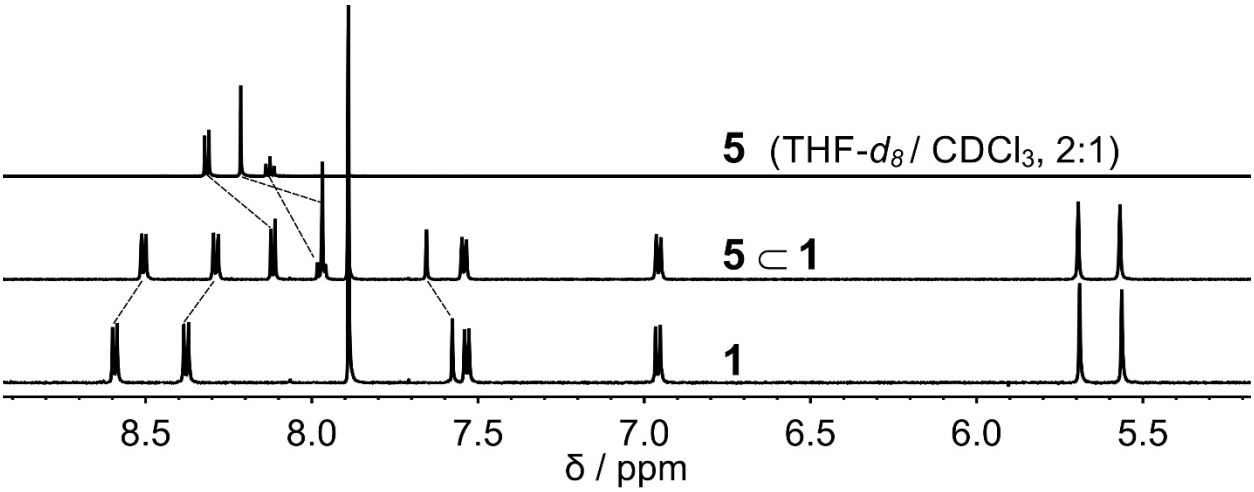

Figure S11. ^{1}H NMR of pyrene ⊂ **1** in THF-d_8/$CDCl_3$ (2:1) showing upfield shift in pyrene (**5**) protons (at 8.3, 8.2 ppm, Δδ= 0.19, 0.24 ppm) as well as in host (**1**) protons (at 8.58, 8.37 ppm, Δδ= 0.08, 0.09 ppm) and downfield shift in host proton (at 7.57 ppm, Δδ= 0.08 ppm).

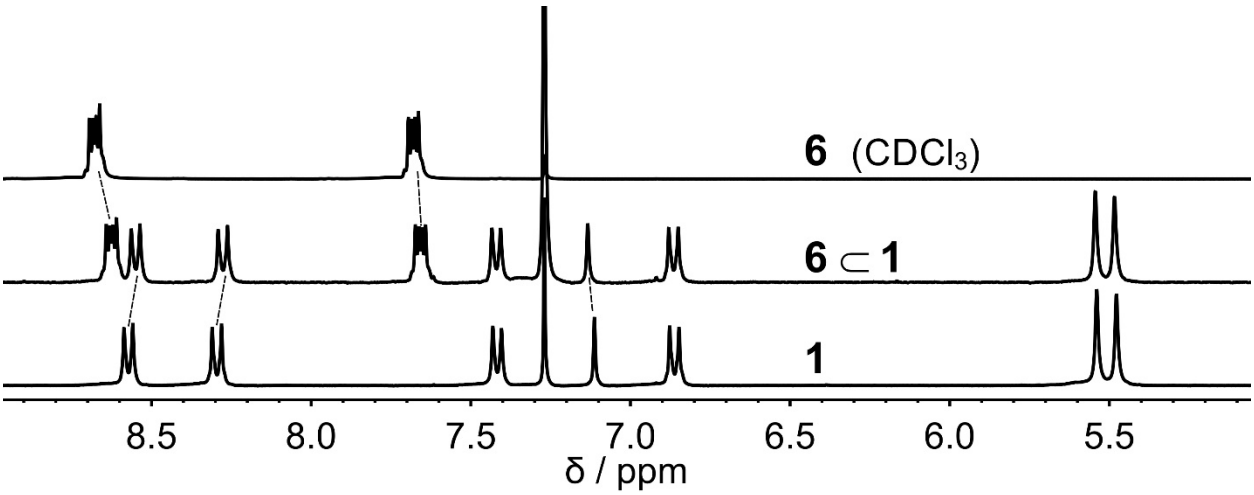

Figure S12. ^{1}H NMR of triphenylene ⊂ **1** in $CDCl_3$ showing negligible shift in triphenylene (**6**) protons (at 8.66, 7.66 ppm, Δδ= 0.06, 0.02 ppm) as well as in host protons (at 8.55, 8.28 ppm Δδ= 0.02, 0.02 ppm) and downfield shift in host proton (at 7.11 ppm, Δδ= 0.02 ppm).

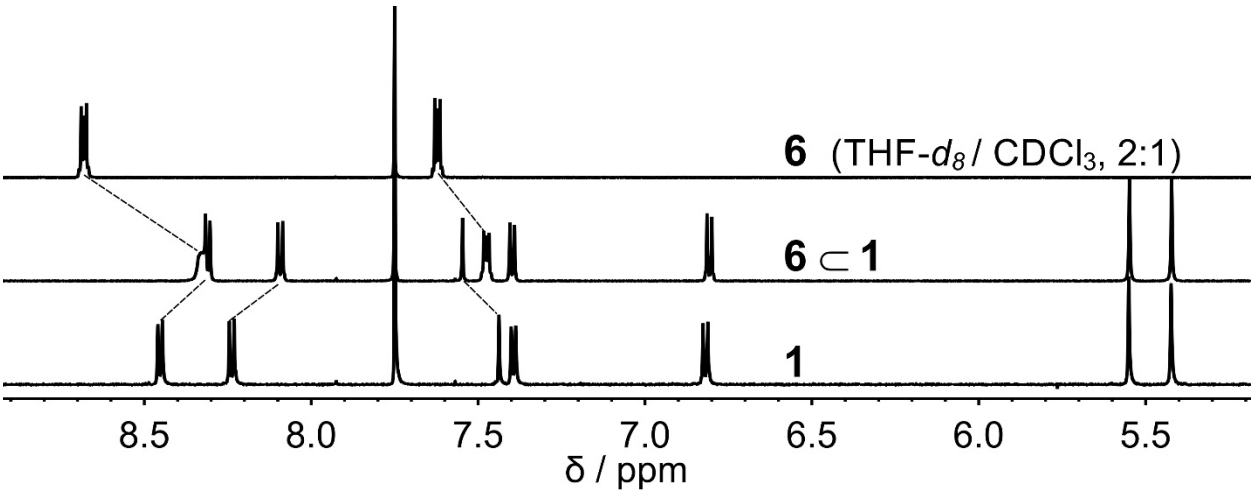

Figure S13. ^{1}H NMR of triphenylene ⊂ **1** in THF-d_8/$CDCl_3$ (2:1) showing upfield shift in triphenylene (**6**) protons (at 8.82, 7.76 ppm, Δδ= 0.35, 0.14 ppm) as well as in host (**1**) protons (at 8.58, 8.37 ppm, Δδ= 0.14, 0.15 ppm) and downfield shift in host proton (at 7.57 ppm, Δδ= 0.11 ppm).

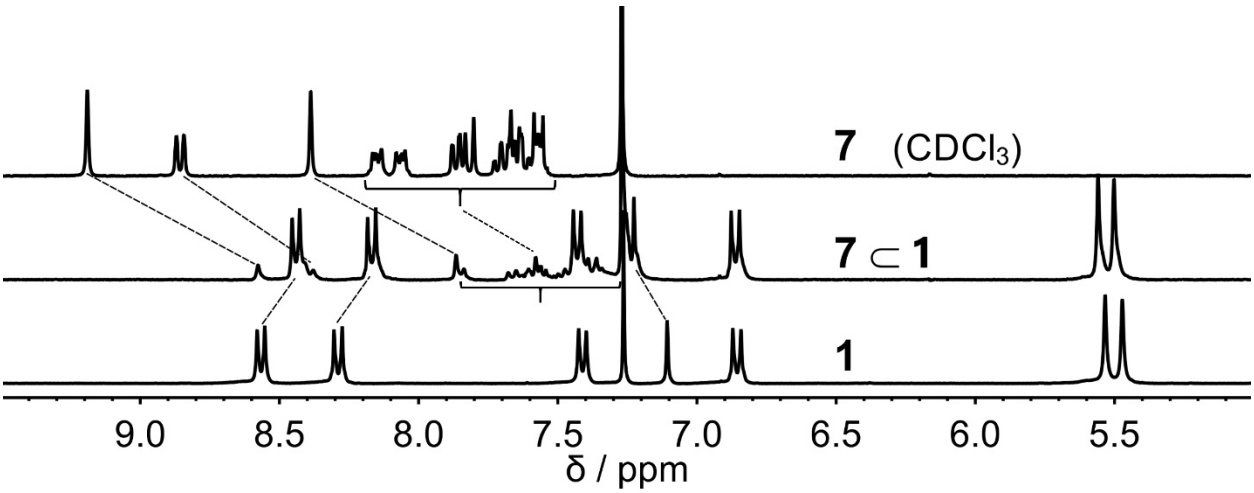

Figure S14. ^{1}H NMR of benz(*a*)anthracene ⊂ **1** in $CDCl_3$ showing upfield shift in benz(*a*)anthracene (**7**) protons (at 9.19, 8.84 ppm, Δδ= 0.62, 0.47 ppm) as well as in host (**1**) protons (at 8.55, 8.28 ppm Δδ= 0.13, 0.13 ppm) and downfield shift in host proton (at 7.11 ppm, Δδ= 0.11 ppm).

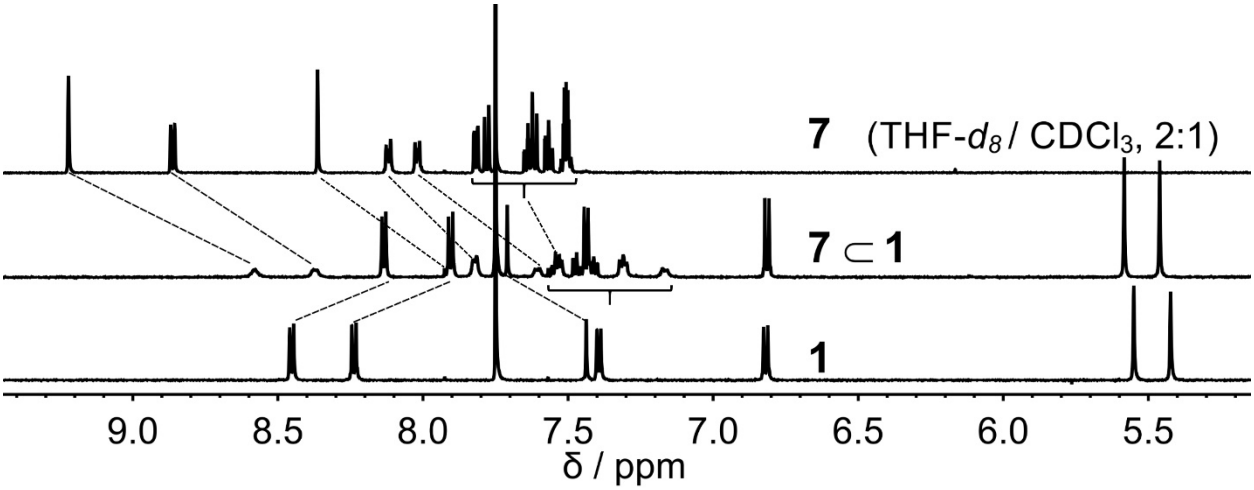

Figure S15. ^{1}H NMR of benz(*a*)anthracene ⊂ **1** in THF-d_8/$CDCl_3$ (2:1) showing upfield shift in benz(*a*)anthracene (**7**) protons (at 9.36, 8.99 ppm, Δδ= 0.64, 0.48 ppm) as well as in host (**1**) protons (at 8.58, 8.37 ppm, Δδ= 0.32, 0.33 ppm) and downfield shift in host proton (at 7.57 ppm, Δδ= 0.27 ppm).

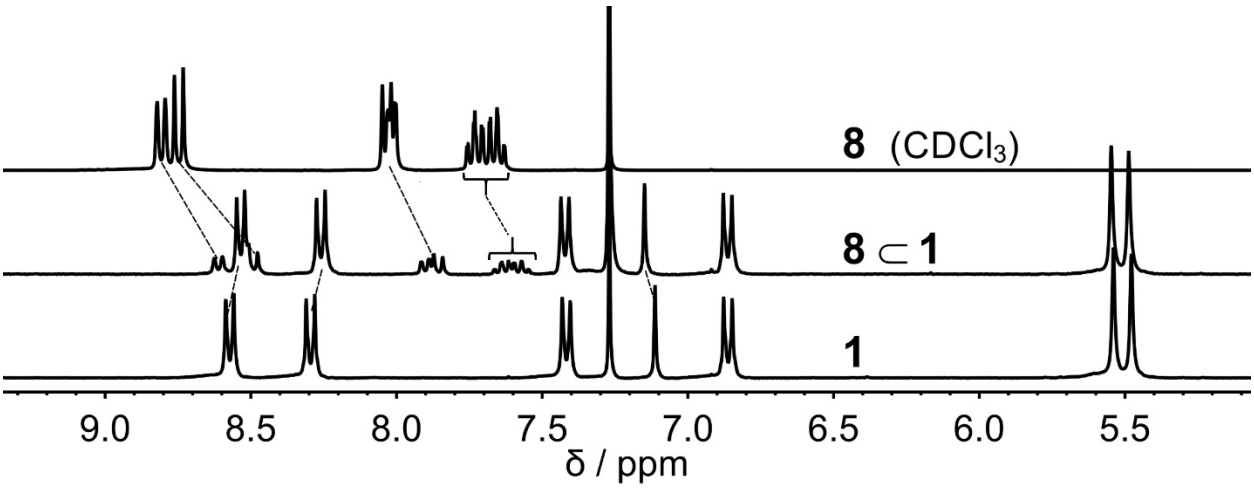

Figure S16. ^{1}H NMR of benzo(*a*)phenanthrene ⊂ **1** in $CDCl_3$ showing upfield shift in benzo(*a*)phenanthrene (**8**) protons (at 8.79, 8.73 ppm, Δδ= 0.2, 0.26 ppm) as well as in host (**1**) protons (at 8.55, 8.28 ppm Δδ= 0.03, 0.04 ppm) and downfield shift in host proton (at 7.11 ppm, Δδ= 0.03 ppm).

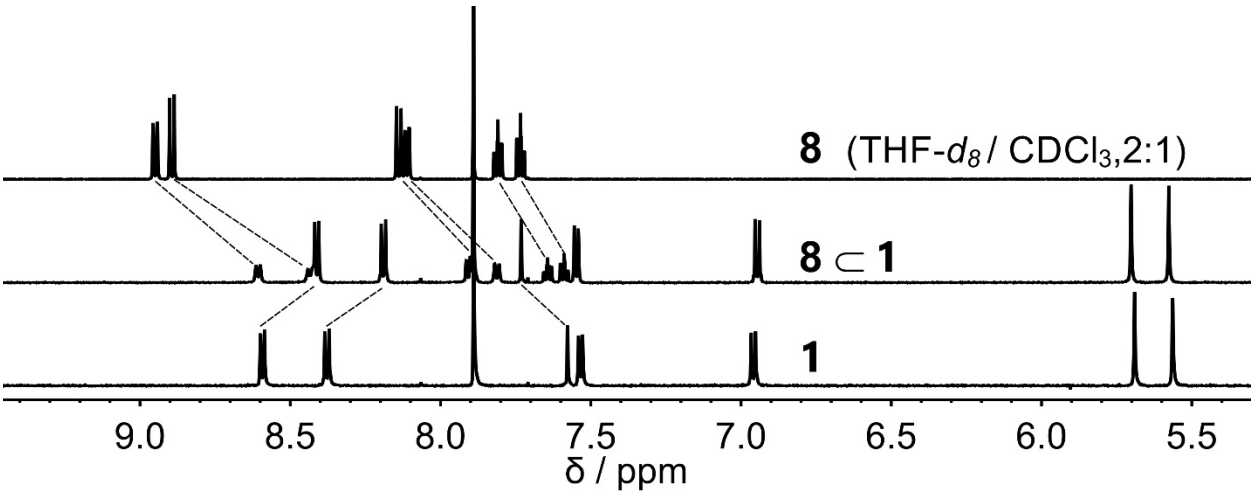

Figure S17. ^{1}H NMR of benzo(*a*)phenanthrene ⊂ **1** in THF-d_8/$CDCl_3$ (2:1) showing upfield shift in benzo(*a*)phenanthrene (**8**) protons (at 8.95, 8.9 ppm, Δδ= 0.34, 0.46 ppm) as well as in host (**1**) protons (at 8.58, 8.37 ppm, Δδ= 0.18, 0.17 ppm) and downfield shift in host proton (at 7.57 ppm, Δδ= 0.16 ppm).

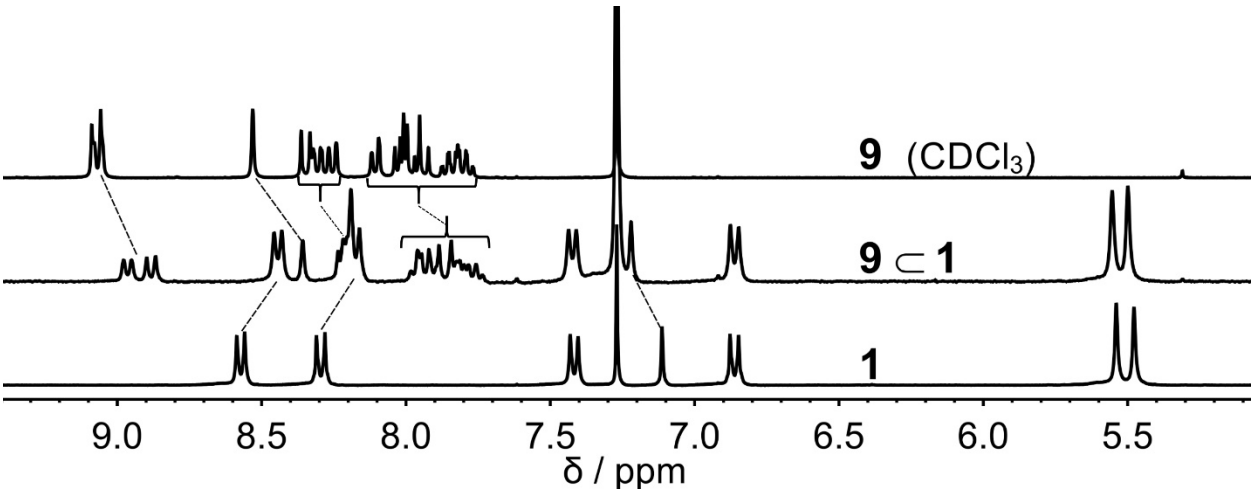

Figure S18. ^{1}H NMR of benzo(*a*)pyrene ⊂ **1** in $CDCl_3$ showing upfield shift in benzo(*a*)pyrene (**9**) protons (at 9.05, 8.53 ppm, Δδ= 0.19, 0.18 ppm) as well as in host (**1**) protons (at 8.55, 8.28 ppm Δδ= 0.13, 0.12 ppm) and downfield shift in host proton (at 7.11 ppm, Δδ= 0.11 ppm).

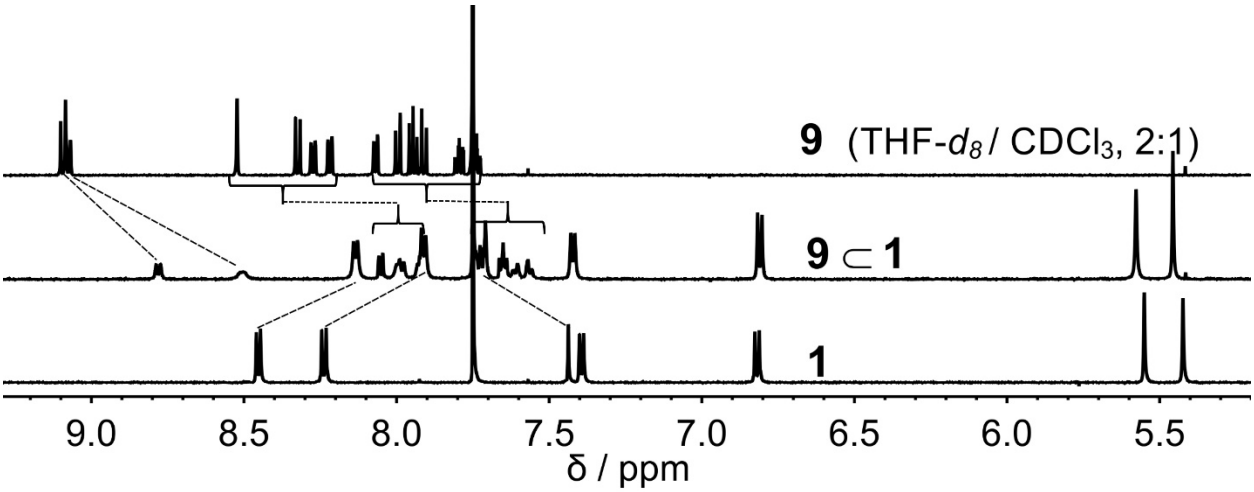

Figure S19. ^{1}H NMR of benzo(*a*)pyrene ⊂ **1** in THF-d_8/$CDCl_3$ (2:1) showing upfield shift in benzo(*a*)pyrene (**9**) protons (at 9.24, 9.2 ppm, Δδ= 0.32, 0.56 ppm) as well as in host (**1**) proton (at 8.58, 8.37 ppm, Δδ= 0.32, 0.33 ppm) and downfield shift in host proton (at 7.57 ppm, Δδ= 0.27 ppm).

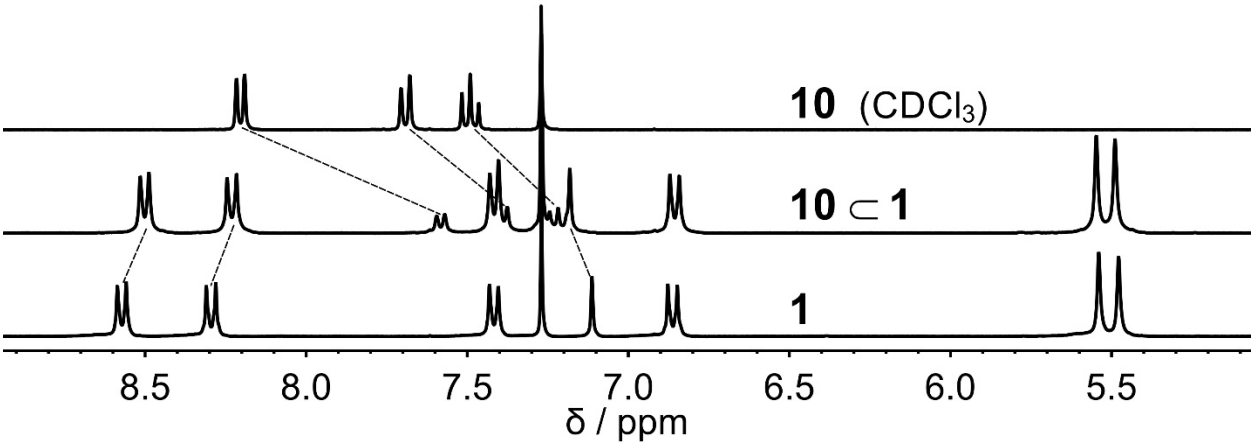

Figure S20. ^{1}H NMR of perylene ⊂ **1** in $CDCl_3$ showing upfield shift in perylene (**10**) protons (at 8.19, 7.67, 7.49 ppm, Δδ= 0.48, 0.23, 0.19 ppm) as well as in host (**1**) proton (at 8.55, 8.28 ppm Δδ= 0.09, 0.09 ppm) and downfield shift in host proton (at 7.11 ppm, Δδ= 0.09 ppm).

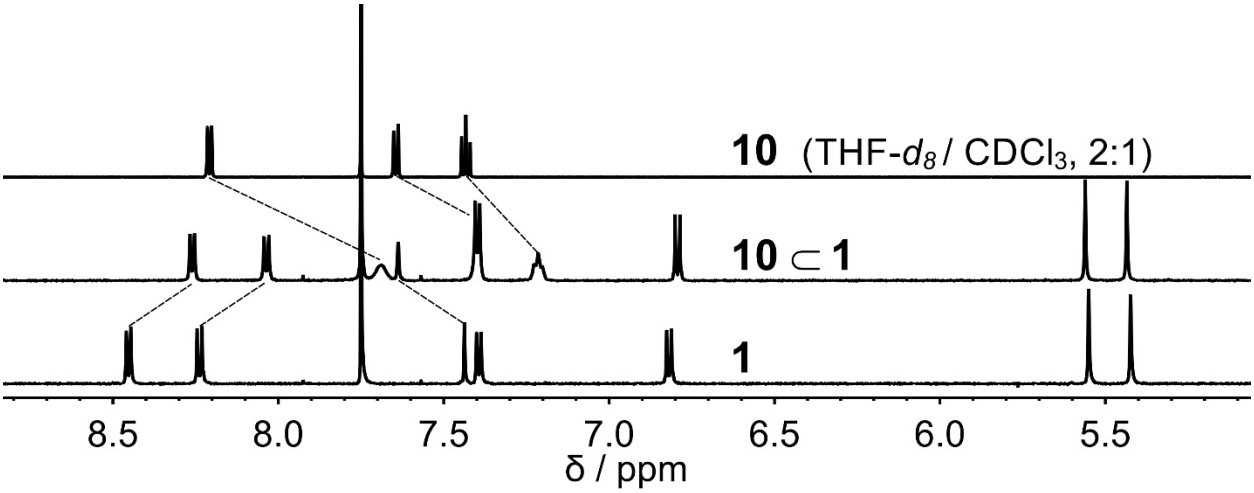

Figure S21. ^{1}H NMR of perylene ⊂ **1** in THF-d_8/$CDCl_3$ (2:1) showing upfield shift in perylene (**10**) protons (at 8.34, 7.77, 7.57 ppm, Δδ= 0.52, 0.24, 0.22 ppm) as well as in host (**1**) protons (at 8.58, 8.37 ppm, Δδ= 0.19, 0.21 ppm) and downfield shift in host proton (at 7.57 ppm, Δδ= 0.2 ppm).

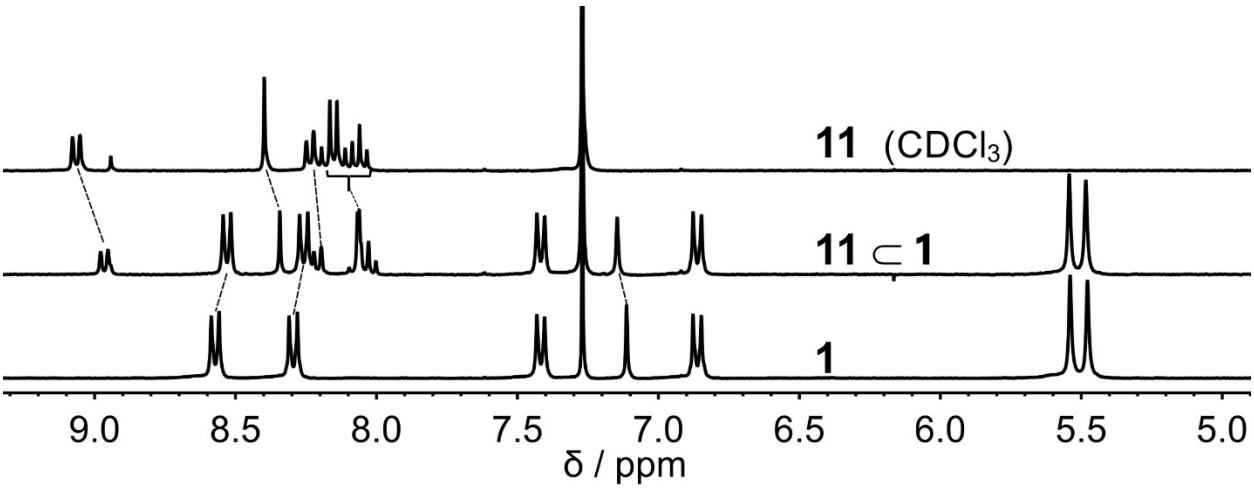

Figure S22. ^{1}H NMR of benzo(*ghi*)perylene ⊂ **1** in $CDCl_3$ showing upfield shift in benzo(*ghi*)perylene (**10**) protons (at 9.05, 8.39 ppm, Δδ= 0.1, 0.05 ppm) as well as in host (**1**) proton (at 8.55, 8.28 ppm Δδ= 0.04, 0.04 ppm) and downfield shift in host proton (at 7.11 ppm, Δδ= 0.03 ppm).

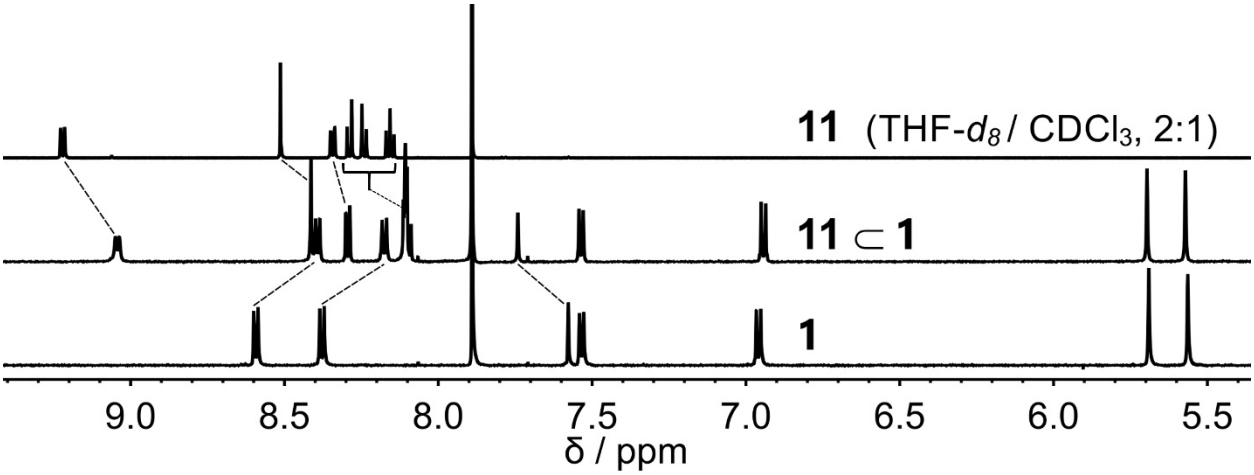

Figure S23. ^{1}H NMR of benzo(*ghi*)perylene ⊂ **1** in THF-d_8/$CDCl_3$ (2:1) showing upfield shift in benzo(*ghi*)perylene (**10**) protons (at 9.21, 8.51 ppm, Δδ= 0.18, 0.1 ppm) as well as in host (**1**) protons (at 8.58, 8.37 ppm, Δδ= 0.2, 0.21 ppm) and downfield shift in host proton (at 7.57 ppm, Δδ= 0.17 ppm).

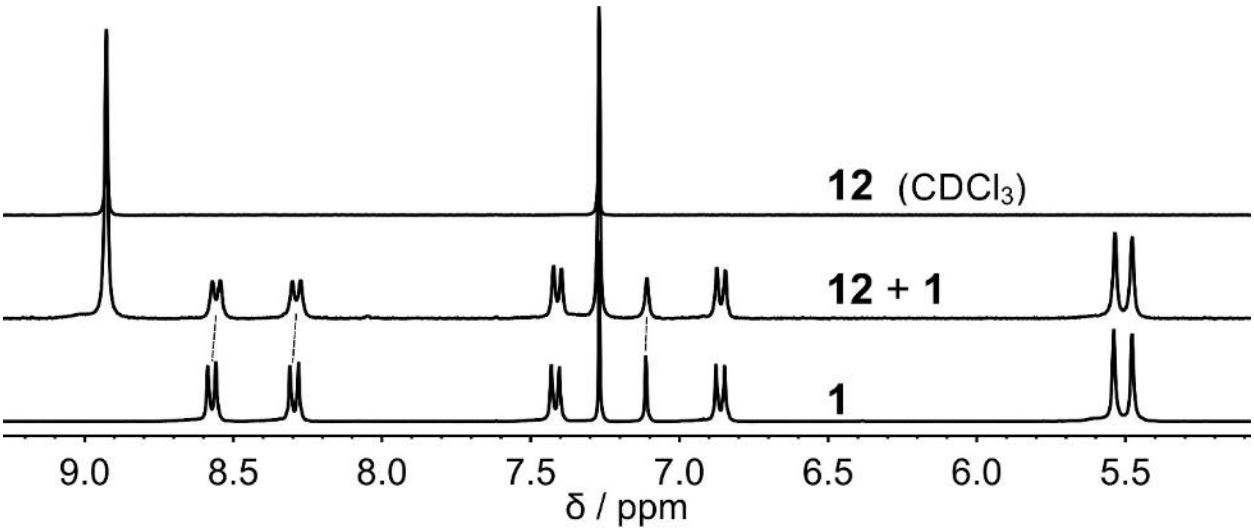

Figure S24. ^{1}H NMR of Coronene + **1** in $CDCl_3$ showing no shift in coronene (**12**) proton (at 8.92 ppm) or in host protons (**1**) (at 8.55, 8.28, 7.11 ppm).

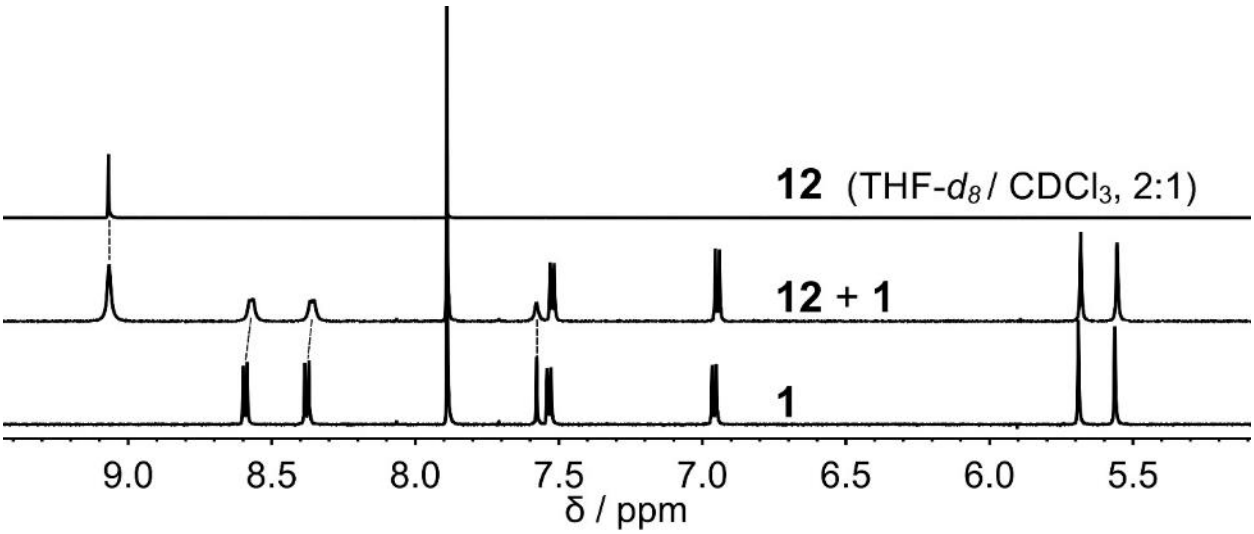

Figure S25. ^{1}H NMR of Coronene + **1** in THF-d_8/$CDCl_3$ (2:1) showing no shift in coronene (**12**) proton (at 9.06 ppm) or in host protons (at 8.58, 8.37, 7.57 ppm).

4. Absorption Spectroscopy of host-guest complexes:

Absorption spectra for 10^{-5} M solution of both **1** and each guest were collected separately. For 1:1 absorption spectra, a 10 μL solution of 10^{-3} M **1** was added to 1 ml 10^{-5} M solution of guest and the solution was mixed properly and data was collected.

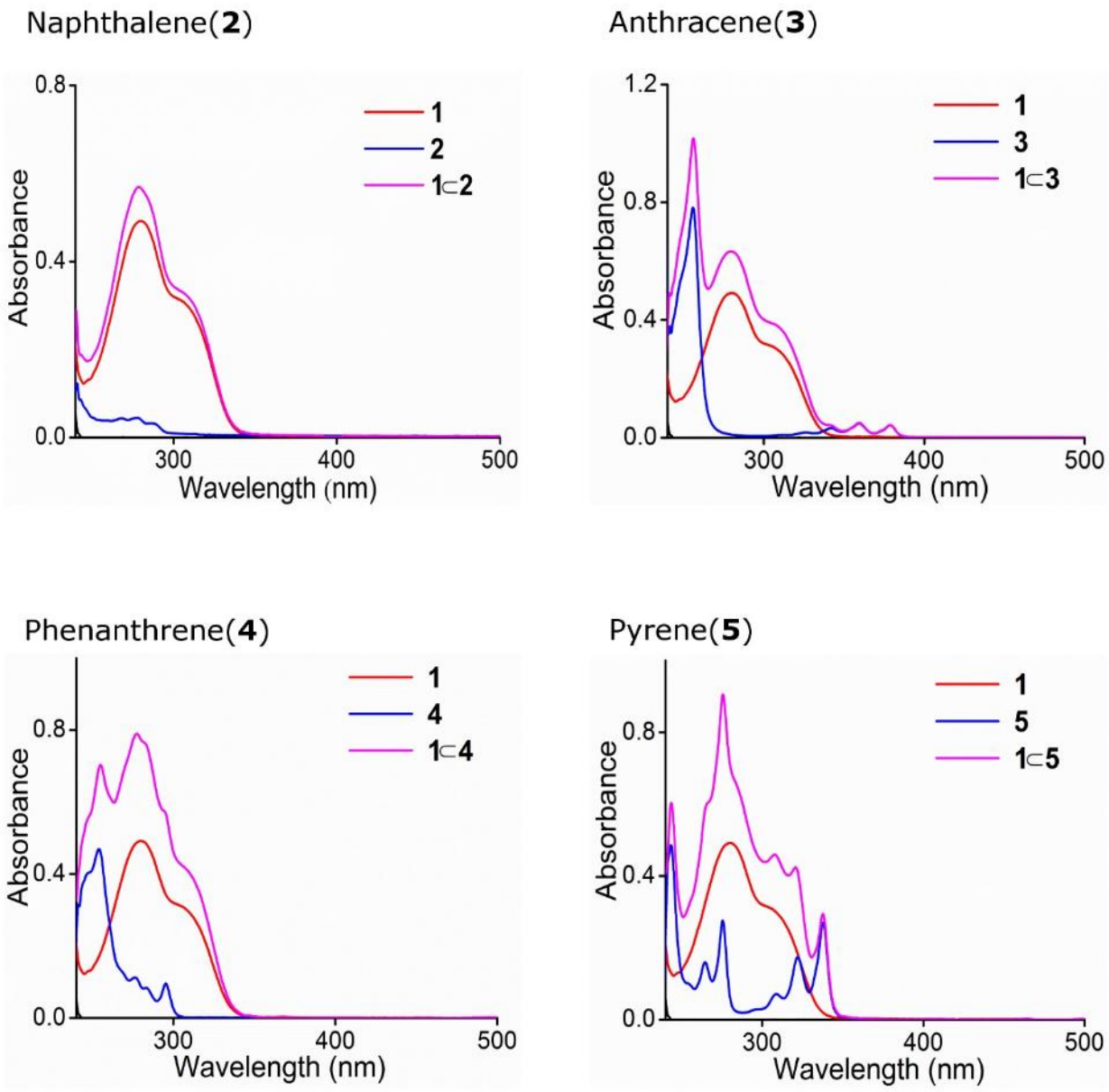

Figure S26. Absorption spectra of **1** (10^{-5} M) in red traces, guest molecules (**2**, **3**, **4** and **5** in 10^{-5} M) in blue traces and 1:1 complex of **1** and the guest molecules (**2**, **3**, **4** and **5**) in magenta traces.

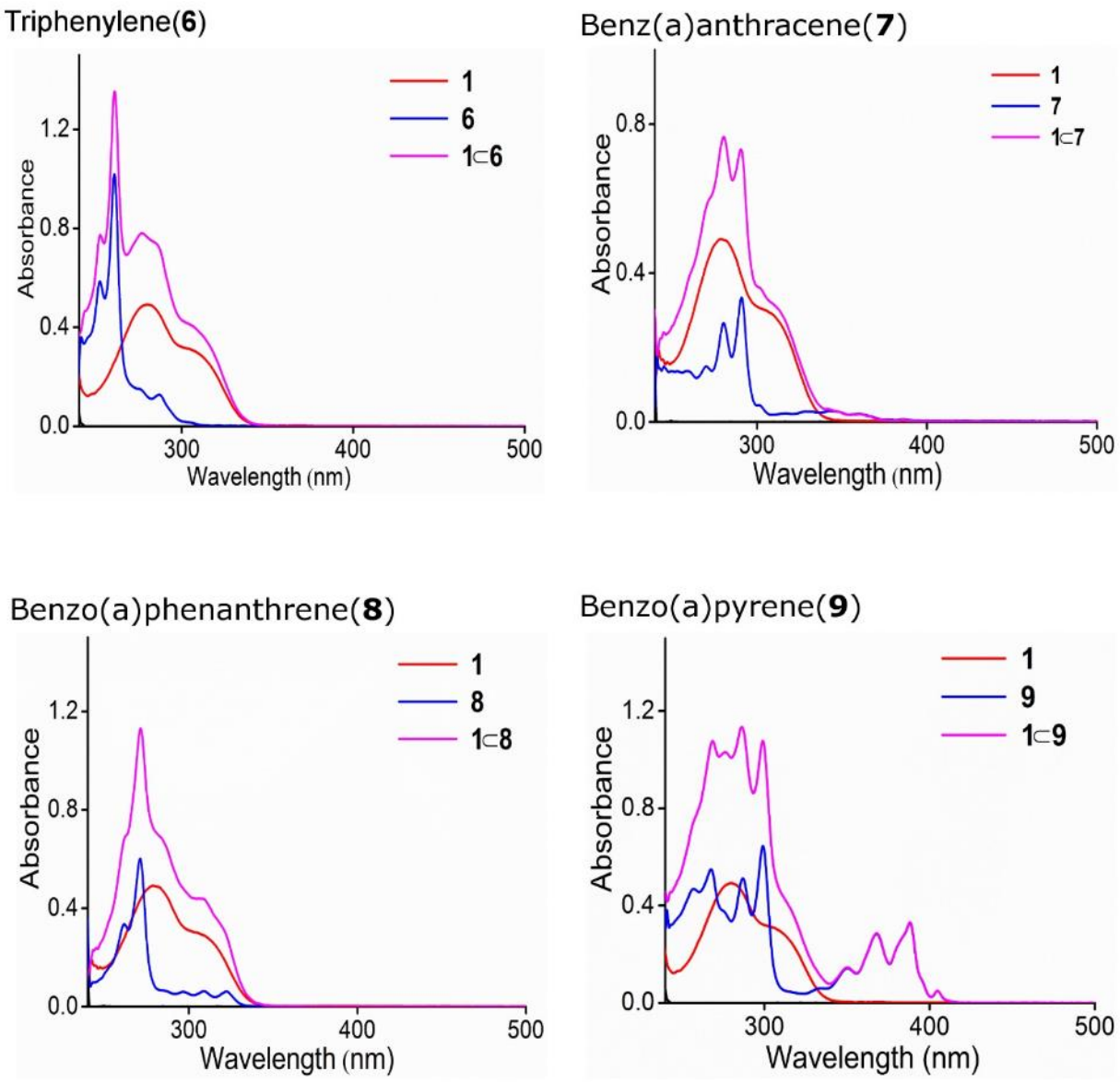

Figure S27. Absorption spectra of **1** (10^{-5} M) in red traces, guest molecules (**6**, **7**, **8** and **9** in 10^{-5} M) in blue traces and 1:1 complex of **1** and the guest molecules (**6**, **7**, **8** and **9**) in magenta traces.

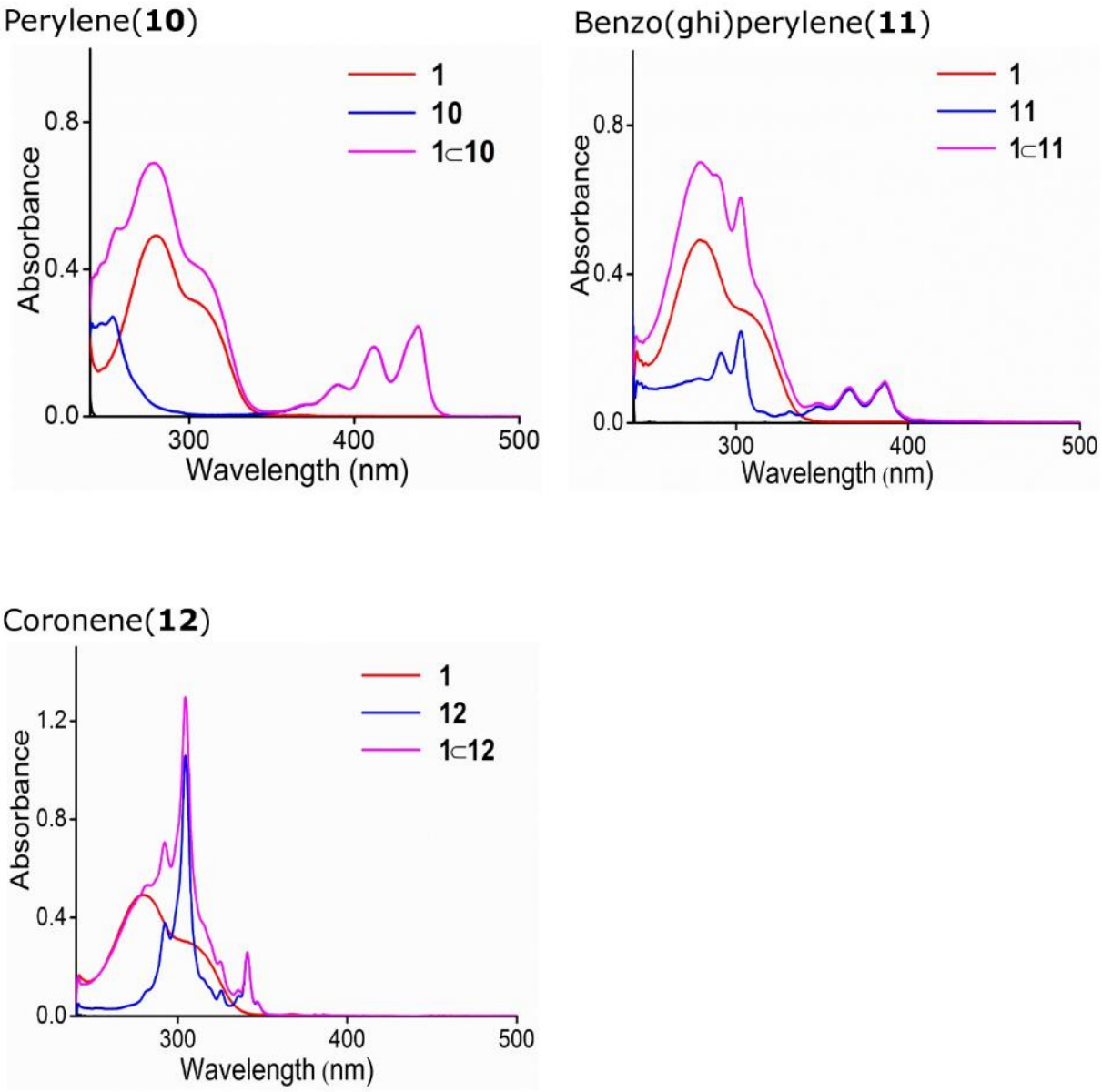

Figure S28. Absorption spectra of **1** (10^{-5} M) in red traces, guest molecules (**10**, **11** and **12** in 10^{-5} M) in blue traces and 1:1 complex of **1** and the guest molecules (**10**, **11** and **12**) in magenta traces.

5. Fluorescence titration of host-guest complexes:

All fluorescence titration experiments were performed in dry chloroform solvent at 298K. Solvent was sonicated for 15 minutes to degas before preparation of stock solution. During titration aliquots of 2 x 10^{-3} M solution of **1** was added to a 2 x 10^{-5} M solution of the guest and stirred for 2 min, the mixture was allowed to settle down for 30 seconds and the data were collected. All data are given in normalized form. Data obtained from fluorescence spectroscopy were fitted by using following equation:

Here we assume that the dilution error, due to addition of small volume of host, compared to large volume of guest, is negligible. Since only the guests are fluorescently active and host is fluorescently silent, the fluorescence of the complex formed is getting static quenched, so it will follow the equation which looks like Stern-Volmer equation

$$F_0/F = 1+K_a[H]$$

Here F_0 = Initial fluorescence of the guest molecule, F = fluorescence after addition of host molecule, K_a = association constant, [H] = host concentration. Change in fluorescence intensity is plotted against the concentration of the host molecule added, and K_a is calculated from a non-linear least square fitting using a 1:1 model.[2] The titrations were repeated for three times to obtain the estimated standard uncertainty. The covariance of fit in all cases is in 10^{-3} range except for the titration with naphthalene.

Naphthalene (**2**):

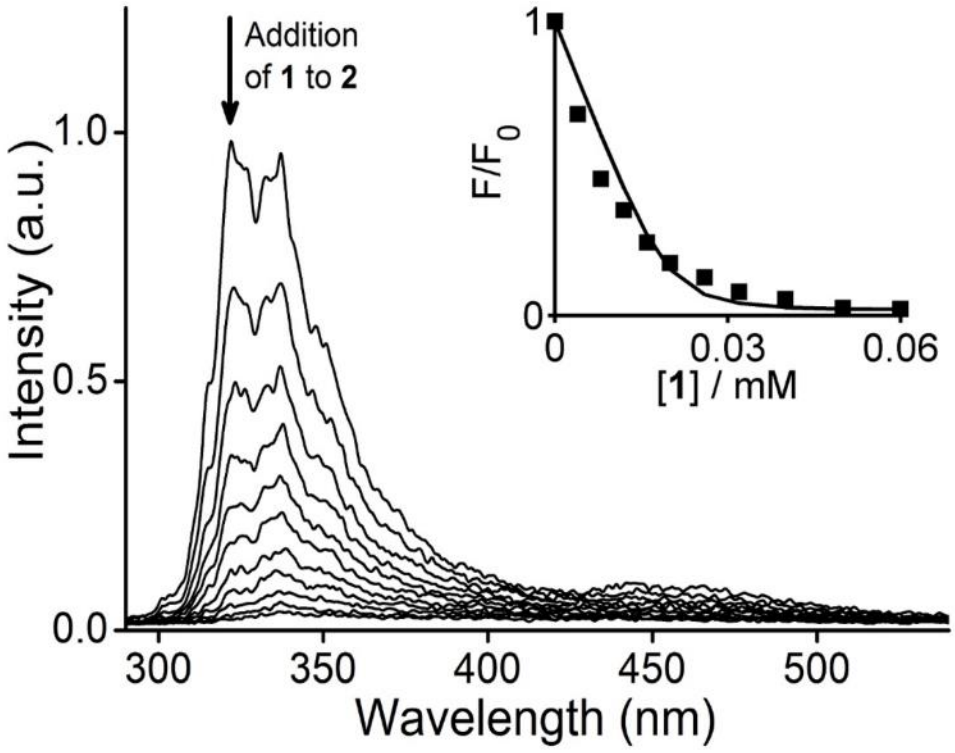

Figure S29. Fluorescence titration of 2 x 10^{-3} M solution of **1** into 2 x 10^{-5} M solution of naphthalene (**2**) (λ_{ex} = 275 nm). Inset: non-linear least square fitting curves of the relative fluorescence intensities vs. the host (**1**) concentration. K_a = (1.2 ± 0.26) x 10^6 M^{-1}, $-\Delta G^0_{298}$ = 34.63 ± 0.54 KJ/M.

Anthracene (**3**):

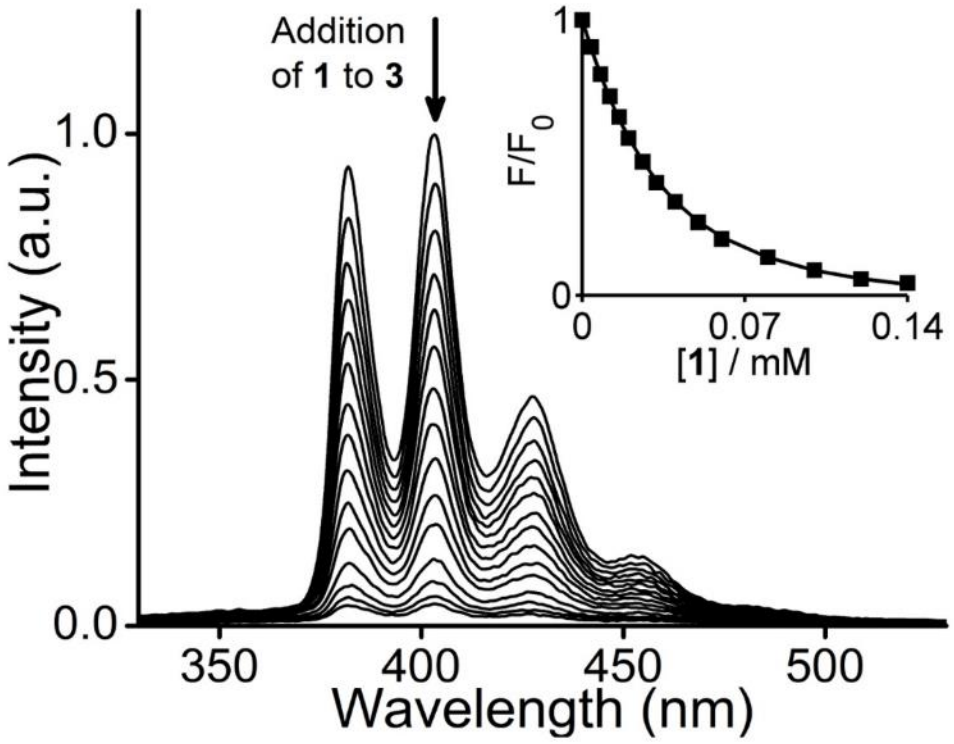

Figure S30. Fluorescence titration of 2 x 10^{-3} M solution of **1** into 2 x 10^{-5} M solution of anthracene (**3**) (λ_{ex} = 320 nm). Inset: non-linear least square fitting curves of the relative fluorescence intensities vs. the host (**1**) concentration. K_a = (3.7 ± 0.42) x 10^4 M^{-1}, $-\Delta G^0_{298}$ = 26.04 ± 0.28 KJ/M.

Phenanthrene (**4**):

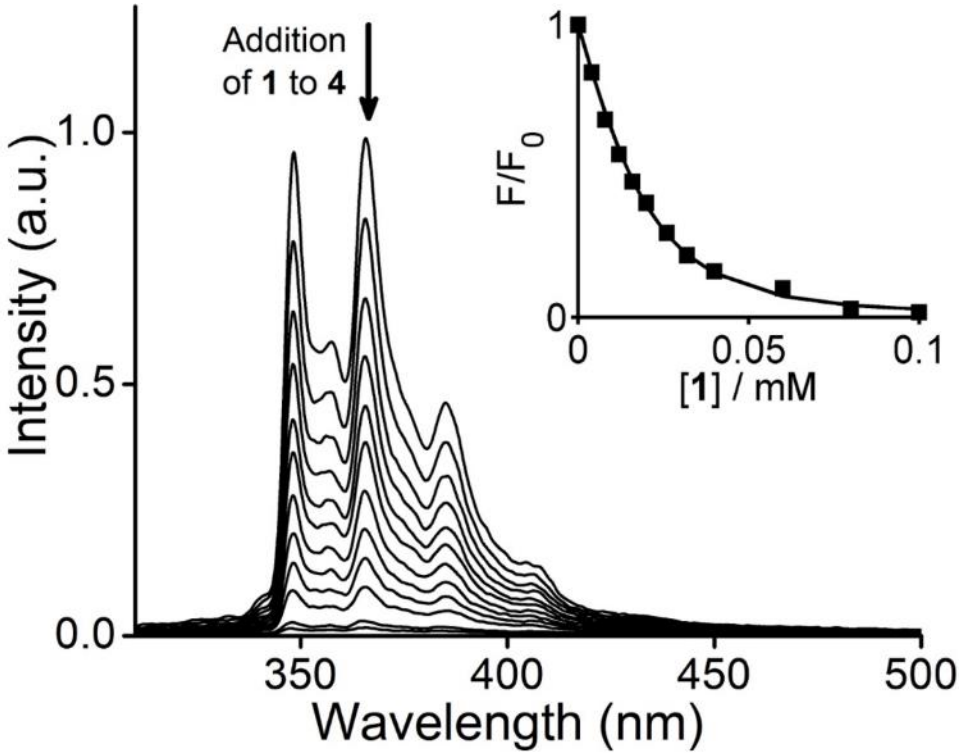

Figure S31. Fluorescence titration of 2 x 10^{-3} M solution of **1** into 2 x 10^{-5} M solution of phenanthrene (**4**) (λ_{ex} = 295 nm). Inset: non-linear least square fitting curves of the relative fluorescence intensities vs. the host (**1**) concentration. K_a = (1.56 ± 0.07) x 10^5 M^{-1}, $-\Delta G^0_{298}$ = 29.62 ± 0.11 KJ/M.

Pyrene (**5**):

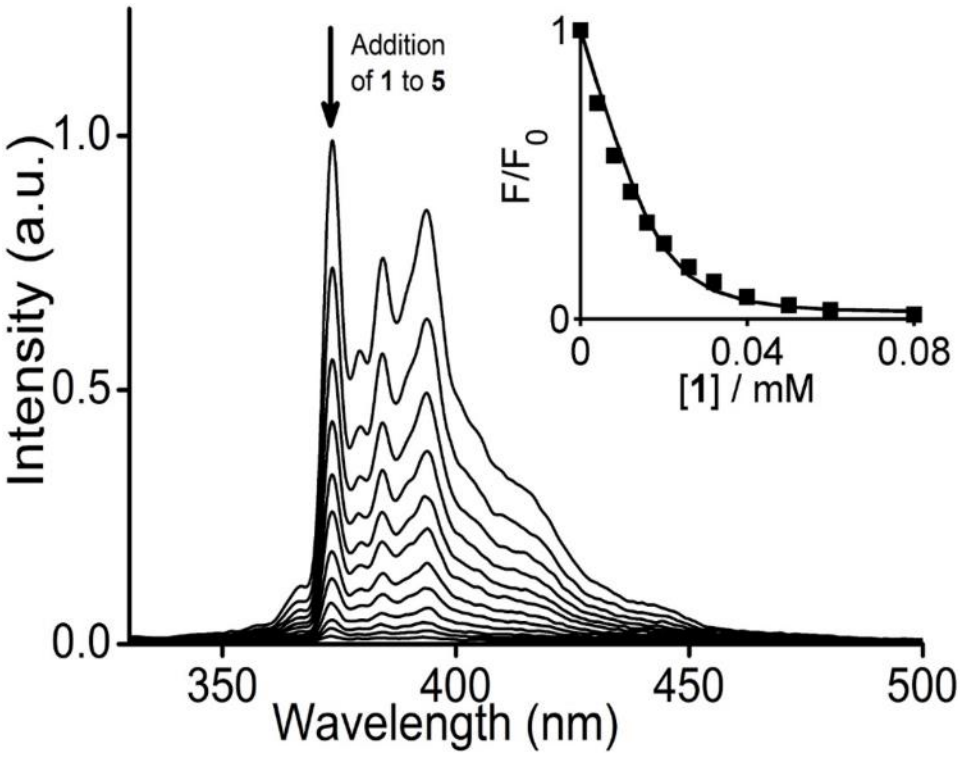

Figure S32. Fluorescence titration of 2 x 10^{-3} M solution of **1** into 2 x 10^{-5} M solution of pyrene (**5**) (λ_{ex} = 275 nm). Inset: non-linear least square fitting curves of the relative fluorescence intensities vs. the host (**1**) concentration. K_a = (5.1 ± 0.19) x 10^5 M^{-1}, $-\Delta G^0_{298}$ = 32.55 ± 0.09 KJ/M.

Triphenylene (**6**):

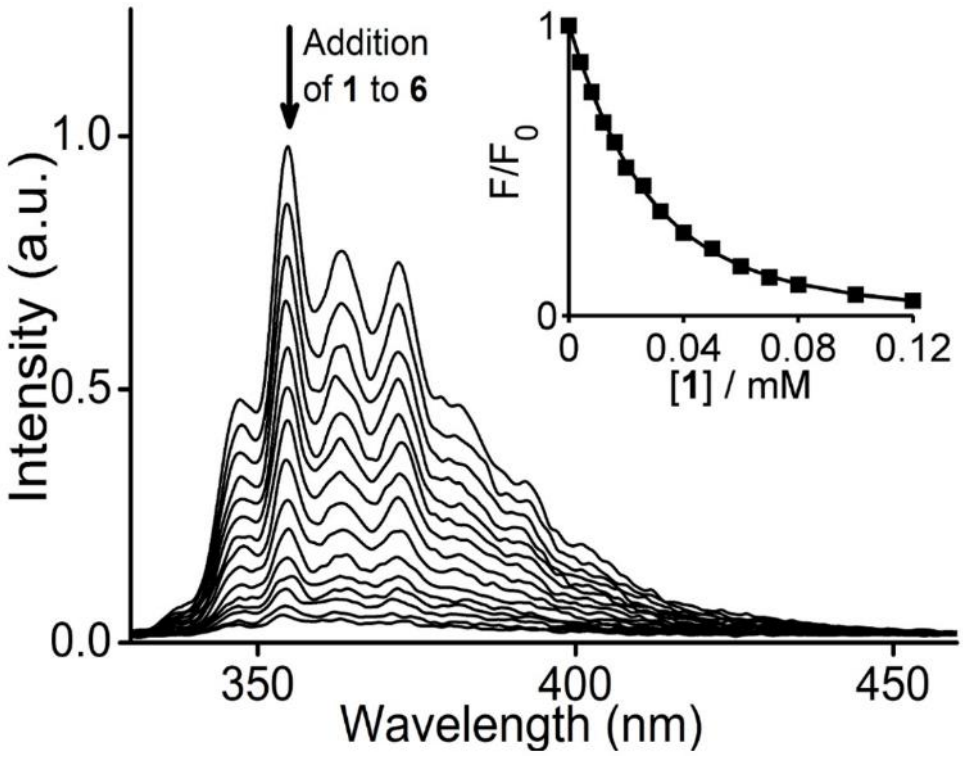

Figure S33. Fluorescence titration of 2 x 10^{-3} M solution of **1** into 2 x 10^{-5} M solution of triphenylene (**6**) (λ_{ex} = 260 nm). Inset: non-linear least square fitting curves of the relative fluorescence intensities vs. the host (**1**) concentration. K_a = (6.27 ± 0.37) x 10^4 M^{-1}, $-\Delta G^0_{298}$ = 27.36 ± 0.15 KJ/M.

Benz(*a*)anthracene (**7**):

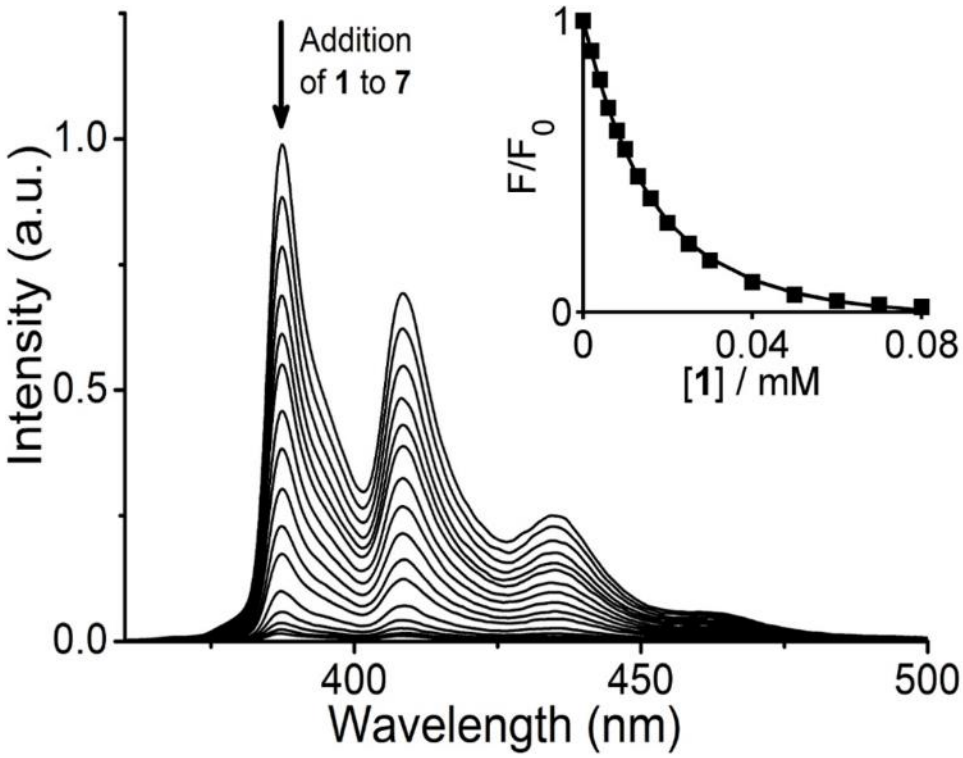

Figure S34. Fluorescence titration of 10^{-3} M solution of **1** into 10^{-5} M solution of benz(*a*)anthracene (**7**) (λ_{ex} = 291 nm). Inset: non-linear least square fitting curves of the relative fluorescence intensities vs. the host (**1**) concentration. K_a = (8.6 ± 0.27) x10^4 M^{-1}, $-\Delta G^0_{298}$ = 28.15 ± 0.08 KJ/M.

Benzo(*a*)phenanthrene (**8**):

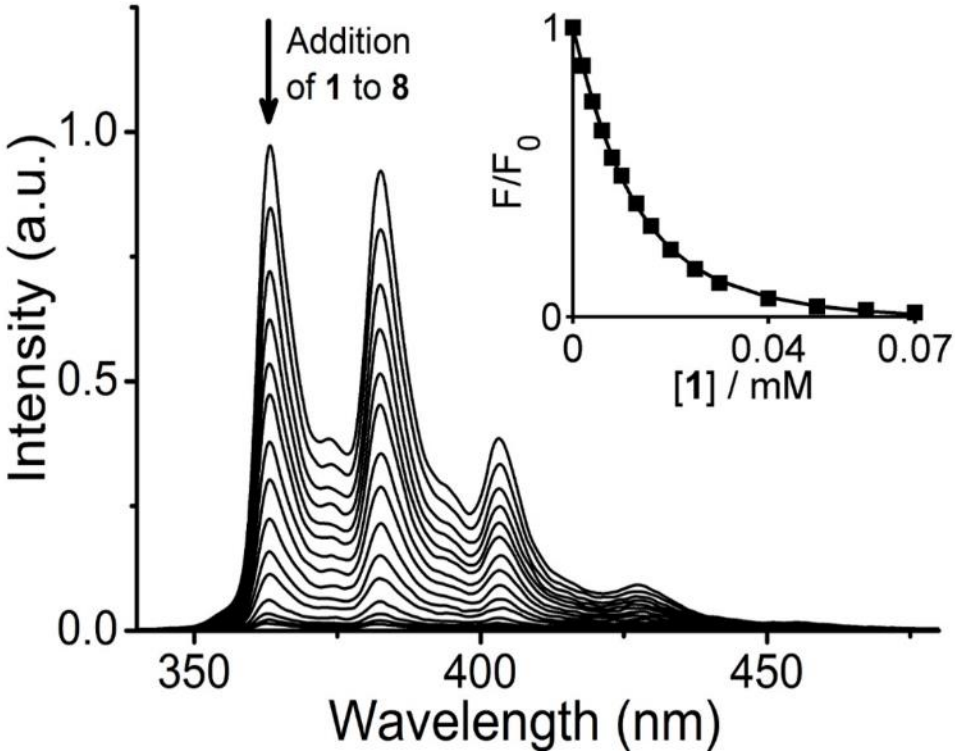

Figure S35. Fluorescence titration of 10^{-3} M solution of **1** into 10^{-5} M solution of benzo(*a*)phenanthrene (**8**) (λ_{ex} = 271 nm). Inset: non-linear least square fitting curves of the relative fluorescence intensities vs. the host (**1**) concentration. K_a = (1.39 ± 0.18) x 10^5 M^{-1}, $-\Delta G^0_{298}$ = 29.81 ± 0.17 KJ/M

Benzo(*a*)pyrene (**9**):

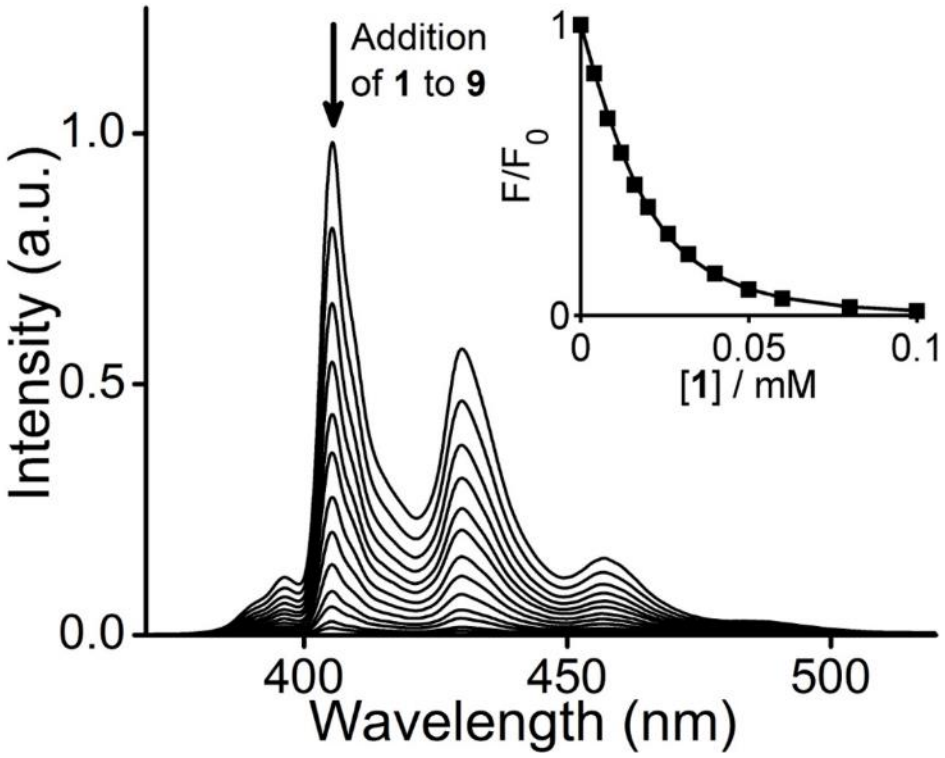

Figure S36. Fluorescence titration of 2 x 10^{-3} M solution of **1** into 2 x 10^{-5} M solution of benzo(*a*)pyrene (**9**) (λ_{ex} = 300 nm). Inset: non-linear least square fitting curves of the relative fluorescence intensities vs. the host (**1**) concentration. K_a = (1.47 ± 0.04) x 10^5 M^{-1}, $-\Delta G^0_{298}$ = 29.48 ± 0.07 KJ/M.

Perylene (**10**):

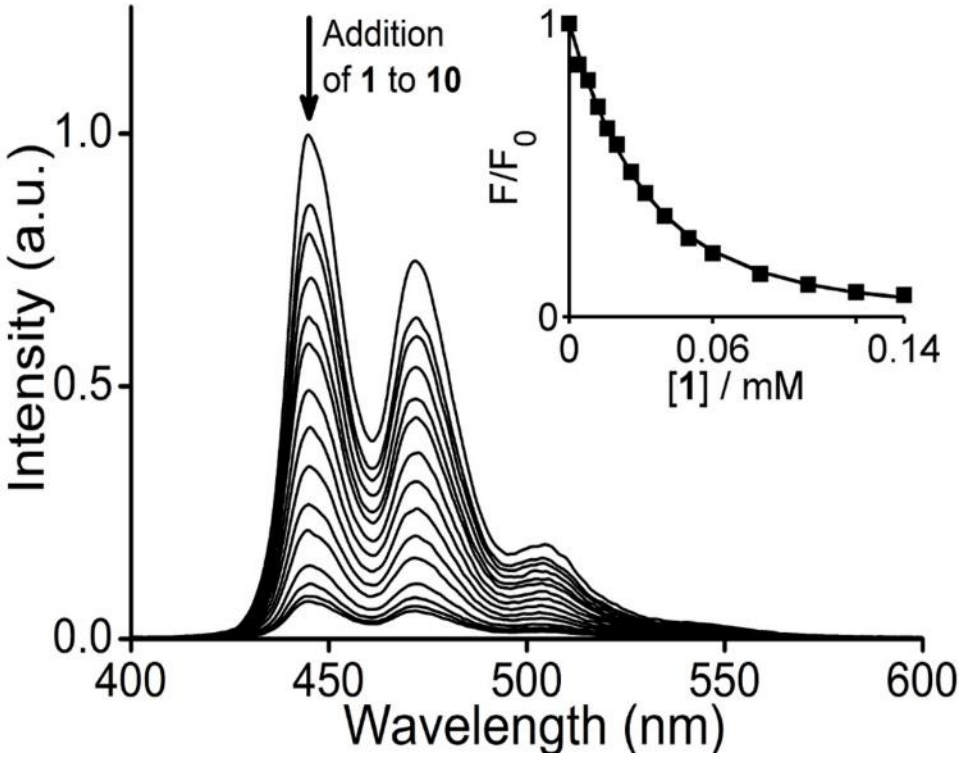

Figure S37. Fluorescence titration of 2 x 10^{-3} M solution of **1** into 2 x 10^{-5} M solution of perylene (**10**) (λ_{ex} = 255 nm). Inset: non-linear least square fitting curves of the relative fluorescence intensities vs. the host (**1**) concentration. K_a = (4.3 ± 0.18) x 10^4 M^{-1}, $-\Delta G^0_{298}$ = 26.42 ± 0.1 KJ/M.

Benzo(*ghi*)perylene (**11**):

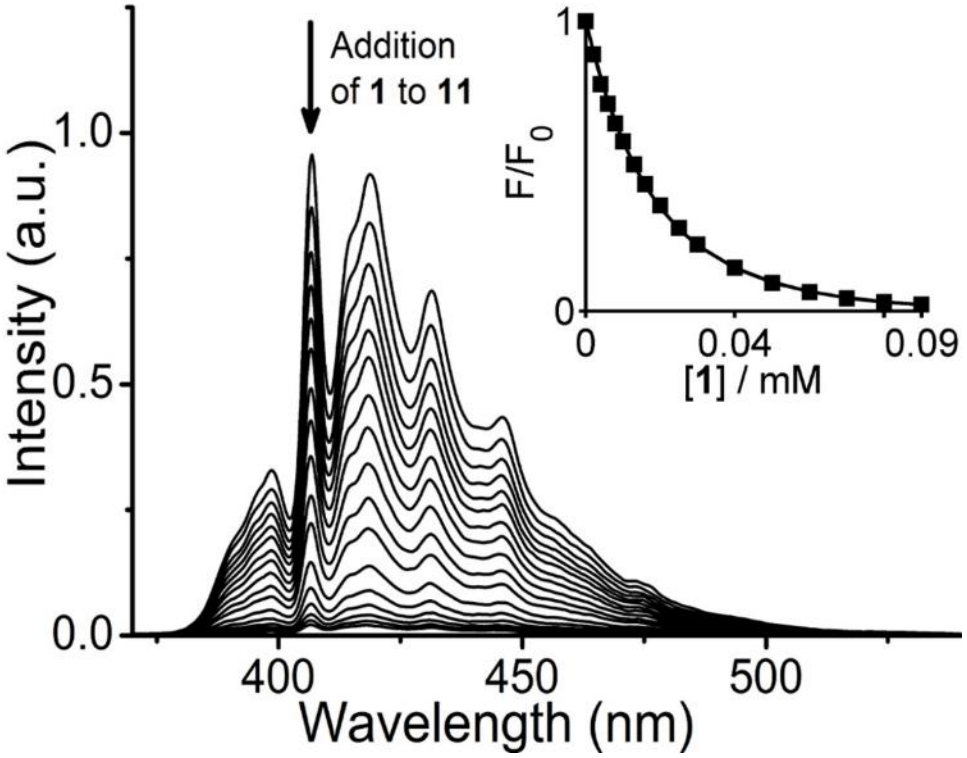

Figure S38. Fluorescence titration of 10^{-3} M solution of **1** into 10^{-5} M solution of benzo(*ghi*)perylene (**11**) at λ_{ex} = 303 nm. Inset: non-linear least square fitting curves of the relative fluorescence intensities vs. the host (**1**) concentration. K_a = (7.2 ± 0.21) x 10^4 M^{-1}, $-\Delta G^0_{298}$ = 27.65 ± 0.13 KJ/M.

Coronene (**12**):

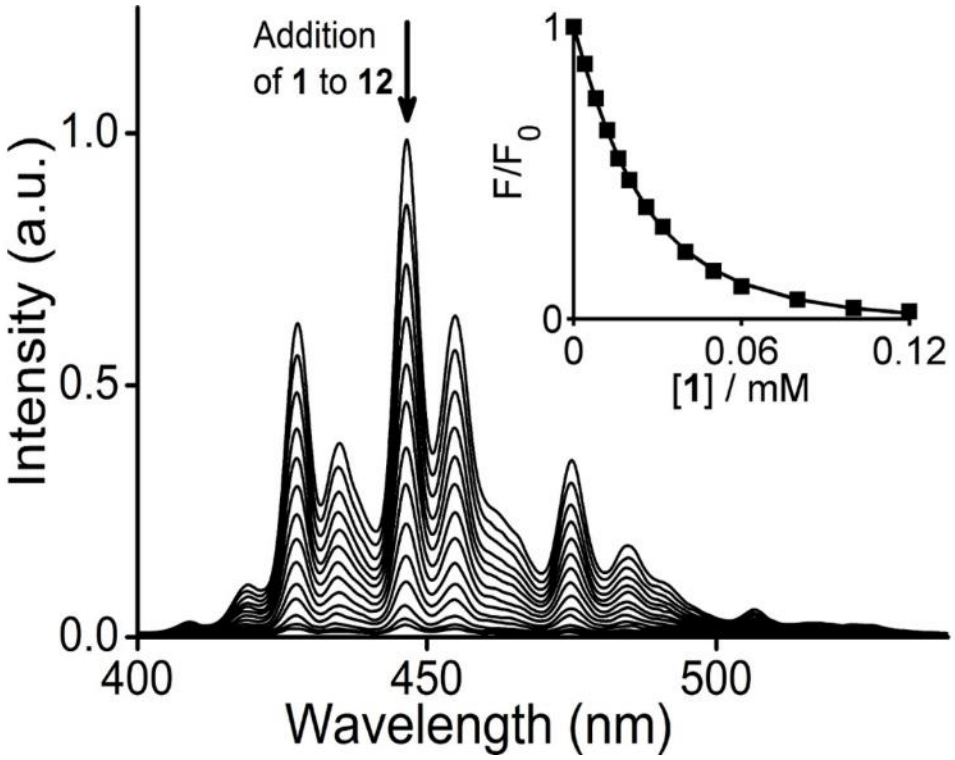

Figure S39. Fluorescence titration of 2 x 10^{-3} M solution of **1** into 2 x 10^{-5} M solution of Coronene (**12**) (λ_{ex} = 305 nm). Inset: non-linear least square fitting curves of the relative fluorescence intensities vs. the host concentration. K_a = (6.75 ± 0.5) x 10^4 M^{-1} and $-\Delta G^0_{298}$ = 27.53 ± 0.2 KJ/M.

6. X-ray Crystallography:

Single crystals of **1** and the complexes, with 4-5 eq excess of the PAH guests were grown by slow evaporation of the solution in $CHCl_3$ or $C_2H_4Cl_2$. Data were collected at 100K on a Bruker Kappa APEX2 CCD diffractometer with MoKα radiation.[3] Preliminary lattice parameters and orientation matrices were obtained from three sets of frames. Then full data were collected using the ω and ϕ scan method with the frame width of 0.5°. Data were processed with the SAINT+ program for reduction and cell refinement.[4] Multiscan absorption corrections were applied by using the SADABS program for area detector.[5] The structures were solved by SHELXT[5] and refined with SHELXL[5] using Olex2 program.[7] Similar 1,2 and 1,3 bond length (SADI, SAME), similar *U*ij (SIMU), rigid body (RIGU) restraints were applied wherever necessary. Equal atomic displacement (EDAP) and planar (FLAT) constraints were applied in a few cases. The CIFs are submitted into CCDC (1451119, 1451120 to 1451123-1451128 and 1478698-1478701) and can be obtained through https://summary.ccdc.cam.ac.uk/structure-summary-form.

Table S1

Identification code	$(CHCl_3)_6 \subset 2(\mathbf{1}).(CHCl_3)_{1.5}$
Empirical formula	$C_{56.75}H_{41.75}Cl_{8.25}N_{15}O_3$
Formula weight	1274.26
Temperature/K	100
Crystal system	triclinic
Space group	P-1
a/Å	10.110(2)
b/Å	21.965(5)
c/Å	27.902(6)
α/°	99.418(11)
β/°	94.933(10)
γ/°	90.930(10)
Volume/Å^3	6087(2)
Z	4
ρ_{calc}g/cm^3	1.391
μ/mm^{-1}	0.438
F(000)	2606.0
Crystal size/mm^3	0.36 × 0.34 × 0.34
Radiation	MoKα (λ = 0.71073)
2Θ range for data collection/°	1.486 to 49.992
Index ranges	$-12 \leq h \leq 11$, $-26 \leq k \leq 25$, $-33 \leq l \leq 33$
Reflections collected	97099
Independent reflections	21026 [R_{int} = 0.0816, R_{sigma} = 0.0862]
Data/restraints/parameters	21026/253/1552
Goodness-of-fit on F^2	1.388
Final R indexes [I>=2σ (I)]	R_1 = 0.1239, wR_2 = 0.3630
Final R indexes [all data]	R_1 = 0.1818, wR_2 = 0.4048
Largest diff. peak/hole / e Å^{-3}	1.77/-1.23

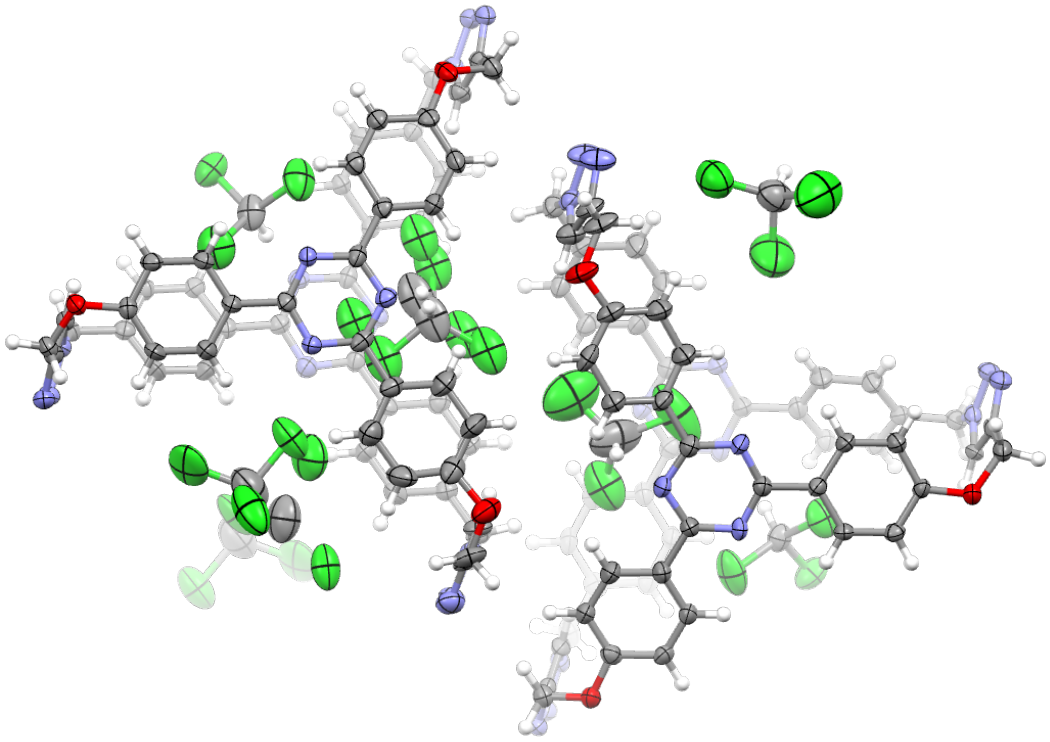

Figure S40. Top and side views of the asymmetric unit in $(CHCl_3)_6 \subset 2(\mathbf{1}).(CHCl_3)_{1.5}$. Thermal ellipsoids are shown in 50% probability level. One of the $CHCl_3$ molecule located inside the cage was disordered over two positions and refined with EADP constraints. Another $CHCl_3$ with 50% is disordered over two positions. Similar bond length restraints (SADI), similar Uij restraints and rigid body (RIGU) restraints were further applied for all solvent molecules.

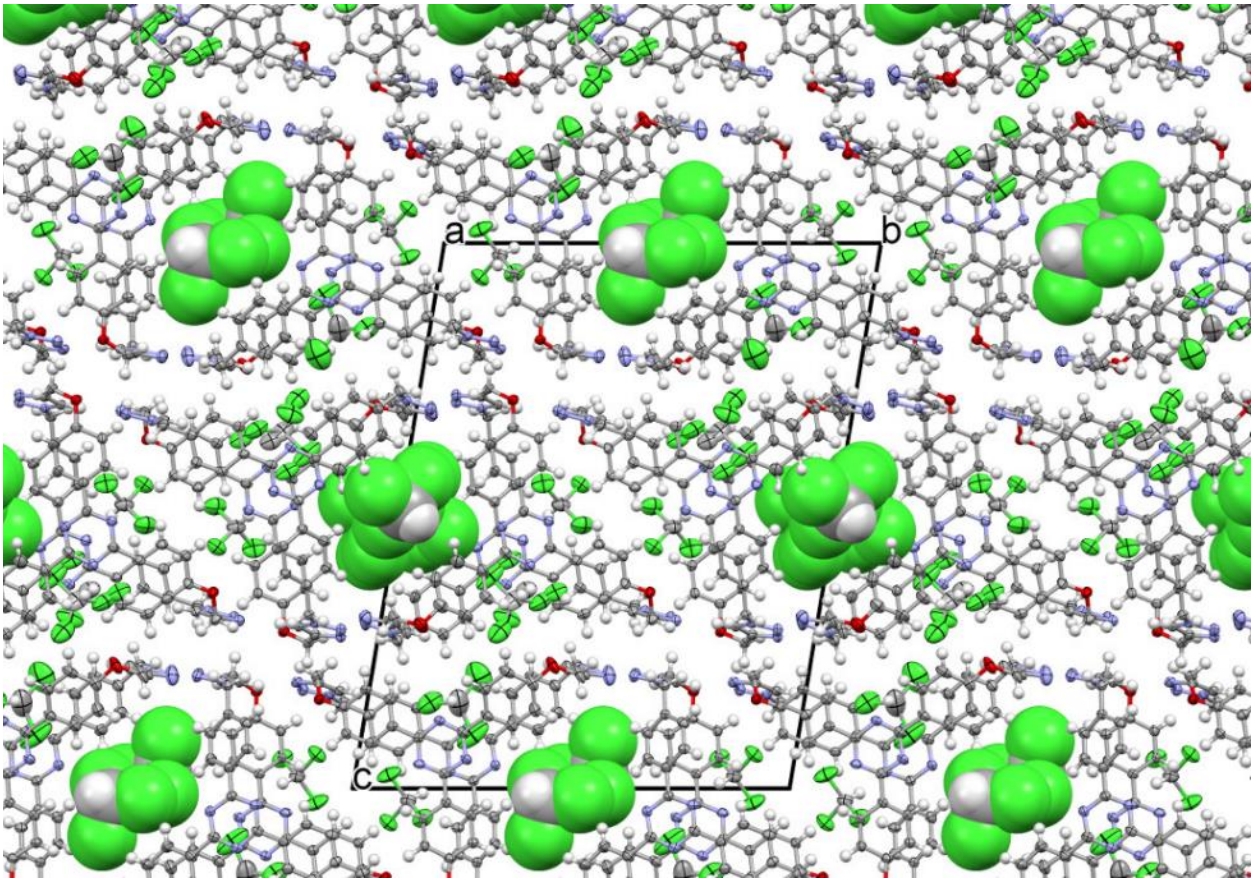

Figure S41. Crystal structure of $(CHCl_3)_6 \subset 2(\mathbf{1}).(CHCl_3)_2$, viewed along *a*-axis, illustrating the layer arrangement. Notice that the $CHCl_3$ molecules located away from the molecular cavity, but filling the lattice void, are shown in space filling mode.

Table S2

Identification code	$(C_2H_4Cl_2)_3 \subset \mathbf{1}.(C_2H_4Cl_2)_{1.5}$
Empirical formula	$C_{61.5}H_{54}Cl_{7.5}N_{15}O_3$
Formula weight	1317.07
Temperature/K	100
Crystal system	monoclinic
Space group	$P2_1/c$
a/Å	10.7001(8)
b/Å	20.2403(14)
c/Å	29.729(2)
α/°	90
β/°	91.170(4)
γ/°	90
Volume/Å^3	6437.2(8)
Z	4
ρ_{calc}g/cm^3	1.359
μ/mm^{-1}	0.386
F(000)	2718.0
Crystal size/mm^3	0.34 × 0.32 × 0.32
Radiation	MoKα (λ = 0.71073)
2Θ range for data collection/°	2.434 to 55.064
Index ranges	$-13 \leq h \leq 13$, $-26 \leq k \leq 24$, $-38 \leq l \leq 38$
Reflections collected	88463
Independent reflections	14748 [R_{int} = 0.0429, R_{sigma} = 0.0387]
Data/restraints/parameters	14748/287/896
Goodness-of-fit on F^2	1.027
Final R indexes [I >2σ (I)]	R_1 = 0.0838, wR_2 = 0.2181
Final R indexes [all data]	R_1 = 0.1103, wR_2 = 0.2374
Largest diff. peak/hole / e Å^{-3}	1.17/-0.90
CCDC number	1451120

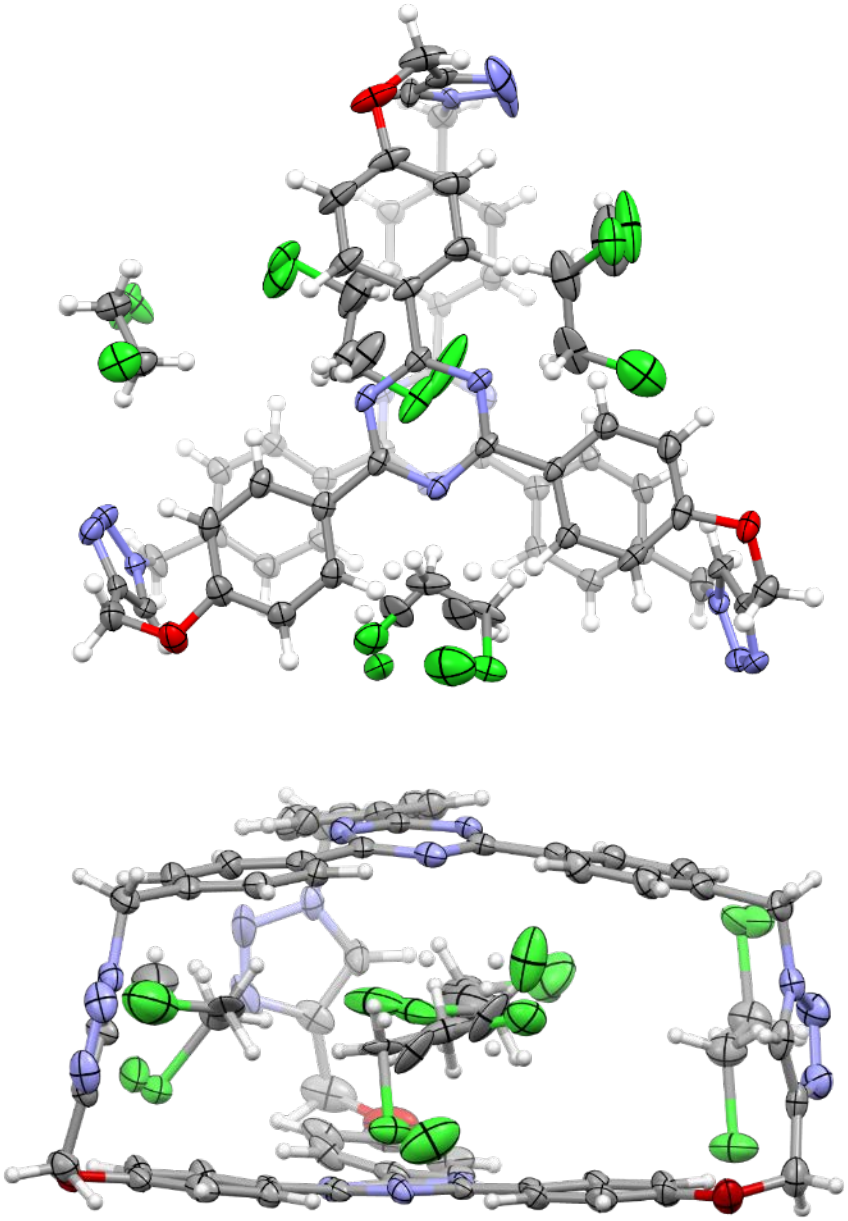

Figure S42. Top and side views of the asymmetric unit in $(C_2H_4Cl_2)_3 \subset$ **1**.$(C_2H_4Cl_2)_{1.5}$. Thermal ellipsoids are shown in 50% probability level. The disordered solvent molecules are refined with similar bond length (SADI), similar *U*ij (SIMU) restraints and rigid body (RIGU) restraints.

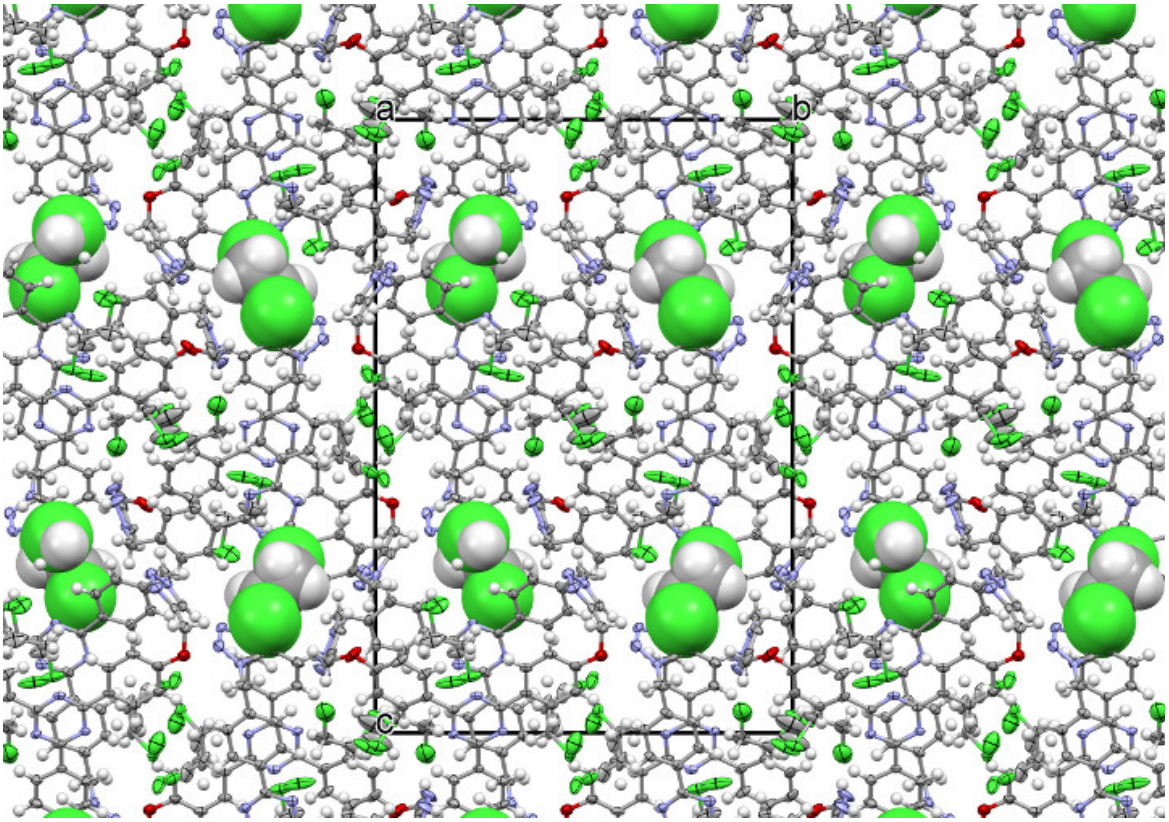

Figure S43. Crystal structure of $(C_2H_4Cl_2)_3 \subset$ **1**.$(C_2H_4Cl_2)_{1.5}$, viewed along *a*-axis. The single $C_2H_4Cl_2$ molecule located away from the molecular cavity is shown in space-filling mode.

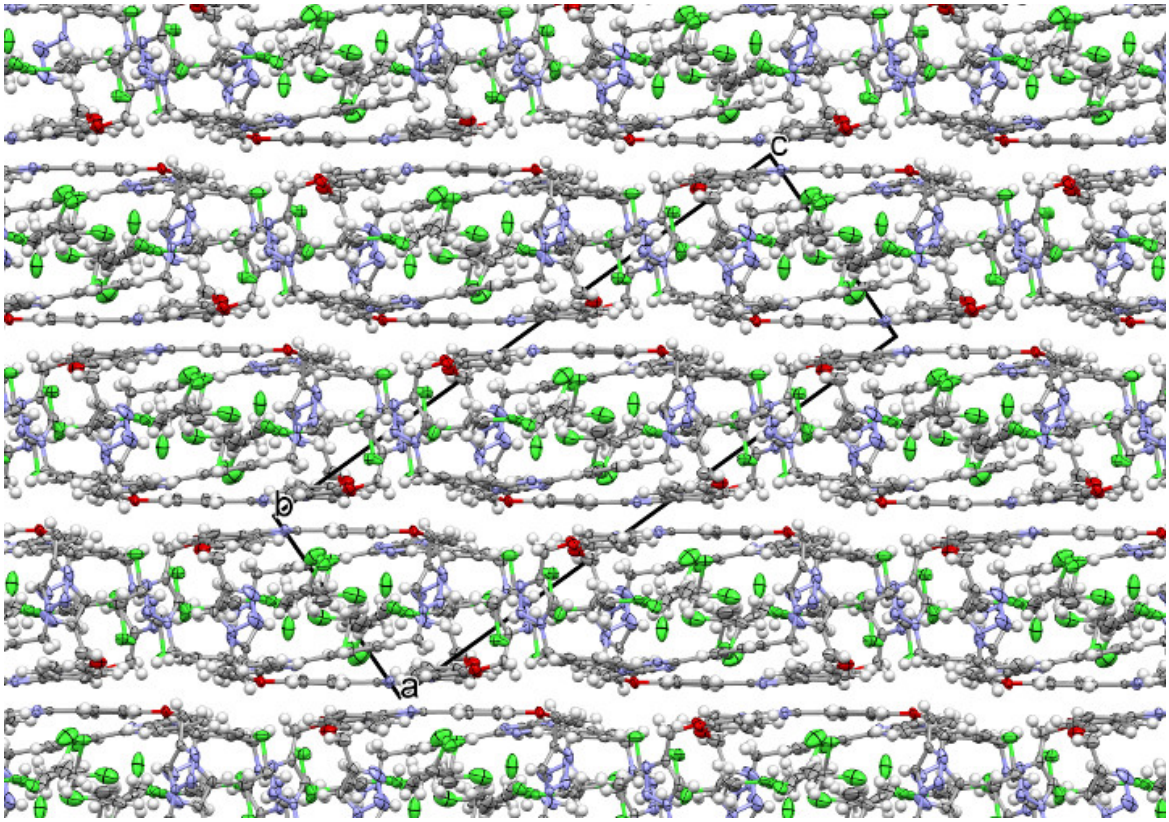

Figure S44. Crystal structure of $(C_2H_4Cl_2)_3 \subset$ **1**.$(C_2H_4Cl_2)_{1.5}$, viewed along *b*-axis, illustrating the layer arrangement.

Table S3

Identification code	Naphthalene(**2**) ⊂ **1**.(**2**)$_{1.8}$($C_2H_4Cl_2$)$_{1.2}$
Empirical formula	$C_{75.47}H_{59}Cl_{2.36}N_{15}O_3$
Formula weight	1307.47
Temperature/K	100
Crystal system	monoclinic
Space group	$P2_1/c$
a/Å	10.7998(10)
b/Å	20.2414(19)
c/Å	29.845(3)
α/°	90
β/°	91.909(5)
γ/°	90
Volume/Å^3	6520.6(10)
Z	4
ρ_{calc}g/cm^3	1.332
μ/mm^{-1}	0.177
F(000)	2723.0
Crystal size/mm^3	0.3 × 0.28 × 0.22
Radiation	MoKα (λ = 0.71073)
2Θ range for data collection/°	3.392 to 55.462
Index ranges	$-13 \leq h \leq 14$, $-20 \leq k \leq 26$, $-38 \leq l \leq 38$
Reflections collected	103965
Independent reflections	14979 [R_{int} = 0.0997, R_{sigma} = 0.1116]
Data/restraints/parameters	14979/585/920
Goodness-of-fit on F^2	1.030
Final R indexes [I>=2σ (I)]	R_1 = 0.1317, wR_2 = 0.3505
Final R indexes [all data]	R_1 = 0.2334, wR_2 = 0.4111
Largest diff. peak/hole / e Å^{-3}	2.28/-0.65

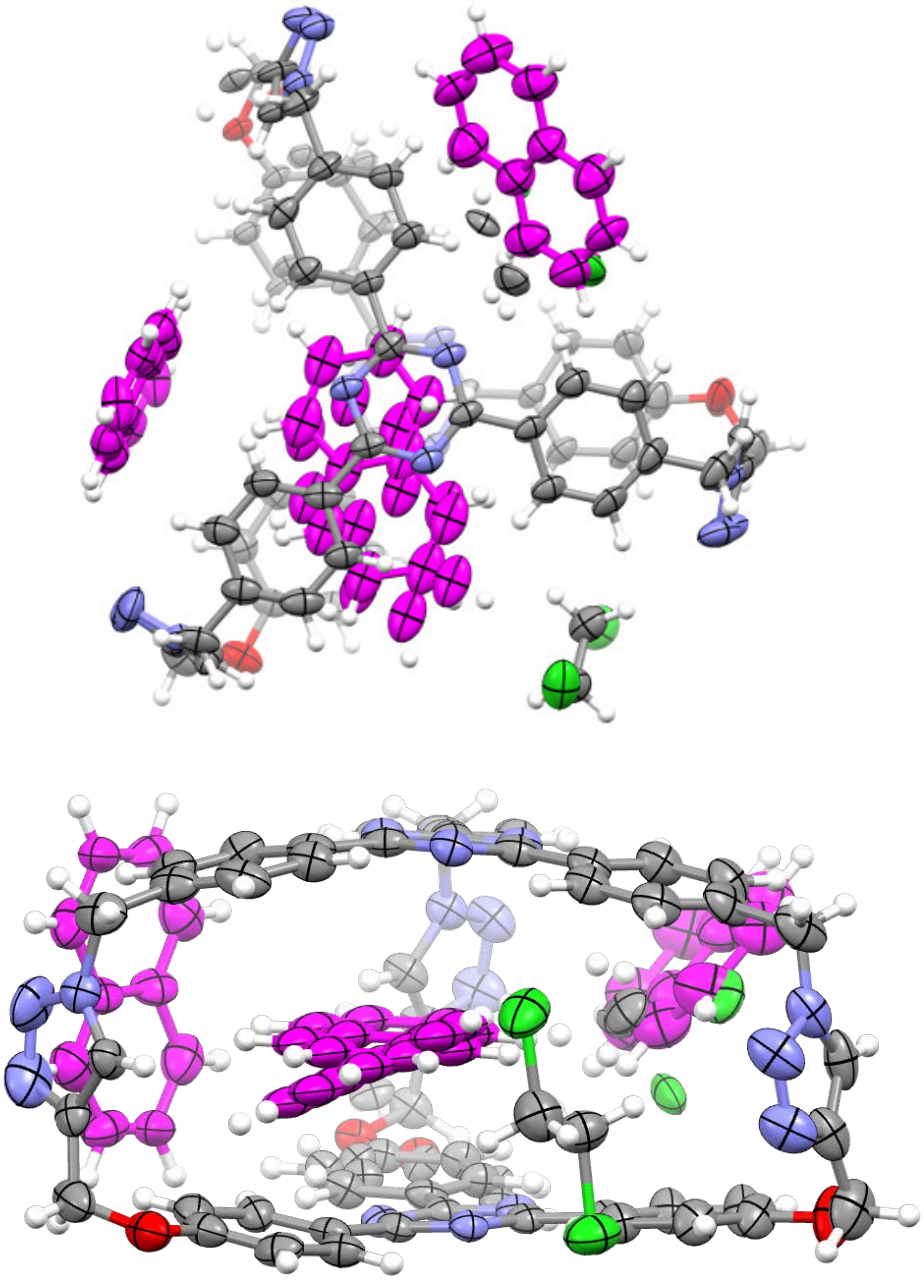

Figure S45. Top and side views of the asymmetric unit in naphthalene(**2**) ⊂ **1**.(**2**)$_{1.8}$($C_2H_4Cl_2$)$_{1.2}$. Thermal ellipsoids are shown in 50% probability level. The naphthalene molecule bound inside the cage is disordered over two positions (85:15). The second component was constrained with DFIX, FLAT and AFIX 116 and EADP. Another site was occupied with naphthalene guest and $C_2H_4Cl_2$ molecule in 80:20 ratio. Restraints such as SIMU, SADI and RIGU were applied to treat. DFIX restraints were further applied to avoid undesired intermolecular contacts. Despite our repeated efforts, the maximum residual electron density, close to the disordered component, cannot be modelled in any meaningful way.

Table S4

Identification code	Anthracene(**3**) ⊂ **1**.$(CHCl_3)_{3.5}$
Empirical formula	$C_{71.5}H_{52.5}Cl_{10.5}N_{15}O_3$
Formula weight	1542.01
Temperature/K	100
Crystal system	monoclinic
Space group	$P2_1/n$
a/Å	16.420(14)
b/Å	13.581(11)
c/Å	32.38(3)
α/°	90
β/°	92.96(3)
γ/°	90
*V*olume/Å^3	7210(10)
Z	4
ρ_{calc}g/cm^3	1.421
μ/mm^{-1}	0.464
F(000)	3156.0
Crystal size/mm^3	0.26 × 0.24 × 0.2
Radiation	MoKα (λ = 0.71073)
2Θ range for data collection/°	2.726 to 54.852
Index ranges	$-20 \leq h \leq 21$, $-14 \leq k \leq 16$, $-41 \leq l \leq 41$
Reflections collected	55200
Independent reflections	15592 [R_{int} = 0.1310, R_{sigma} = 0.2414]
Data/restraints/parameters	15592/0/919
Goodness-of-fit on F^2	0.882
Final *R* indexes [$I > 2\sigma(I)$]	R_1 = 0.0853, wR_2 = 0.2148
Final *R* indexes [all data]	R_1 = 0.2592, wR_2 = 0.2908
Largest diff. peak/hole / e Å^{-3}	0.97/-0.73
CCDC number	1451123

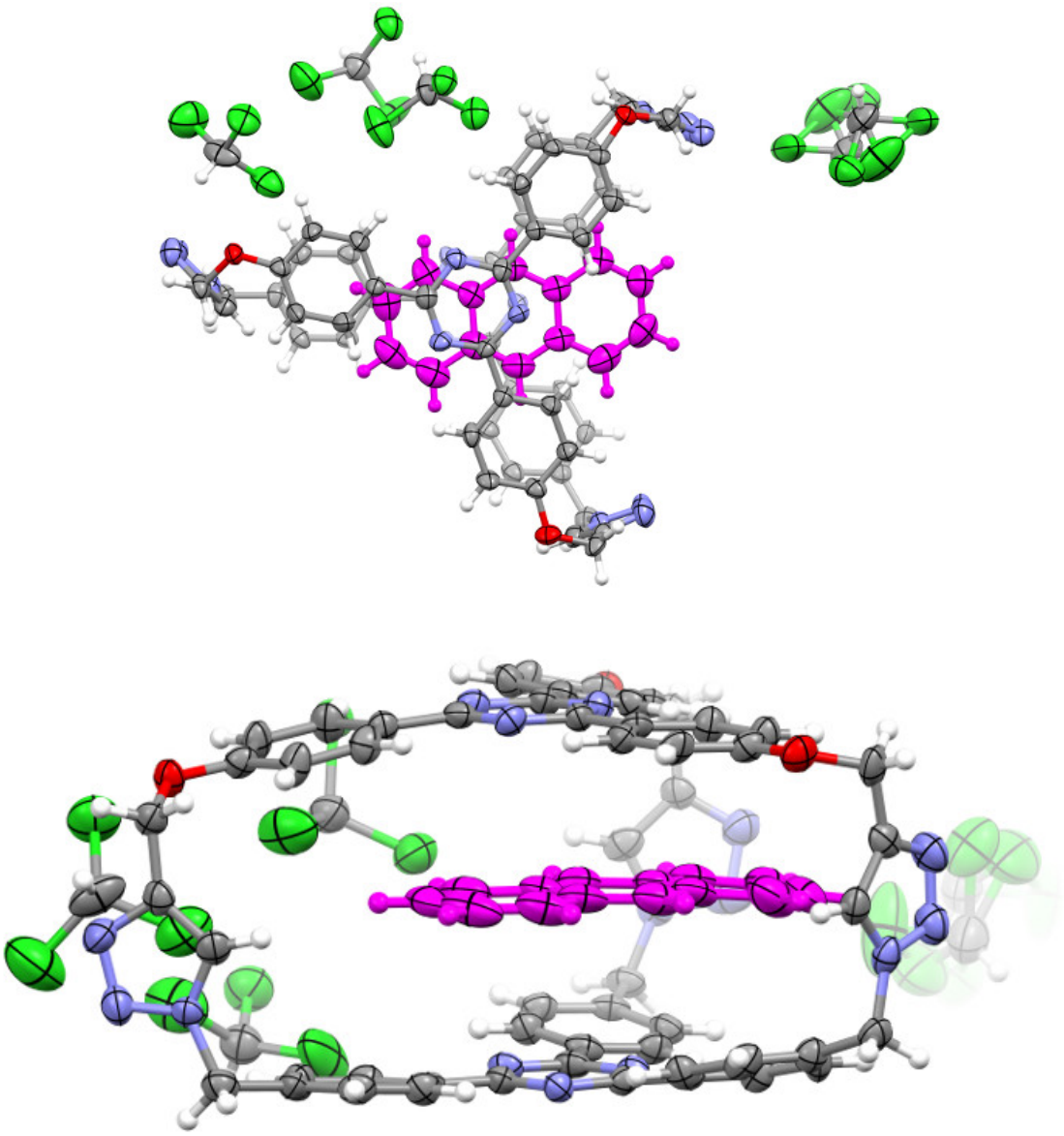

Figure S46. Top and side views of the asymmetric unit in anthracene(**3**) ⊂ **1**.$(CHCl_3)_{3.5}$ Thermal ellipsoids are shown in 50% probability level. One of the chloroform molecules was disordered and treated with same distance SADI, similar *U*ij (SIMU) and rigid body restraints (RIGU).

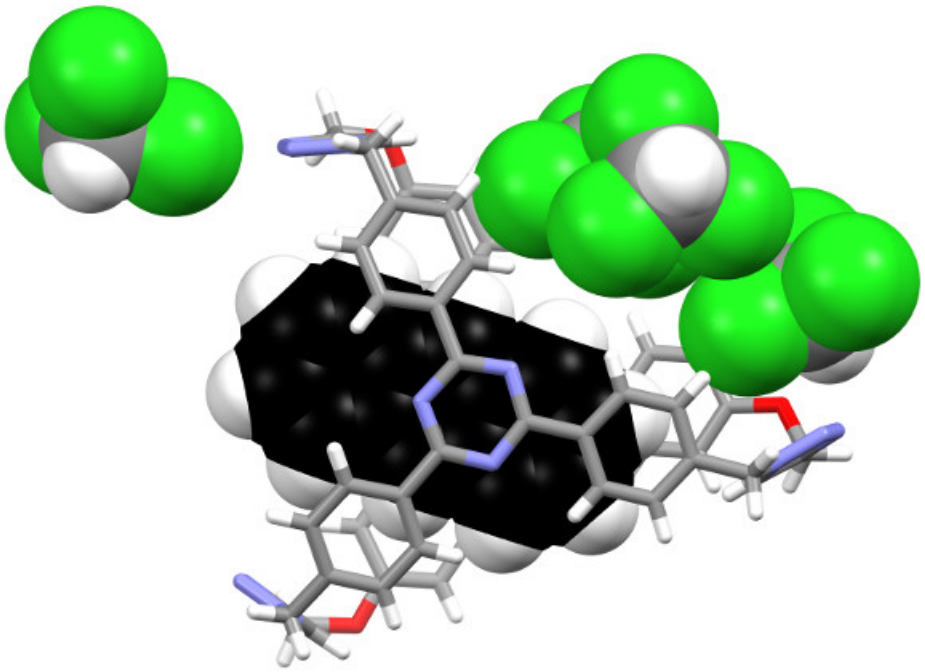

Figure S47. The asymmetric unit of anthracene(**3**) ⊂ **1**.$(CHCl_3)_{3.5}$ in which the guest and solvent molecules are shown in space filling mode. The shortest $d_{C\text{-}Cl\ldots C}$ is 4.1 Å

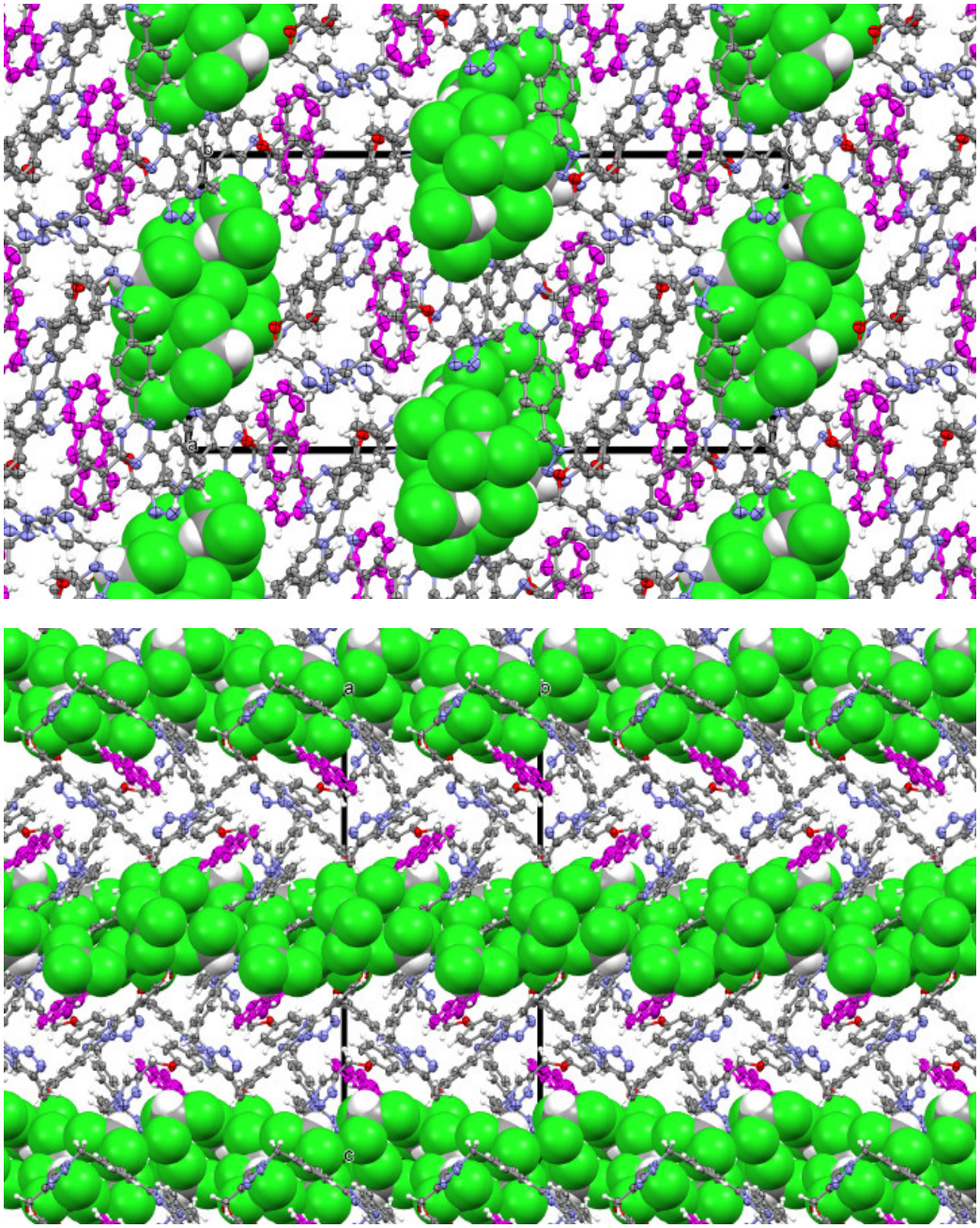

Figure S48. Crystal structure of anthracene ⊂ **1**.$(CHCl_3)_{3.5}$ viewed along *b*-axis in top and *a*-axis in the bottom. The solvent molecules are shown in the space filling mode.

Table **S5**

Identification code	Phenanthrene (**4**) ⊂**1**($C_2H_4Cl_2$)$_3$
Empirical formula	$C_{74}H_{61}Cl_6N_{15}O_3$
Formula weight	1421.07
Temperature/K	293.15
Crystal system	monoclinic
Space group	$P2_1/n$
a/Å	16.154(4)
b/Å	13.571(3)
c/Å	31.638(6)
α/°	90
β/°	90.061(14)
γ/°	90
Volume/Å^3	6936(3)
Z	4
ρ_{calc}g/cm^3	1.361
μ/mm^{-1}	0.308
F(000)	2944.0
Crystal size/mm^3	0.29 × 0.21 × 0.16
Radiation	MoKα (λ = 0.71073)
2Θ range for data collection/°	2.574 to 50.572
Index ranges	-18 ≤ h ≤ 19, -15 ≤ k ≤ 15, -37 ≤ l ≤ 37
Reflections collected	67978
Independent reflections	12141 [R_{int} = 0.0965, R_{sigma} = 0.1788]
Data/restraints/parameters	12141/509/986
Goodness-of-fit on F^2	1.041
Final *R* indexes [*I*>=2σ (*I*)]	R_1 = 0.1040, wR_2 = 0.2792
Final *R* indexes [all data]	R_1 = 0.2291, wR_2 = 0.3517
Largest diff. peak/hole / e Å^{-3}	1.05/-0.46
CCDC number	1478700

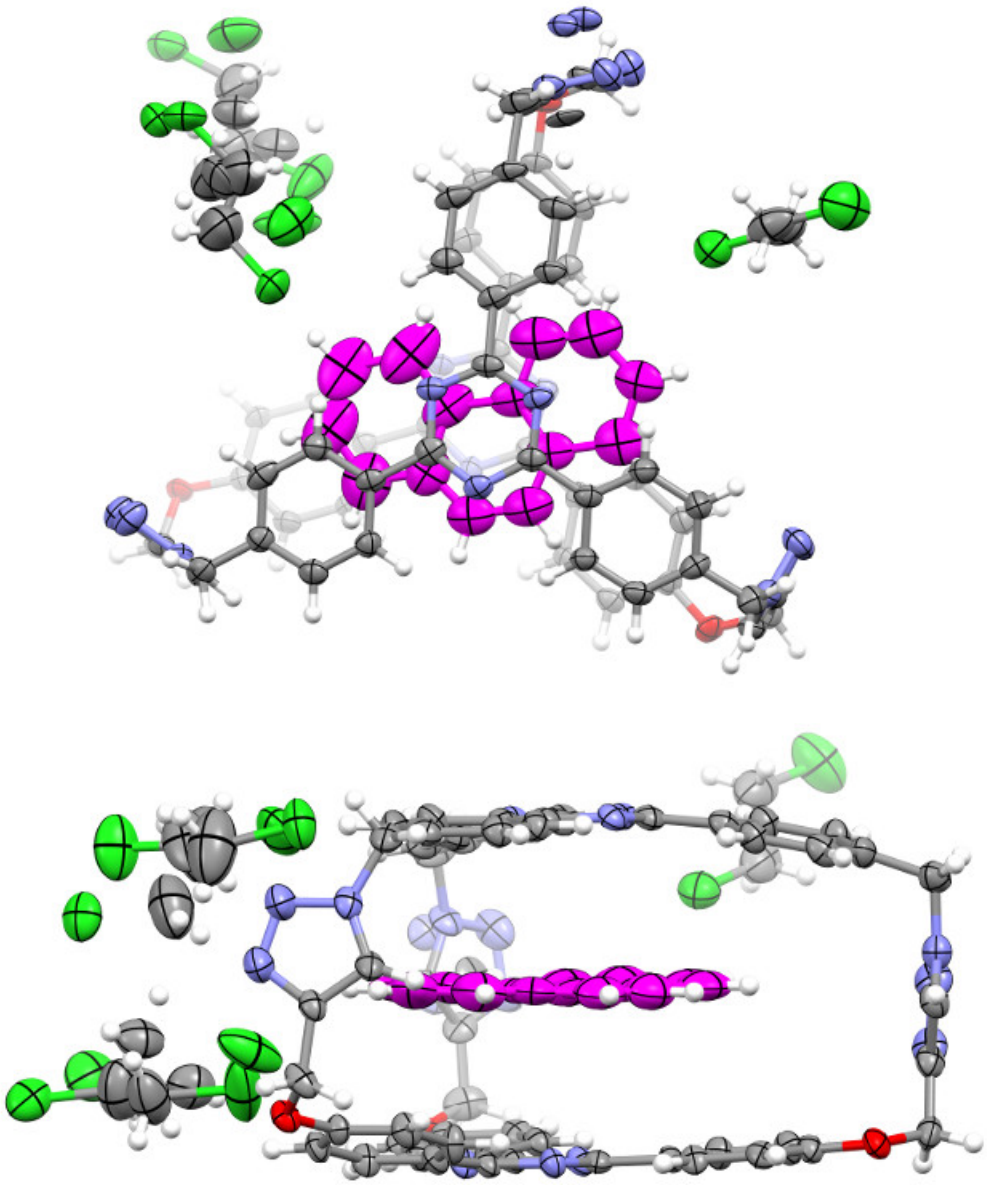

Figure S49. Top and side views of the asymmetric unit in phenanthrene(**4**) ⊂ **1**($C_2H_4Cl_2$)$_3$. Thermal ellipsoids are shown in 50% probability level. Two of the dichloroethane solvent molecules were disordered and treated with same distance (SADI), similar *U*ij (SIMU) and rigid body (RIGU) restraints.

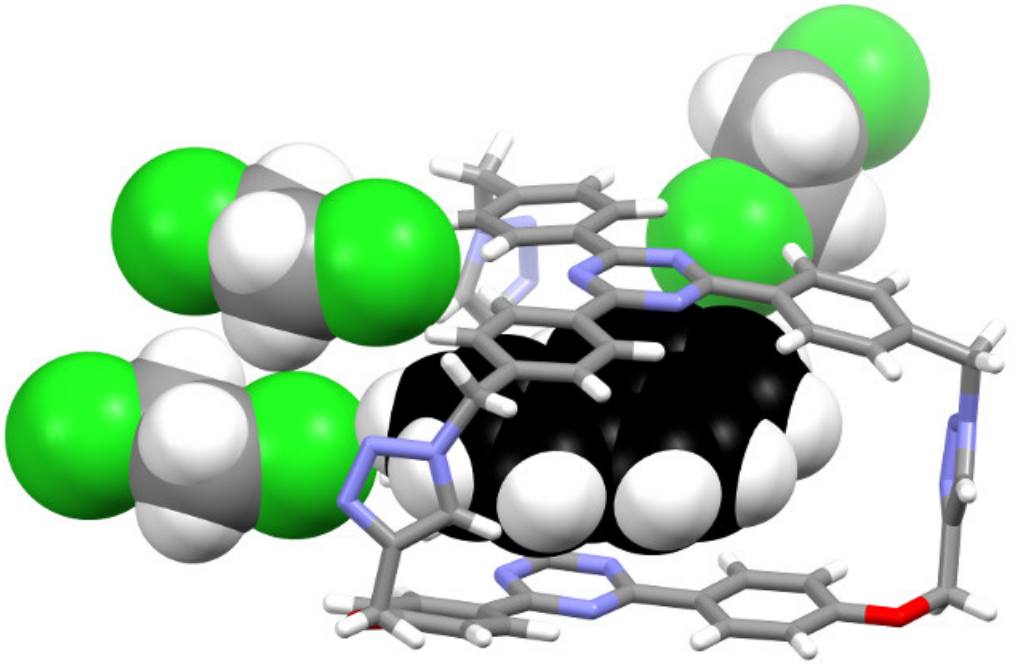

Figure S50. The asymmetric unit of phenanthrene(**4**) ⊂ **1**($C_2H_4Cl_2$)$_3$ in which the guest and solvent molecules are shown in space filling mode. The shortest $d_{C\text{-}Cl\ldots C}$ are 3.7 and 3.9 Å

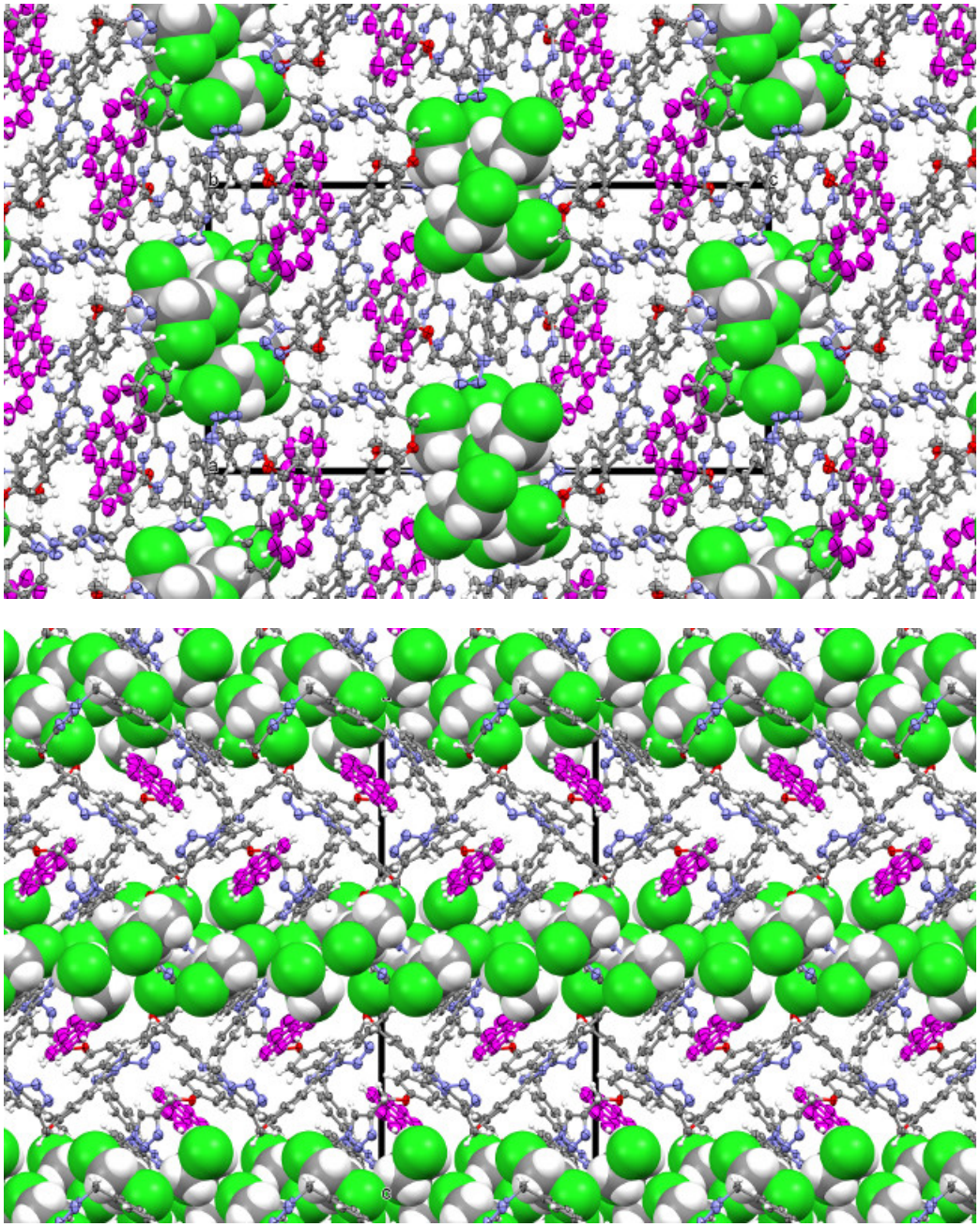

Figure S51. Crystal structure of phenanthrene(**4**) ⊂ **1**$(C_2H_4Cl_2)_3$ viewed along *b*-axis in top and *a*-axis in the bottom. The solvent molecules are shown in the space filling mode.

Table S6

Identification code	Pyrene(**5**) ⊂ **1**. $(CHCl_3)_3$
Empirical formula	$C_{73}H_{52}Cl_9N_{15}O_3$
Formula weight	1506.73
Temperature/K	100
Crystal system	monoclinic
Space group	$P2_1/n$
a/Å	16.133(5)
b/Å	13.761(4)
c/Å	32.115(9)
α/°	90
β/°	92.117(18)
γ/°	90
Volume/Å^3	7125(4)
Z	4
ρ_{calc}g/cm^3	1.405
μ/mm^{-1}	0.414
F(000)	3089.0
Crystal size/mm^3	0.26 × 0.24 × 0.2
Radiation	MoKα (λ = 0.71073)
2Θ range for data collection/°	2.538 to 50.192
Index ranges	$-18 \leq h \leq 19$, $-16 \leq k \leq 16$, $-37 \leq l \leq 37$
Reflections collected	127040
Independent reflections	12583 [R_{int} = 0.1152, R_{sigma} = 0.0884]
Data/restraints/parameters	12583/1438/1187
Goodness-of-fit on F^2	1.038
Final *R* indexes [I>=2σ (I)]	R_1 = 0.1047, wR_2 = 0.2882
Final *R* indexes [all data]	R_1 = 0.1792, wR_2 = 0.3751
Largest diff. peak/hole / e Å^{-3}	0.86/-0.57
CCDC number	1451125

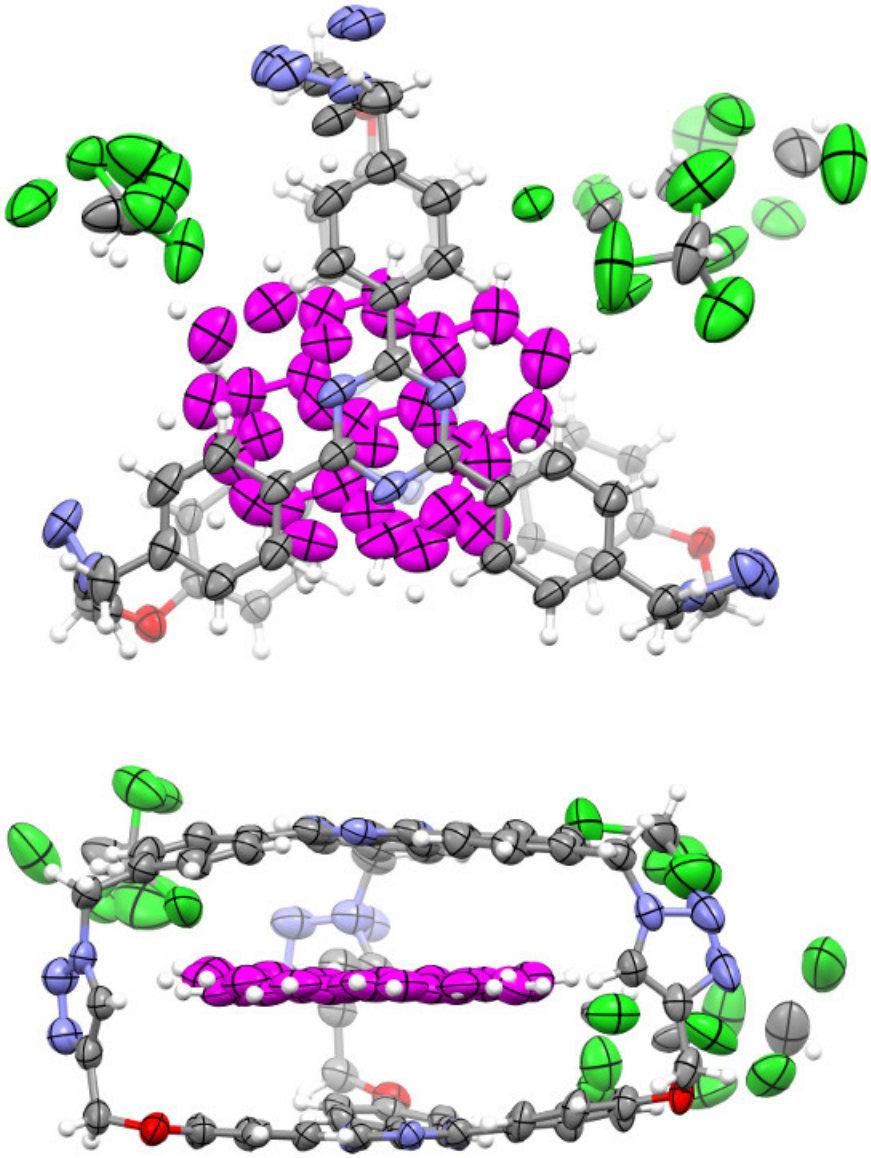

Figure S52. Top and side views of the asymmetric unit in pyrene(**5**) ⊂ **1**.$(CHCl_3)_3$. Thermal ellipsoids are shown in 50% probability level. One of the triazole rings in **1** is disordered over two orientations and treated with similar distance (SADI), similar *U*ij (SIMU) and rigid body (RIGU) restraints. The pyrene molecule is also disordered over two orientations in same plane and refined with the above restraints. The chloroform molecules are also disordered and were treated similarly. One of the chloroform molecule is disordered over three positions and refined with SUMP to obtain single molecule.

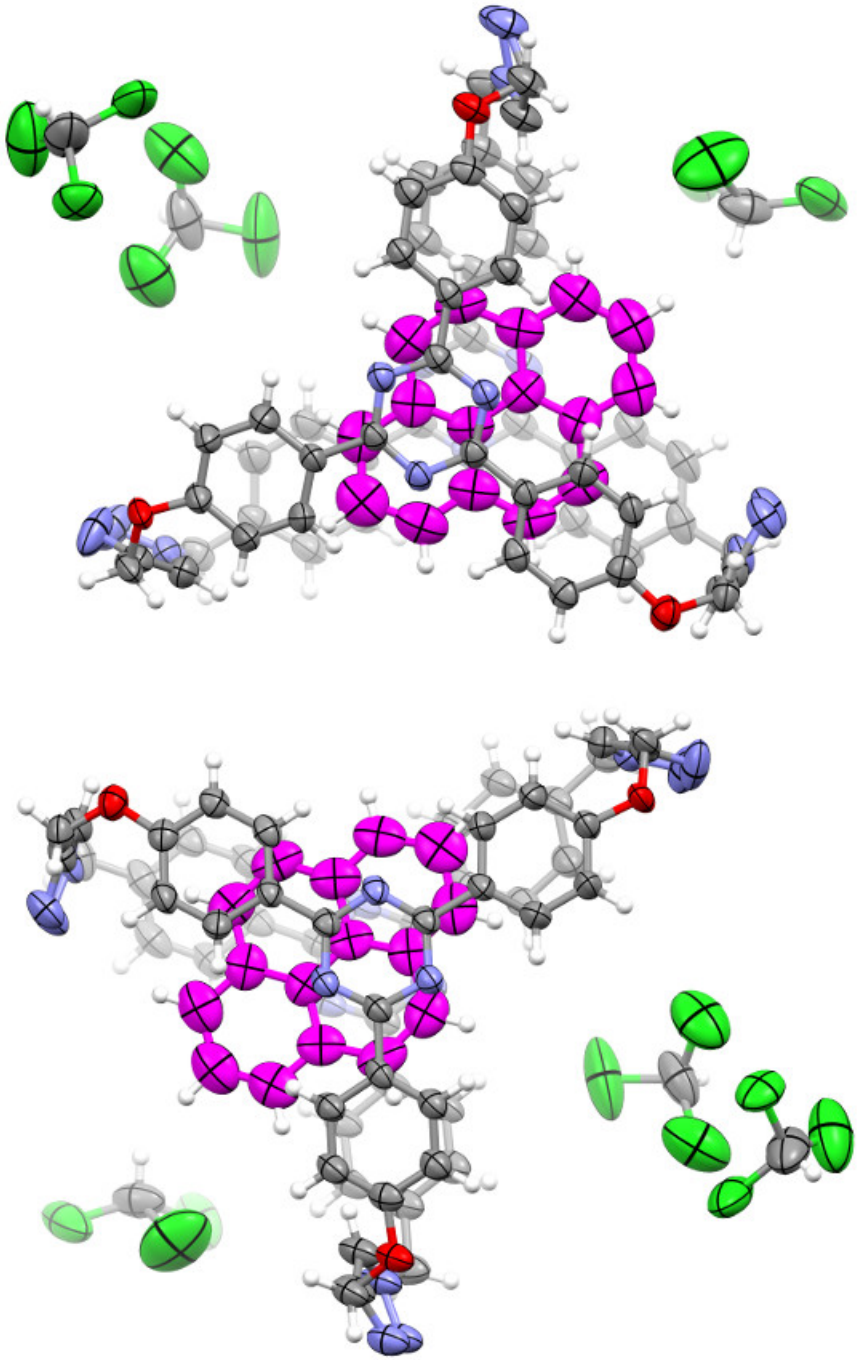

Figure S53. The disordered pyrene molecules of pyrene(**5**) ⊂ **1**.$(CHCl_3)_3$ are shown in two separate models for clarity.

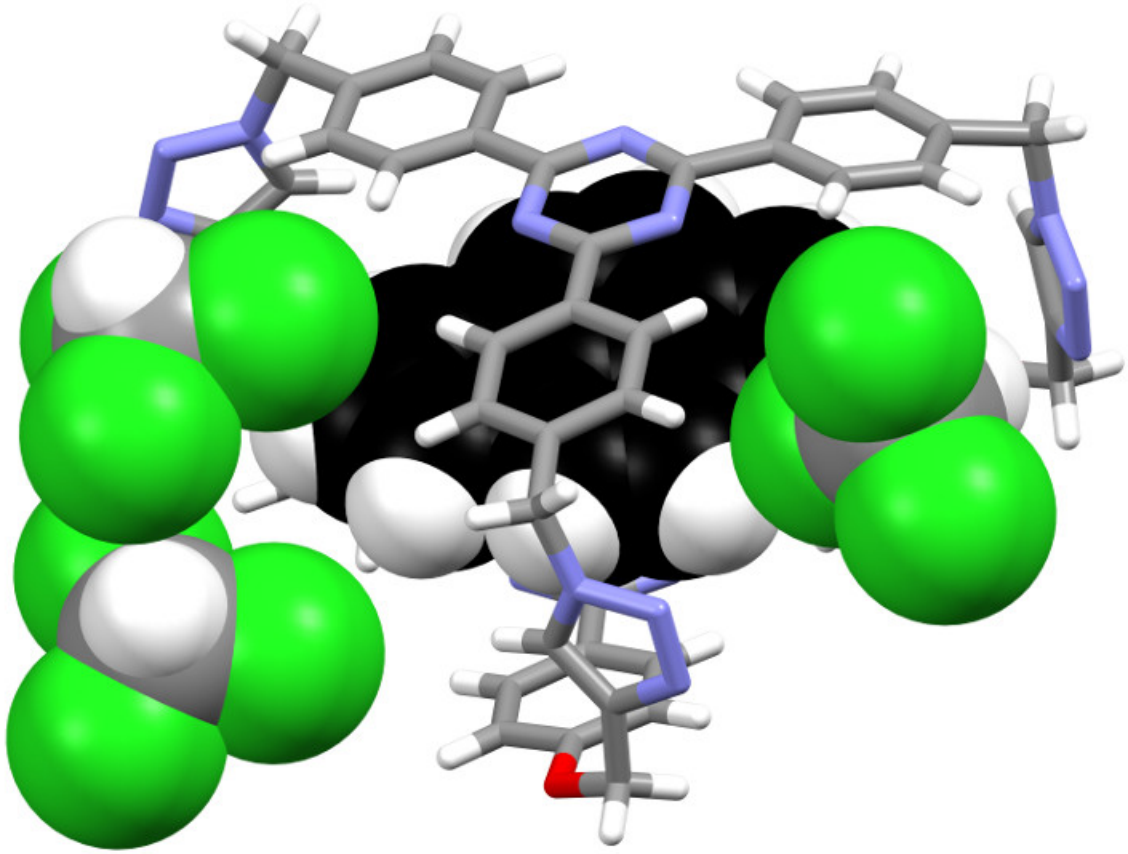

Figure S54. The asymmetric unit of pyrene(**5**) ⊂ **1**.$(CHCl_3)_3$ in which the guest and solvent molecules are shown in space filling mode. The shortest $d_{C\text{-}Cl\ldots C}$ is 3.8 Å

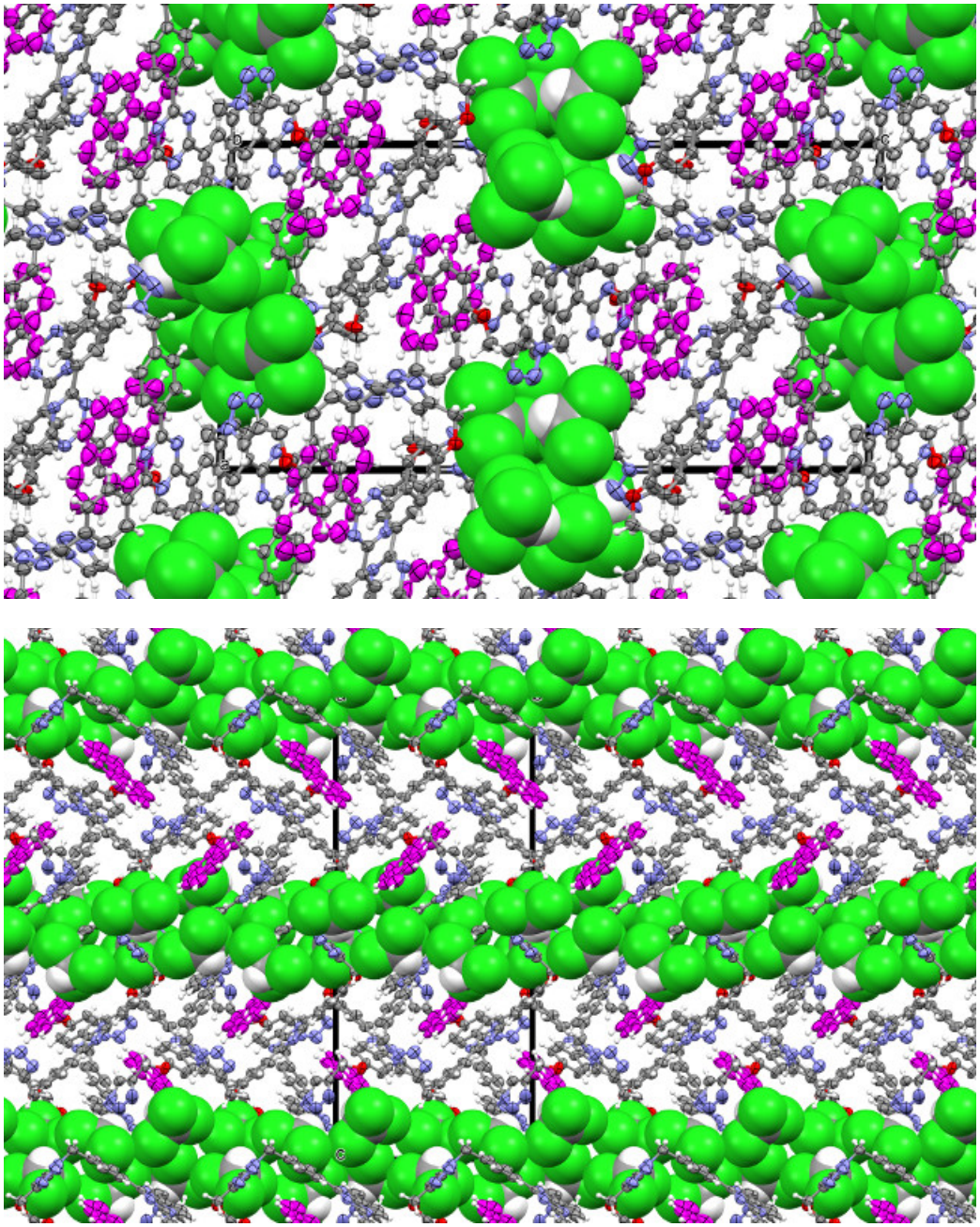

Figure S55. Crystal structure of pyrene ⊂ **1**.$(CHCl_3)_3$ viewed along *b*-axis in top and *a*-axis in the bottom. The solvent molecules are shown in the space filling mode.

Table S7

Identification code	Triphenylene(**6**) ⊂ **1**.$(CHCl_3)_3$
Empirical formula	$C_{75}H_{54}Cl_9N_{15}O_3$
Formula weight	1532.38
Temperature/K	100
Crystal system	monoclinic
Space group	$P2_1/n$
a/Å	16.056(2)
b/Å	13.8514(17)
c/Å	32.082(4)
α/°	90
β/°	91.878(7)
γ/°	90
*V*olume/Å^3	7131.1(16)
Z	4
ρ_{calc}g/cm^3	1.427
μ/mm^{-1}	0.415
F(000)	3144.0
Crystal size/mm^3	0.34 × 0.32 × 0.3
Radiation	MoKα (λ = 0.71073)
2Θ range for data collection/°	2.8 to 54.564
Index ranges	$-20 \le h \le 20$, $-17 \le k \le 15$, $-40 \le l \le 40$
Reflections collected	71481
Independent reflections	15592 [R_{int} = 0.1207, R_{sigma} = 0.1334]
Data/restraints/parameters	15592/1099/1058
Goodness-of-fit on F^2	1.075
Final *R* indexes [$I > 2\sigma(I)$]	R_1 = 0.0980, wR_2 = 0.2734
Final *R* indexes [all data]	R_1 = 0.1930, wR_2 = 0.3441
Largest diff. peak/hole / e Å^{-3}	1.65/-0.54
CCDC number	1451124

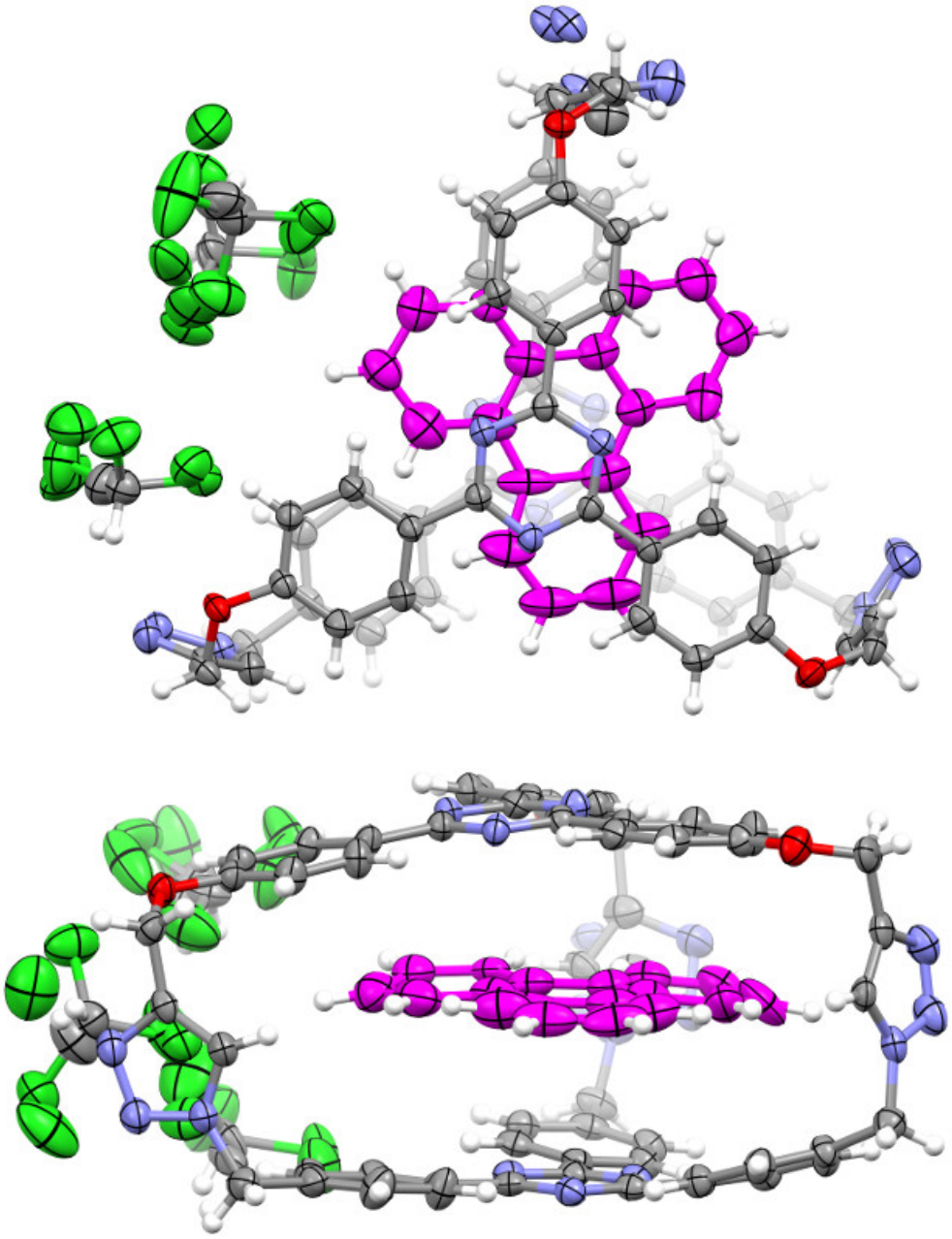

Figure S56. Top and side views of the asymmetric unit in triphenylene(**6**) ⊂ **1**.$(CHCl_3)_3$. Thermal ellipsoids are shown in 50% probability level. One of the triazole rings is disordered over two orientations and treated with similar distance (SADI), similar *U*ij (SIMU) and rigid body (RIGU) restraints. The chloroform molecules are disordered and were treated similarly.

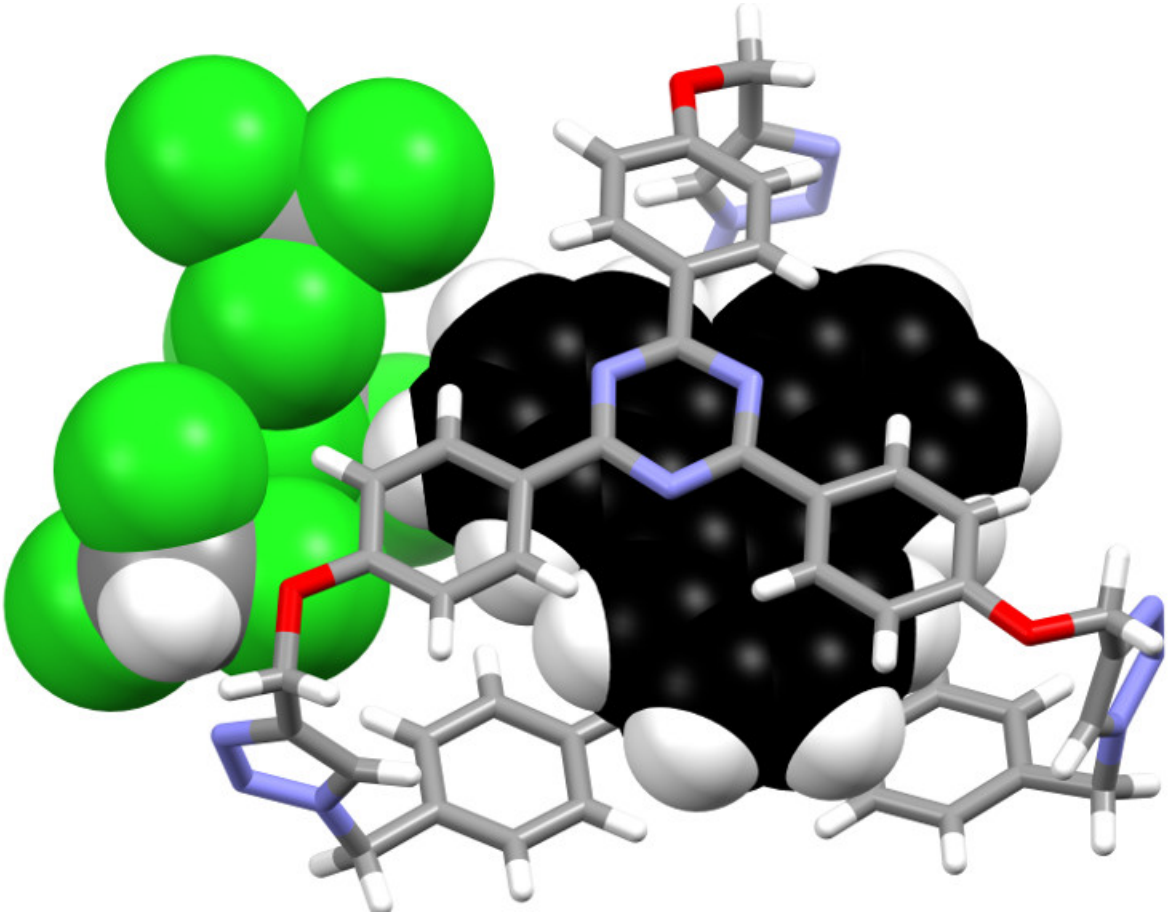

Figure S57. The asymmetric unit of triphenylene(**6**) ⊂ **1**.$(CHCl_3)_3$ in which the guest and solvent molecules are shown in space filling mode. The shortest $d_{C\text{-}Cl\ldots C}$ is 4.0 Å

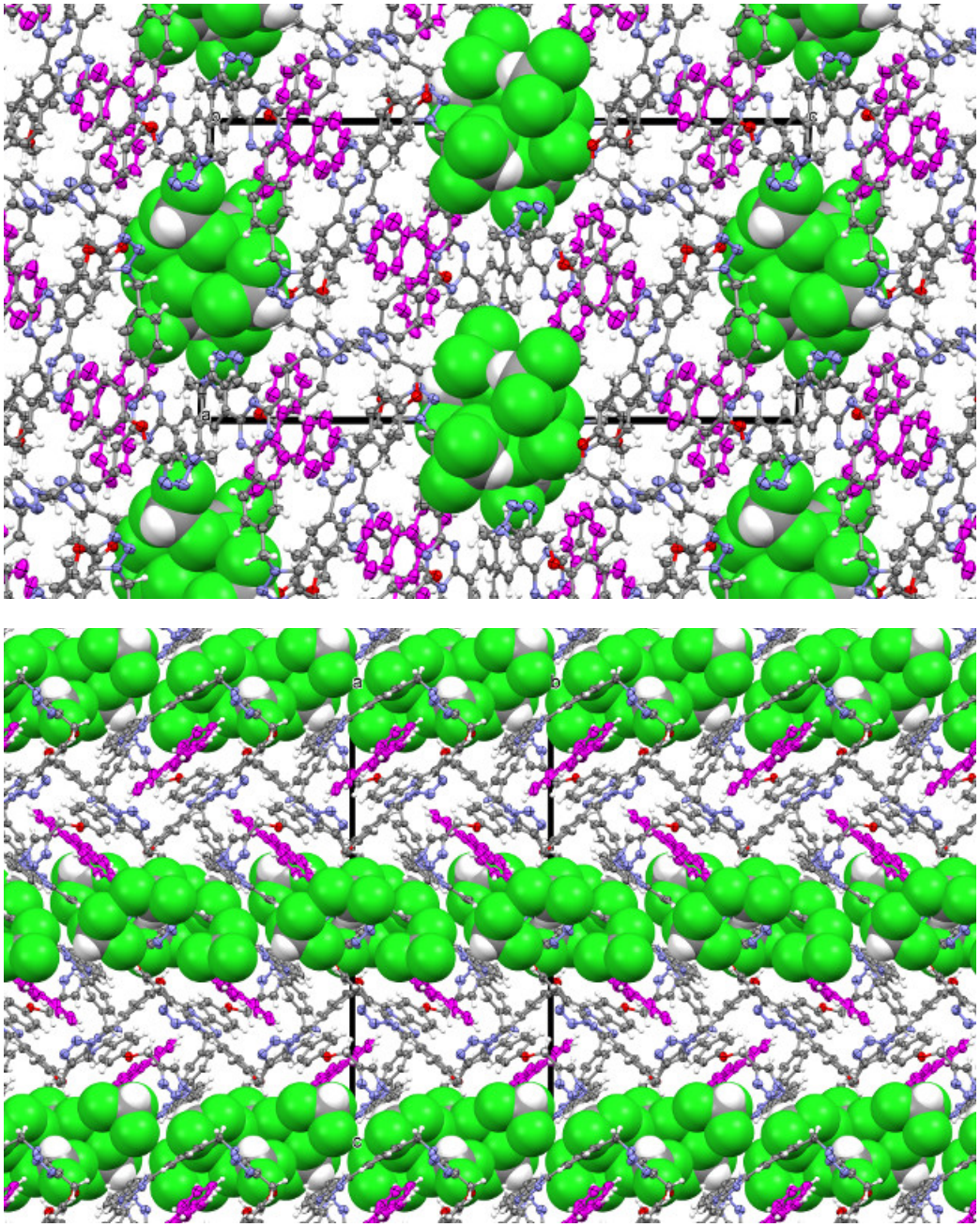

Figure S58. Crystal structure of triphenylene(**6**) ⊂ **1**.$(CHCl_3)_3$ viewed along *b*-axis in top and *a*-axis in the bottom. The solvent molecules are shown in the space filling mode.

Table S8

Identification code	Benz(*a*)anthracene(**7**) ⊂ **1**. C2H4Cl2
Empirical formula	$C_{74}H_{55}Cl_2N_{15}O_3$
Formula weight	1273.23
Temperature/K	293.15
Crystal system	monoclinic
Space group	$P2_1/c$
a/Å	21.861(3)
b/Å	15.4737(18)
c/Å	18.600(2)
α/°	90
β/°	98.075(7)
γ/°	90
Volume/Å^3	6229.4(13)
Z	4
ρ_{calc}g/cm^3	1.358
μ/mm^{-1}	0.169
F(000)	2648.0
Crystal size/mm^3	0.32 × 0.22 × 0.18
Radiation	MoKα (λ = 0.71073)
2Θ range for data collection/°	3.236 to 50.408
Index ranges	-26 ≤ h ≤ 25, -18 ≤ k ≤ 16, -21 ≤ l ≤ 22
Reflections collected	63306
Independent reflections	11018 [R_{int} = 0.1223, R_{sigma} = 0.1610]
Data/restraints/parameters	11018/0/847
Goodness-of-fit on F^2	1.042
Final *R* indexes [*I*>=2σ (*I*)]	R_1 = 0.0756, wR_2 = 0.1847
Final *R* indexes [all data]	R_1 = 0.1604, wR_2 = 0.2258
Largest diff. peak/hole / e Å^{-3}	0.70/-0.71
CCDC number	1478698

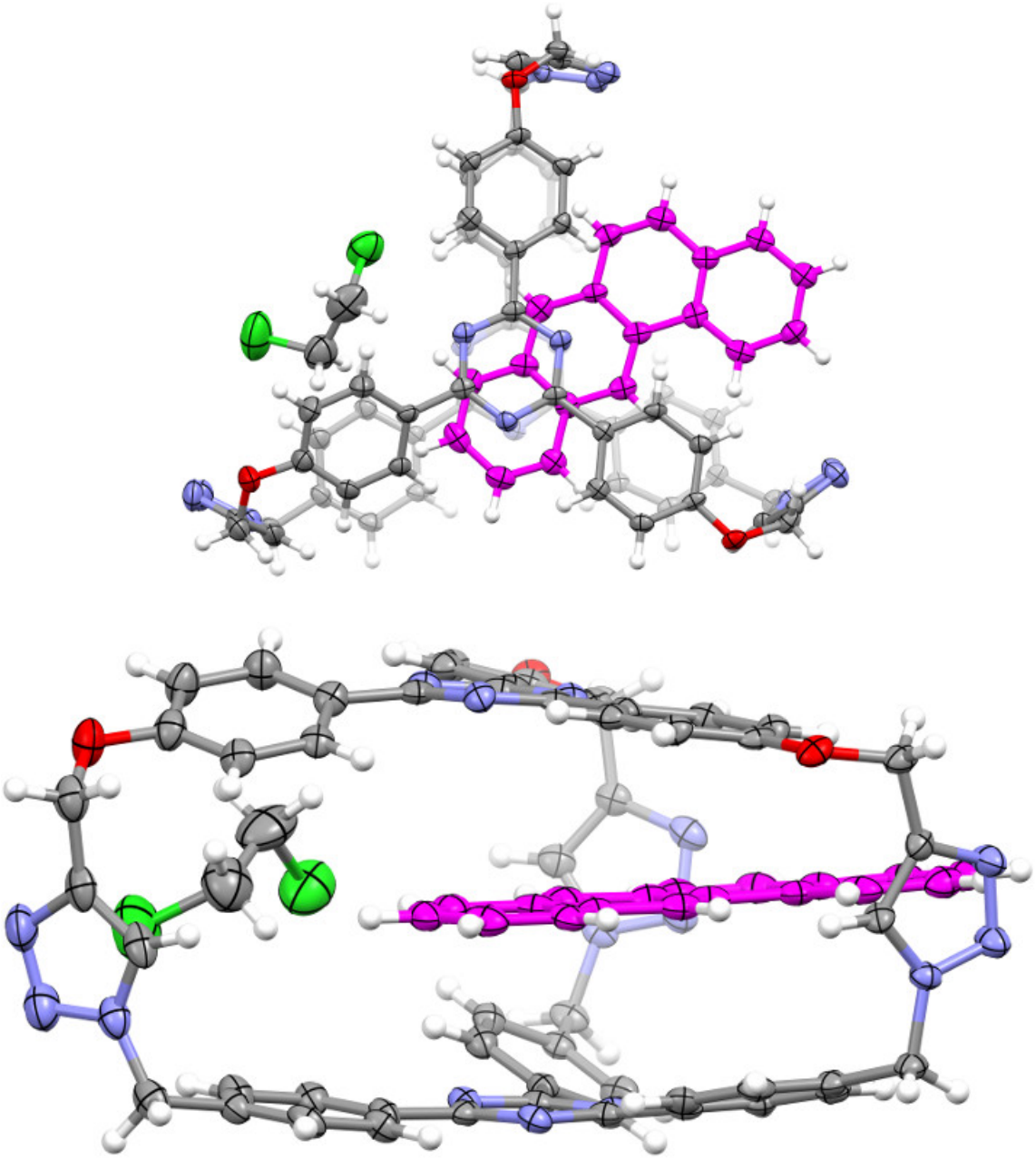

Figure S59. Top and side views of the asymmetric unit in benz(*a*)anthracene(**8**) ⊂ **1**.$C_2H_4Cl_2$. Thermal ellipsoids are shown in 50% probability level.

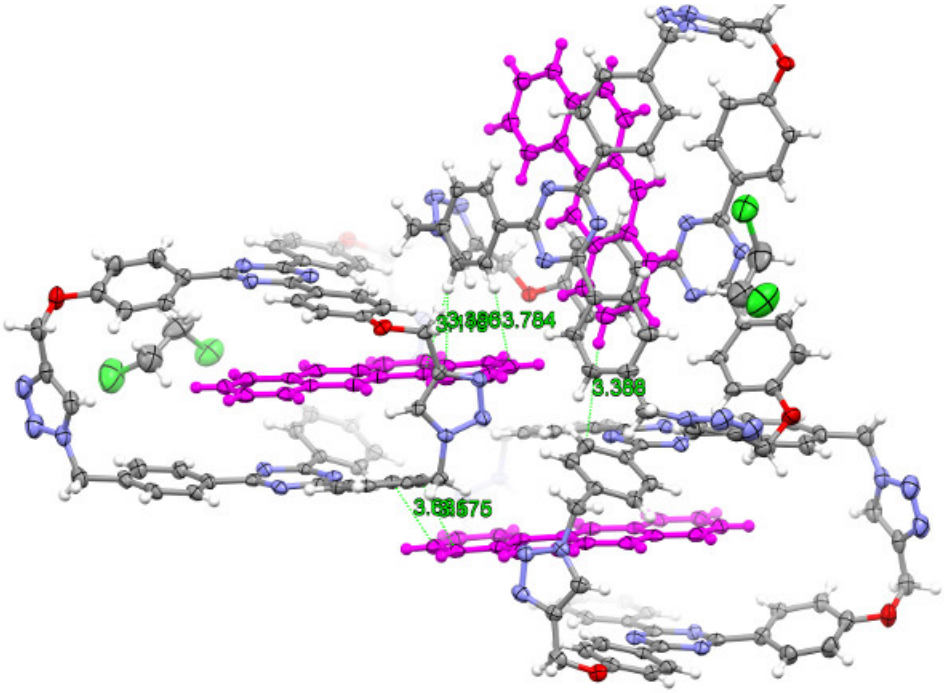

Figure S60. The figure illustrating significant C-H…π contacts between the host and guest in benz(*a*)anthracene(**8**) ⊂ **1**.$C_2H_4Cl_2$

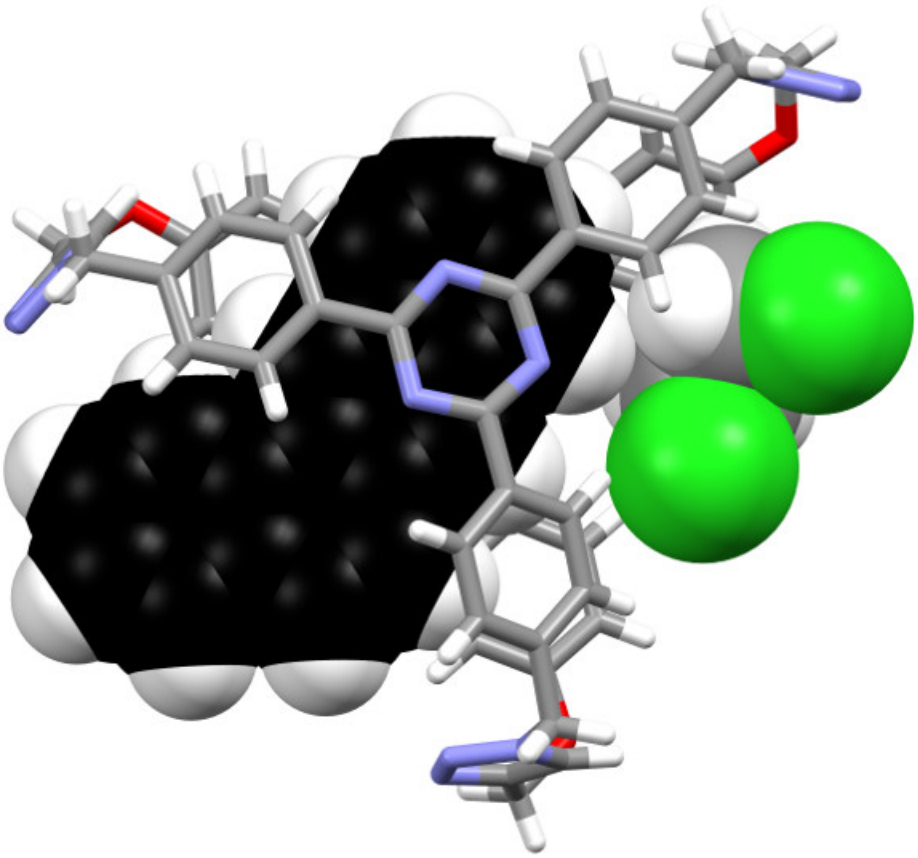

Figure S61. The asymmetric unit of benz(*a*)anthracene(**8**) ⊂ **1**.$C_2H_4Cl_2$ in which the guest and solvent molecules are shown in space filling mode. The shortest $d_{C\text{-}Cl\ldots C}$ is 4.1 Å

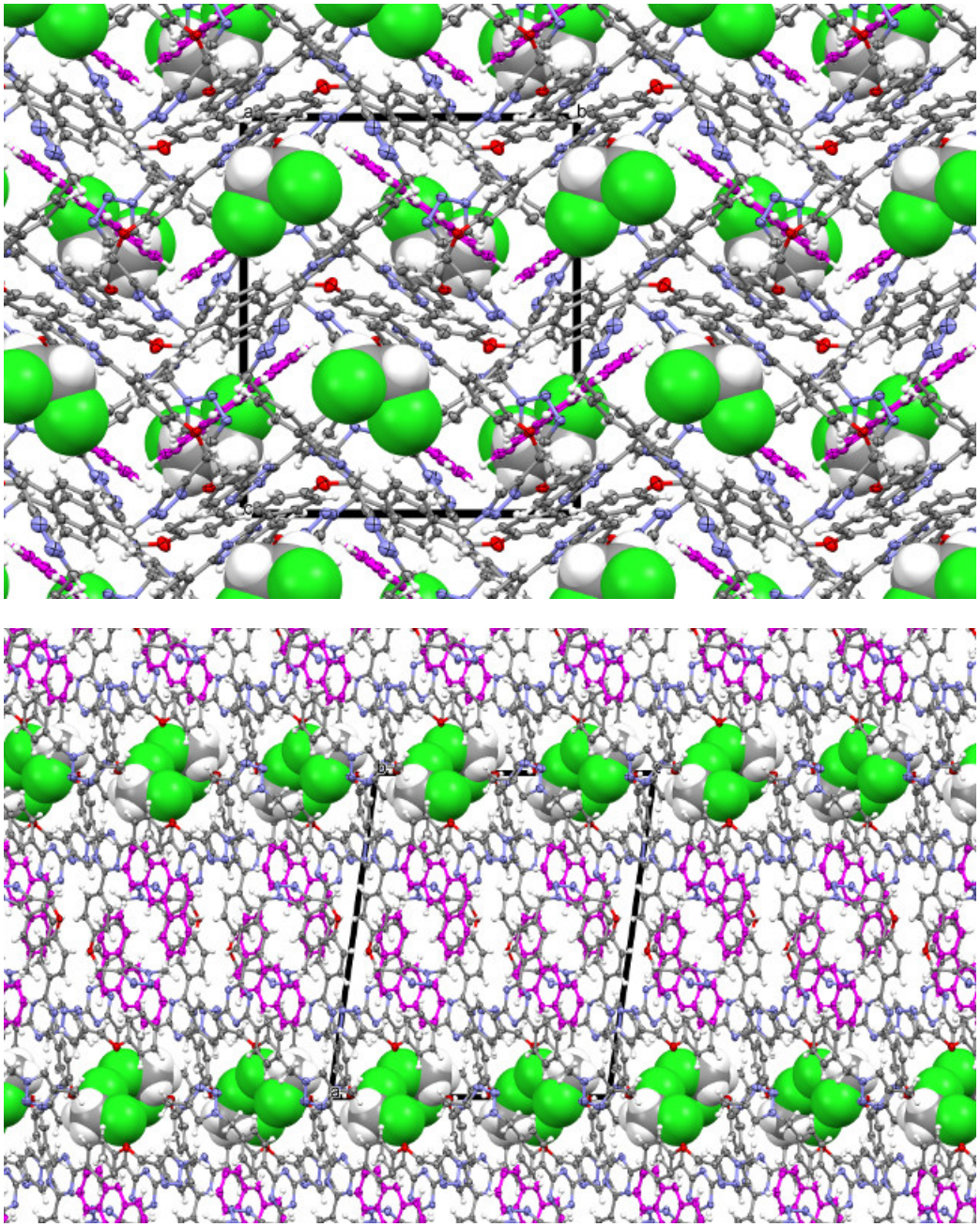

Figure S62. The crystal structure of benz(*a*)anthracene(**8**) ⊂ **1**.$C_2H_4Cl_2$ viewed along *a*-axis in top and *b*-axis in bottom. The solvent molecules are shown in space filling mode to highlight that they occupy isolated voids, rather than continuous channel.

Table S9

Identification code	{benzo(*a*)phenanthrene(**8**)}$_2$ ⊂ (**1**)$_2$.($C_2H_4Cl_2$)$_7$
Empirical formula	$C_{76}H_{59}Cl_4N_{15}O_3$
Formula weight	1372.18
Temperature/K	293.15
Crystal system	monoclinic
Space group	$P2_1/n$
a/Å	17.7889(16)
b/Å	21.013(2)
c/Å	37.032(3)
α/°	90
β/°	102.091(5)
γ/°	90
Volume/Å^3	13535(2)
Z	8
ρ_{calc}g/cm^3	1.347
μ/mm^{-1}	0.237
F(000)	5696.0
Crystal size/mm^3	0.24 × 0.21 × 0.18
Radiation	MoKα (λ = 0.71073)
2Θ range for data collection/°	2.24 to 54.942
Index ranges	$-23 \leq h \leq 23$, $-27 \leq k \leq 27$, $-47 \leq l \leq 47$
Reflections collected	181530
Independent reflections	30814 [R_{int} = 0.0886, R_{sigma} = 0.0707]
Data/restraints/parameters	30814/707/1738
Goodness-of-fit on F^2	1.012
Final R indexes [I>=2σ (I)]	R_1 = 0.1274, wR_2 = 0.3329
Final R indexes [all data]	R_1 = 0.1978, wR_2 = 0.3887
Largest diff. peak/hole / e Å^{-3}	1.72/-1.36

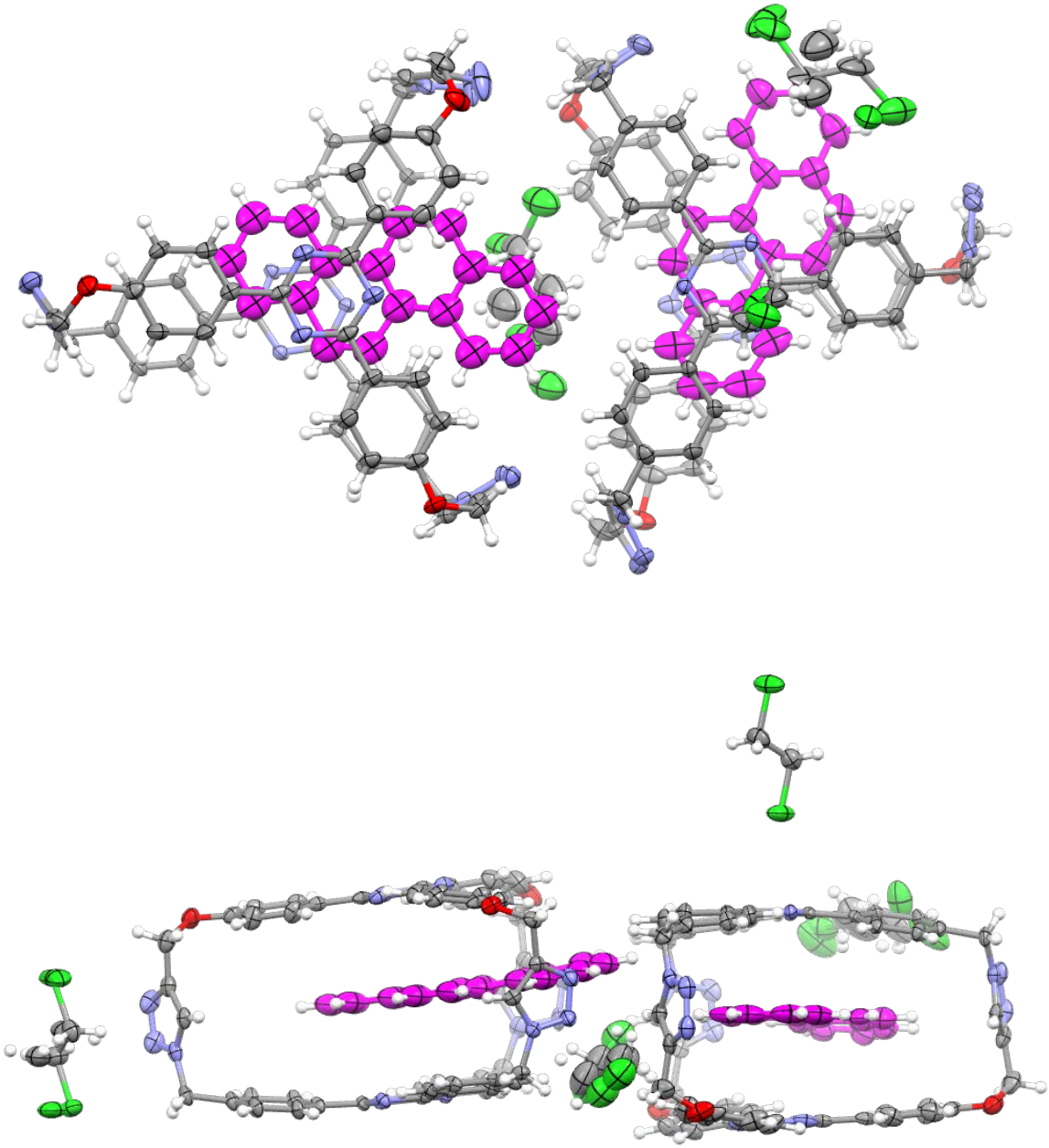

Figure S63. Top and side views of the asymmetric unit in {benzo(*a*)phenanthrene(**8**)}$_2$ ⊂ (**1**)$_2$.($C_2H_4Cl_2$)$_7$. Thermal ellipsoids are shown in 50% probability level. One of the benzo(a)phenanthrene was refined with EADP constraint and the DFIX 1.38 for C-C bond lengths. The dichloroethane solvent molecules are disordered over two positions and treated with similar distance (SADI), similar *U*ij (SIMU) and rigid body (RIGU) restraints. One of them was constrained with EADP.

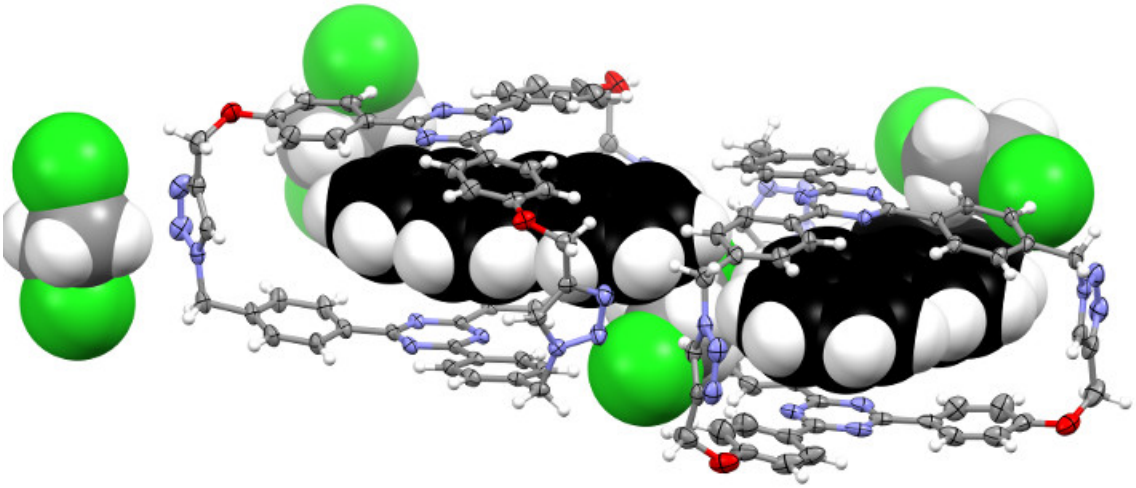

Figure S64. The asymmetric unit of {benzo(*a*)phenanthrene(**8**)}$_2$ ⊂ (**1**)$_2$.($C_2H_4Cl_2$)$_7$ in which the guest and solvent molecules are shown in space filling mode. The shortest $d_{C\text{-}Cl\ldots C}$ is 4.0 Å.

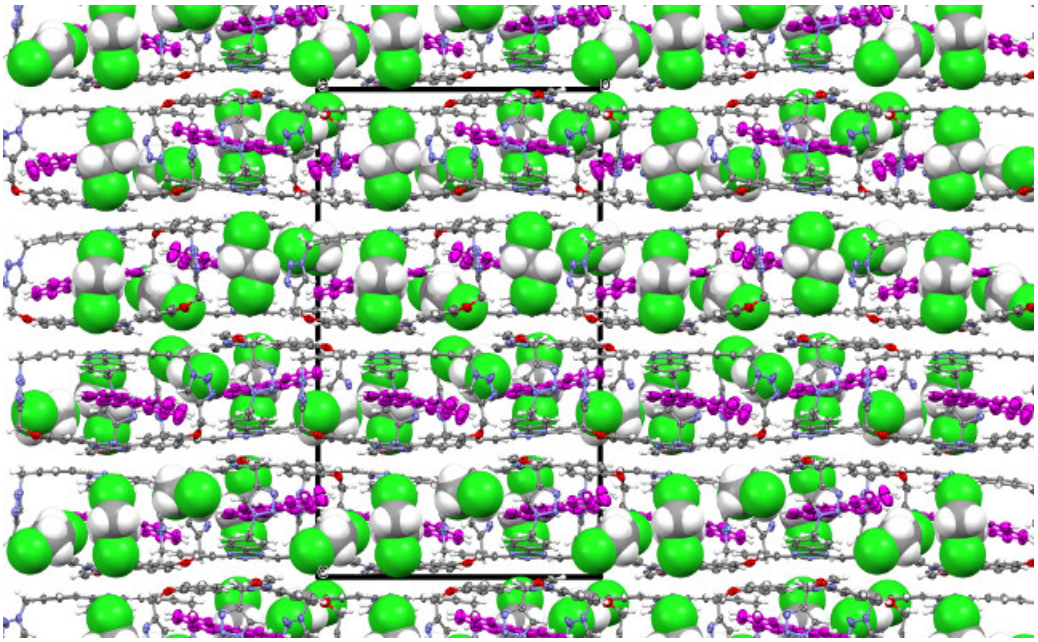

Figure S65. The crystal structure of {benzo(*a*)phenanthrene(**8**)}$_2$ ⊂ (**1**)$_2$.($C_2H_4Cl_2$)$_7$.

Table S10

Identification code	benzo(*a*)pyrene(**9**) ⊂ **1**.$(C_2H_4Cl_2)_3$
Empirical formula	$C_{80}H_{63}Cl_6N_{15}O_3$
Formula weight	1495.15
Temperature/K	100
Crystal system	monoclinic
Space group	$P2_1/n$
a/Å	16.1736(17)
b/Å	13.7072(16)
c/Å	31.887(3)
α/°	90
β/°	92.389(6)
γ/°	90
*V*olume/Å^3	7063.1(13)
Z	4
ρ_{calc}g/cm^3	1.406
μ/mm^{-1}	0.307
F(000)	3096.0
Crystal size/mm^3	0.26 × 0.24 × 0.18
Radiation	MoKα (λ = 0.71073)
2Θ range for data collection/°	2.556 to 50.332
Index ranges	-19 ≤ h ≤ 19, -15 ≤ k ≤ 15, -37 ≤ l ≤ 34
Reflections collected	69263
Independent reflections	12050 [R_{int} = 0.1512, R_{sigma} = 0.2526]
Data/restraints/parameters	12050/2105/1257
Goodness-of-fit on F^2	1.025
Final *R* indexes [$I > 2\sigma(I)$]	R_1 = 0.1179, wR_2 = 0.2958
Final *R* indexes [all data]	R_1 = 0.3066, wR_2 = 0.4008
Largest diff. peak/hole / e Å^{-3}	0.80/-0.54
CCDC number	1451127

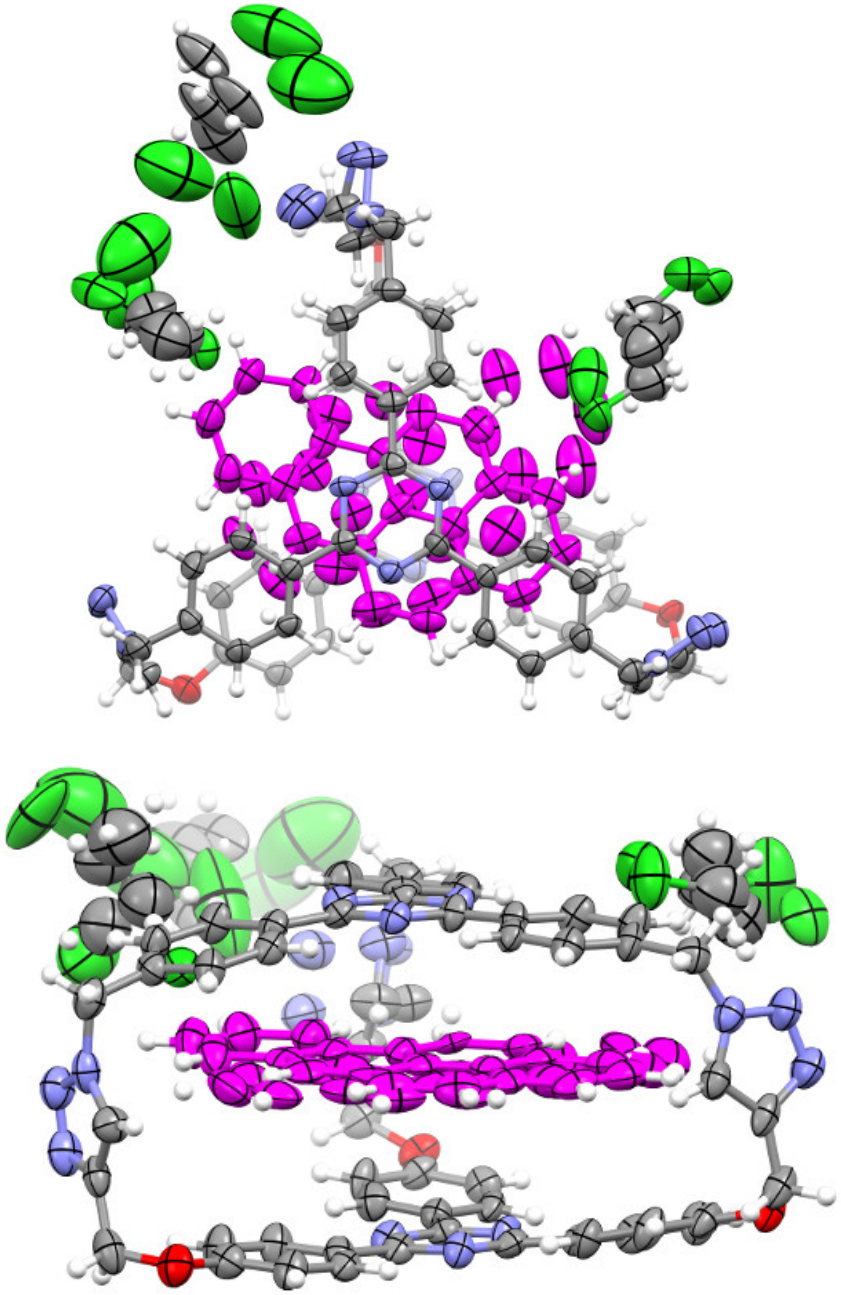

Figure S66. Top and side views of the asymmetric unit in benzo(*a*)pyrene(**9**) ⊂ **1**.$(C_2H_4Cl_2)_3$. Thermal ellipsoids are shown in 50% probability level. The benzo(a)pyrene molecules are disordered over two positions and refined with same distance (SADI), similar Uij (SIMU) and rigid body (RIGU) restraints. The dichloroethane solvent molecules are also disordered over two positions and refined in a similar manner.

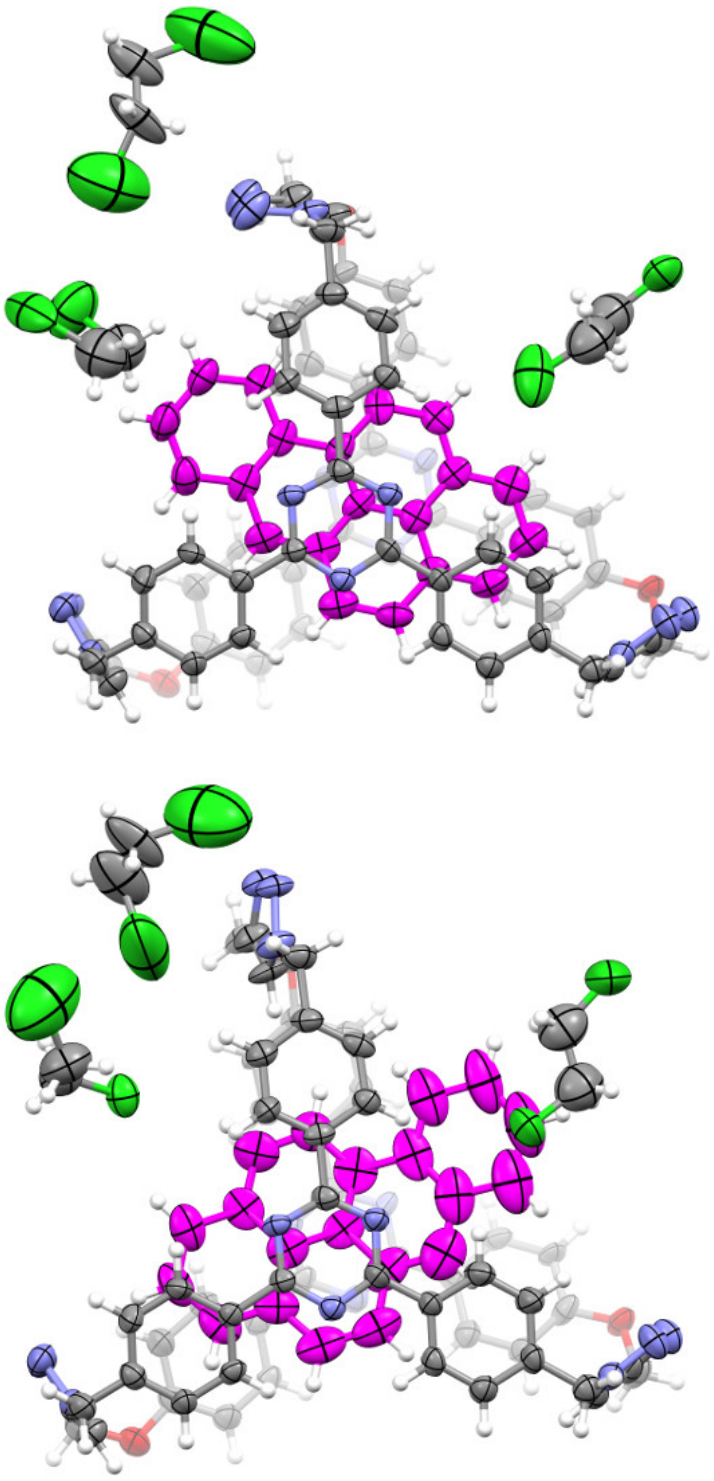

Figure S67. The disordered benzo(*a*)pyrene molecules of benzo(*a*)pyrene(**9**) ⊂ **1**.$(C_2H_4Cl_2)_3$are shown in two separate models for clarity.

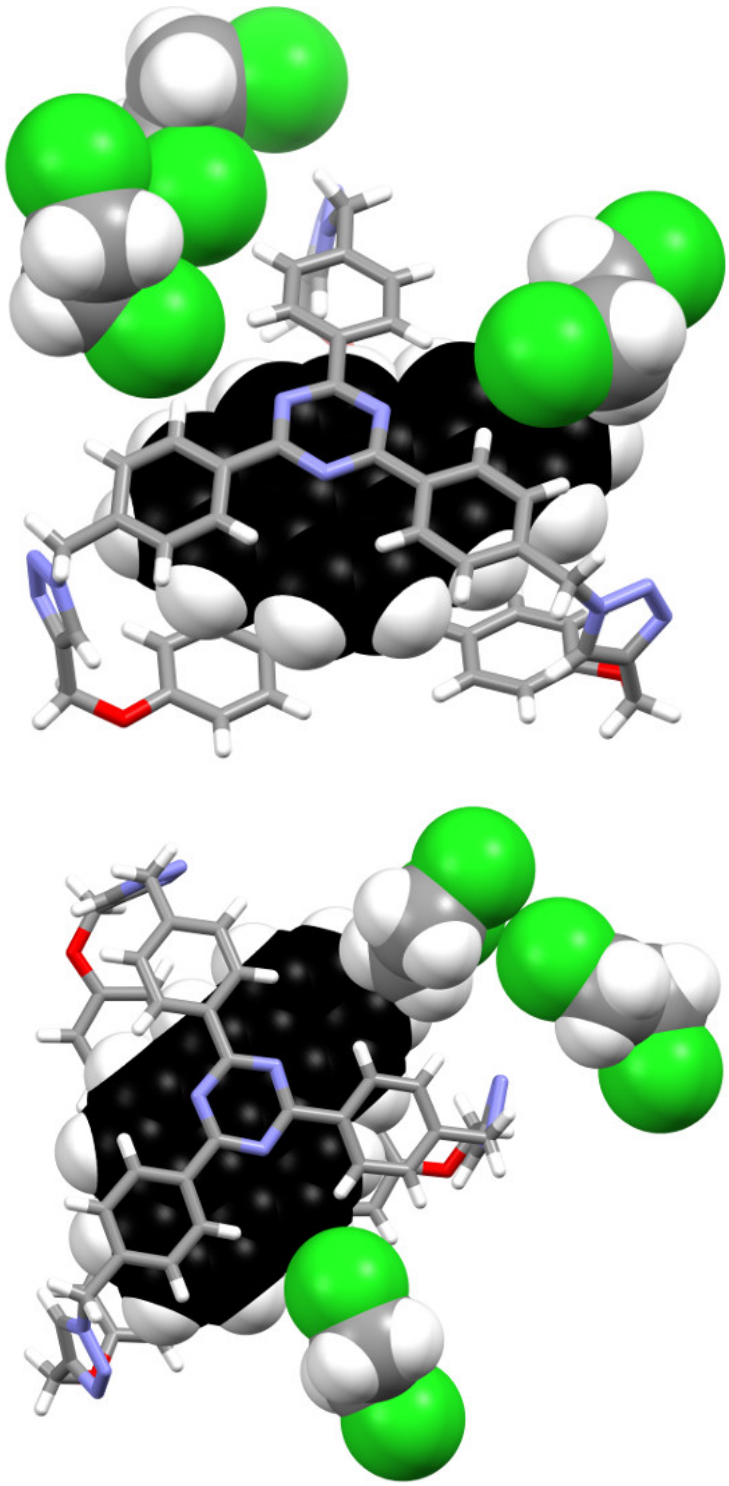

Figure S68. The asymmetric unit of benzo(*a*)pyrene(**9**) ⊂ **1**.$(C_2H_4Cl_2)_3$ in two different models, according to the disorder, in which the guest and solvent molecules are shown in space filling mode to illustrate the close contacts between them. The shortest $d_{C\text{-}Cl\ldots C}$ is 4.0 Å.

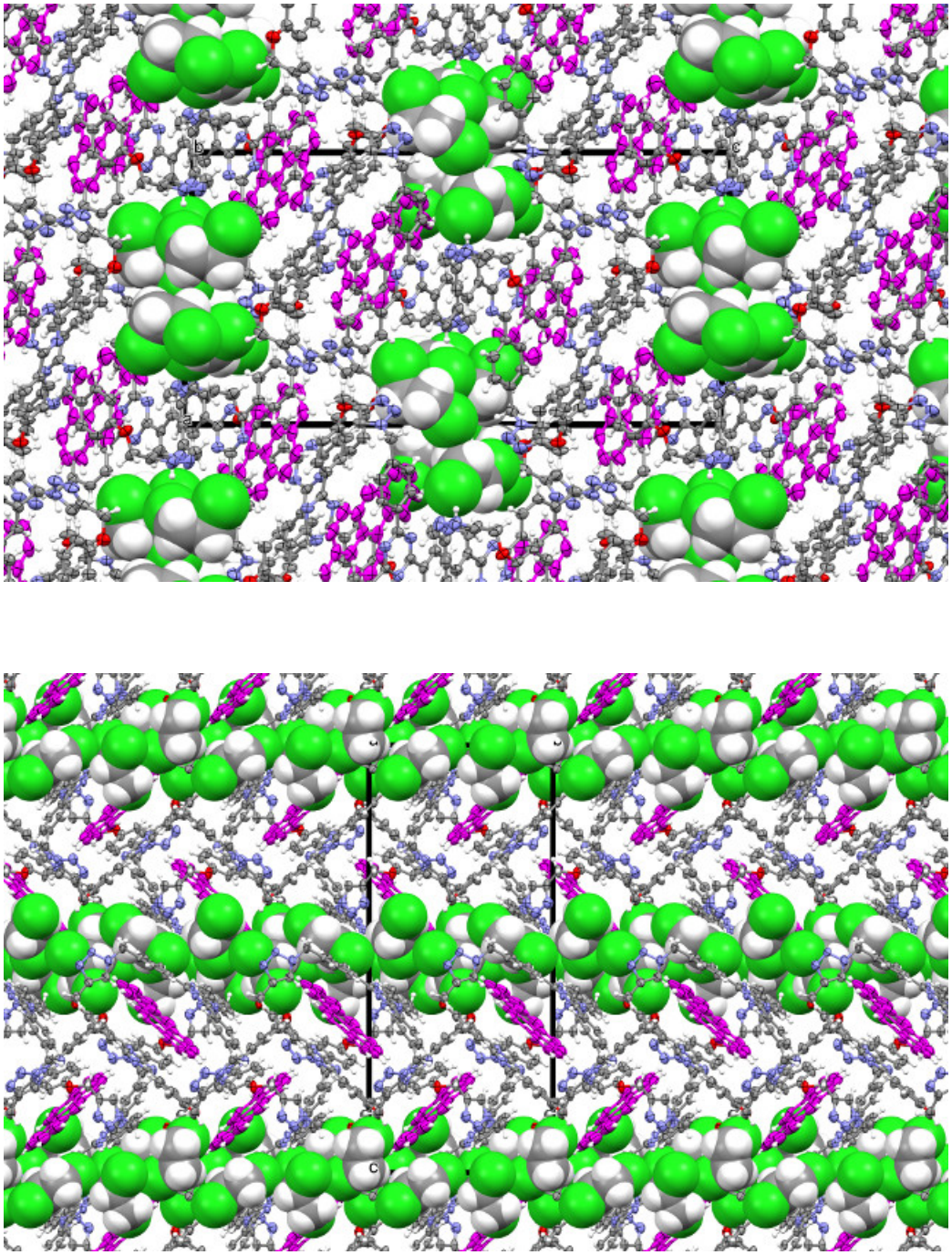

Figure S69. Crystal structure of benzo(*a*)pyrene(**9**) ⊂ **1**. 3($C_2H_4Cl_2$) viewed along *b*-axis in top and *a*-axis in the bottom. The solvent molecules are shown in the space filling mode.

Table S11

Identification code	Perylene(**10**) ⊂ **1**.$(C_2H_4Cl_2)_3$
Empirical formula	$C_{80}H_{63}Cl_6N_{15}O_3$
Formula weight	1495.15
Temperature/K	100
Crystal system	monoclinic
Space group	$P2_1/n$
a/Å	16.2180(16)
b/Å	13.8125(12)
c/Å	31.653(3)
α/°	90
β/°	92.288(6)
γ/°	90
*V*olume/Å^3	7085.0(11)
Z	4
ρ_{calc}g/cm^3	1.402
μ/mm^{-1}	0.306
F(000)	3096.0
Crystal size/mm^3	0.32 × 0.3 × 0.3
Radiation	MoKα (λ = 0.71073)
2Θ range for data collection/°	3.874 to 50.314
Index ranges	-19 ≤ h ≤ 19, -16 ≤ k ≤ 16, -37 ≤ l ≤ 37
Reflections collected	92937
Independent reflections	12511 [R_{int} = 0.1069, R_{sigma} = 0.1212]
Data/restraints/parameters	12511/853/1077
Goodness-of-fit on F^2	1.194
Final *R* indexes [$I > 2\sigma(I)$]	R_1 = 0.1265, wR_2 = 0.3332
Final *R* indexes [all data]	R_1 = 0.2277, wR_2 = 0.3891
Largest diff. peak/hole / e Å^{-3}	1.41/-0.80
CCDC number	1451126

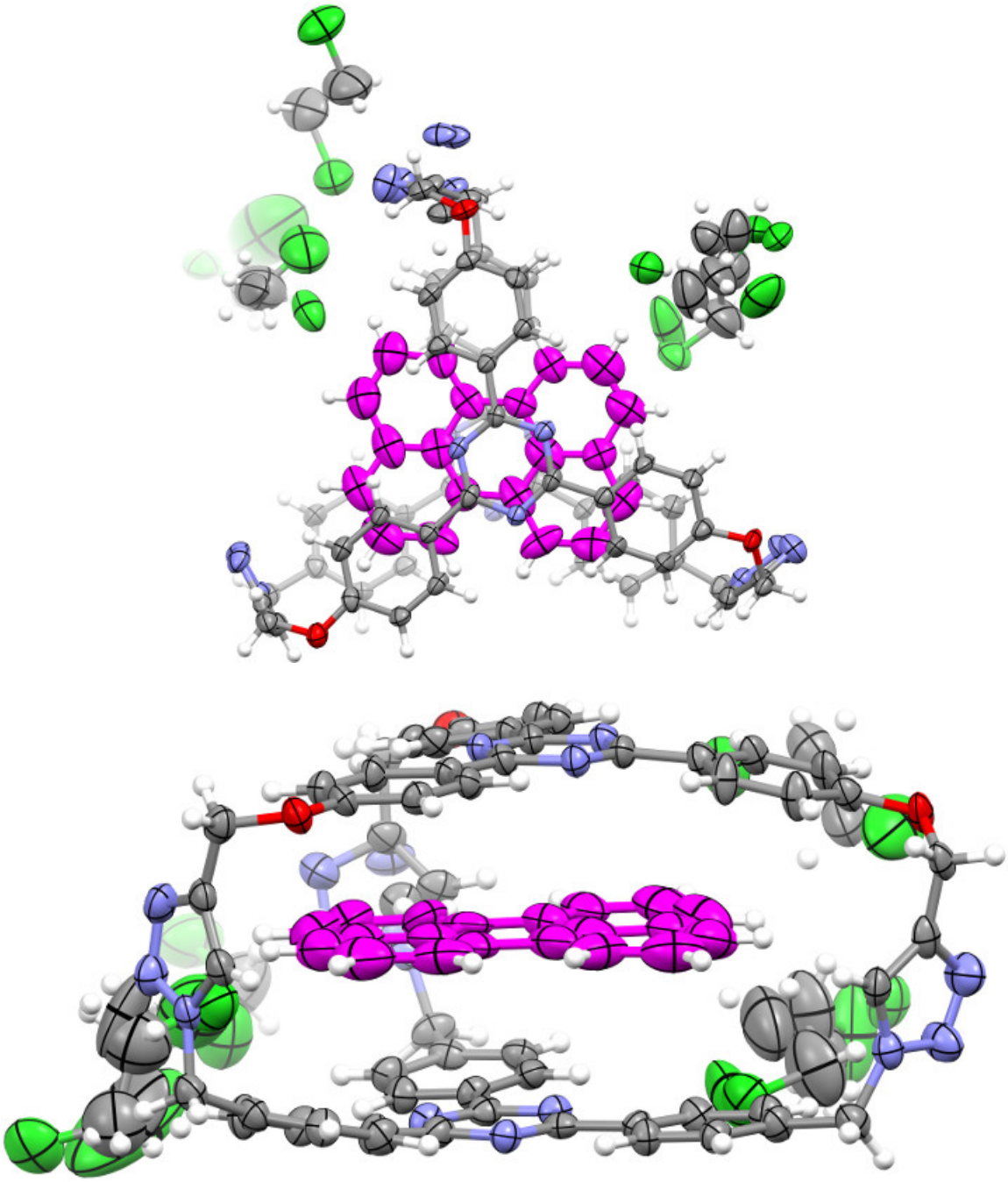

Figure S70. Top and side views of the asymmetric unit in perylene ⊂ **1**. 3($C_2H_4Cl_2$). Thermal ellipsoids are shown in 50% probability level. The dichloroethane molecules are disordered over two positions; thus refined with same distance (SADI), similar Uij (SIMU) and rigid body restraints (RIGU).

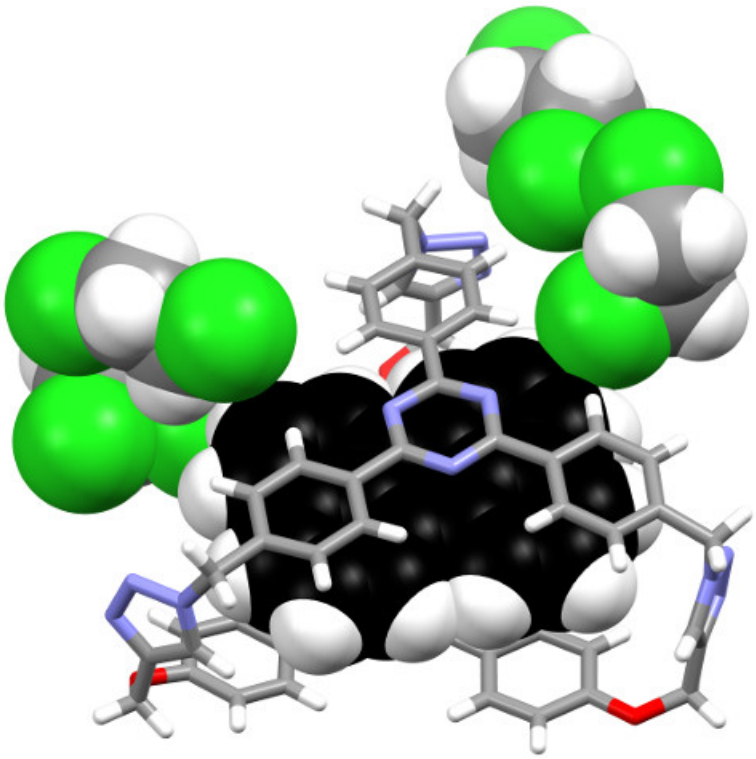

Figure S71. The figure illustrating the close contacts between $C_2H_4Cl_2$ and perylene molecules bound inside **1**. The shortest distance observed between chlorine and perylene ($d_{C\text{-}Cl\cdots C}$) is 3.2 Å.

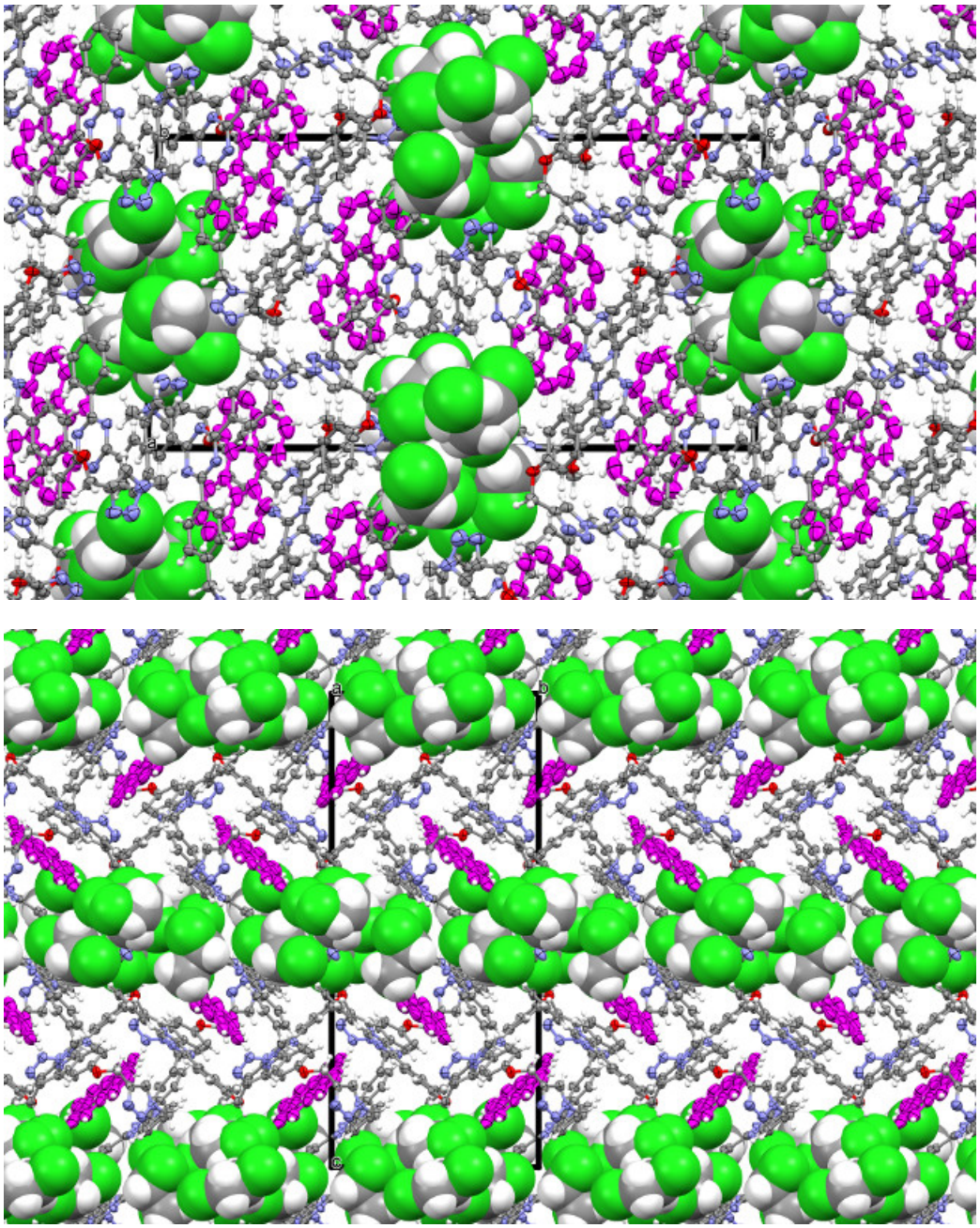

Figure S72. Crystal structure of perylene(**10**) ⊂ **1**.$(C_2H_4Cl_2)_3$ viewed along viewed along *b*-axis in top and *a*-axis in the bottom. The solvent molecules are shown in the space filling mode.

Table S12

Identification code	Benzo(*ghi*)perylene(**11**) ⊂ **1**.$(C_2H_4Cl_2)_3$
Empirical formula	$C_{82}H_{63}Cl_6N_{15}O_3$
Formula weight	1519.05
Temperature/K	293.15
Crystal system	monoclinic
Space group	$P2_1/n$
a/Å	16.1030(17)
b/Å	13.8295(15)
c/Å	31.954(4)
α/°	90
β/°	92.721(6)
γ/°	90
*V*olume/Å^3	7108.1(13)
Z	4
ρ_{calc}g/cm^3	1.419
μ/mm^{-1}	0.306
F(000)	3144.0
Crystal size/mm^3	0.26 × 0.21 × 0.18
Radiation	MoKα (λ = 0.71073)
2Θ range for data collection/°	2.552 to 52.864
Index ranges	$-19 \leq h \leq 20$, $-17 \leq k \leq 16$, $-39 \leq l \leq 39$
Reflections collected	92449
Independent reflections	14393 [R_{int} = 0.0843, R_{sigma} = 0.1193]
Data/restraints/parameters	14393/1824/1271
Goodness-of-fit on F^2	1.047
Final *R* indexes [$I > 2\sigma(I)$]	R_1 = 0.0757, wR_2 = 0.1987
Final *R* indexes [all data]	R_1 = 0.1702, wR_2 = 0.2489
Largest diff. peak/hole / e Å^{-3}	0.60/-0.62
CCDC number	1478699

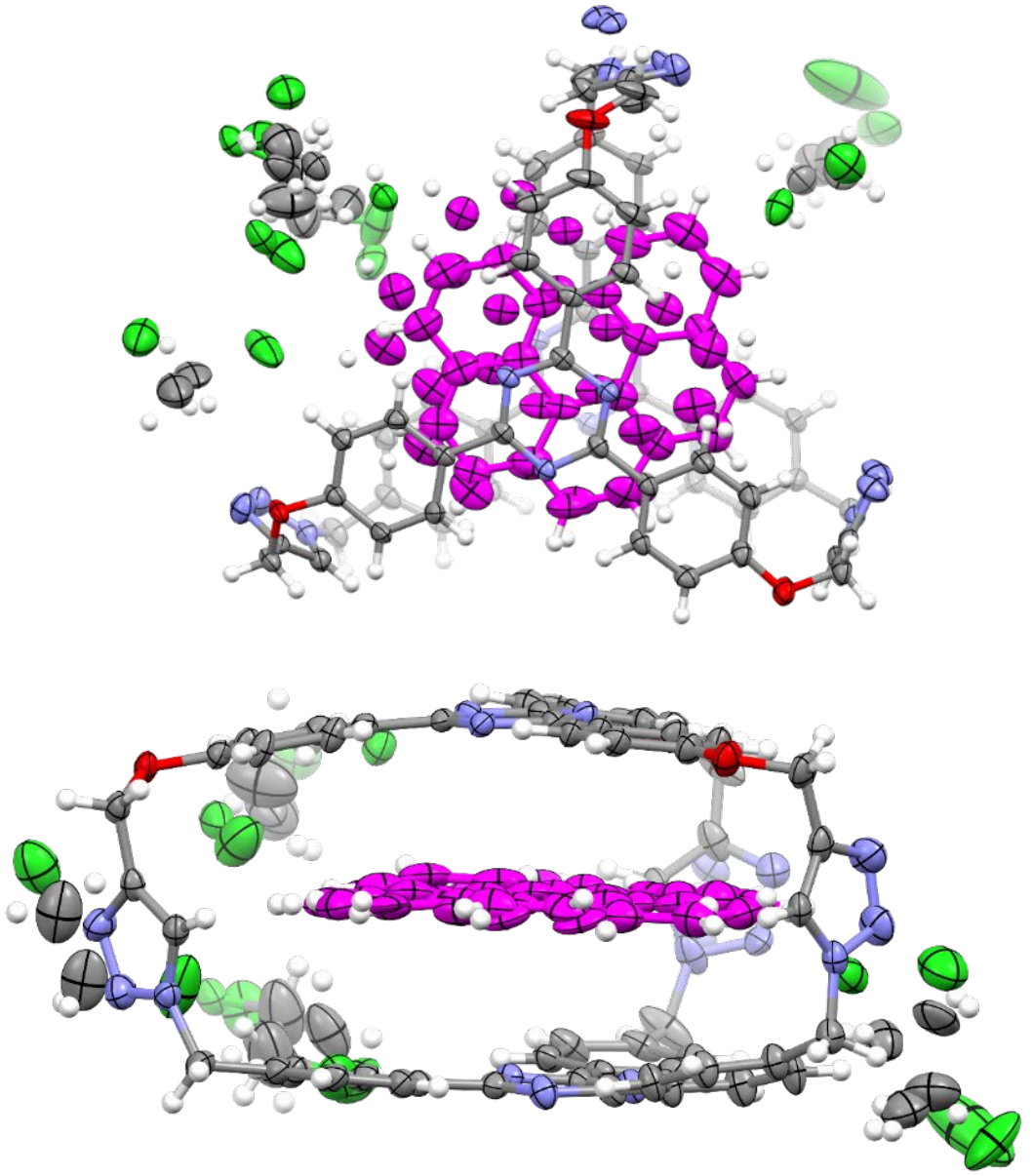

Figure S73. Top and side views of the asymmetric unit in benzo(*ghi*)perylene(**11**) ⊂ **1**.$(C_2H_4Cl_2)_3$. Thermal ellipsoids are shown in 50% probability level. The benzo(*ghi*)perylene molecule is disordered over two positions; thus refined with same distance (SADI), similar Uij (SIMU) and rigid body restraints (RIGU). The dichloroethane molecule is also disordered over two positions and refined in a similar manner.

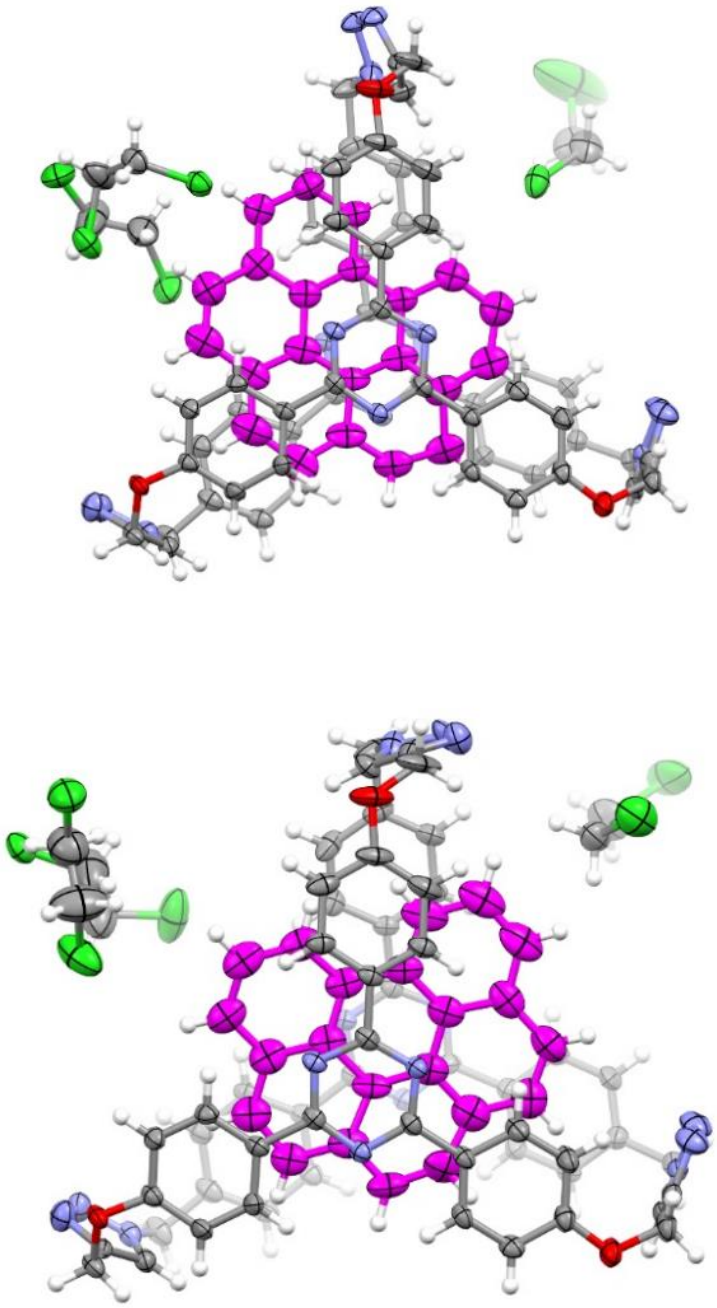

Figure S74. The disordered components benzo(*ghi*)perylene(**11**) ⊂ **1**.$(C_2H_4Cl_2)_3$ asymmetric unit is shown in two different models for better clarity.

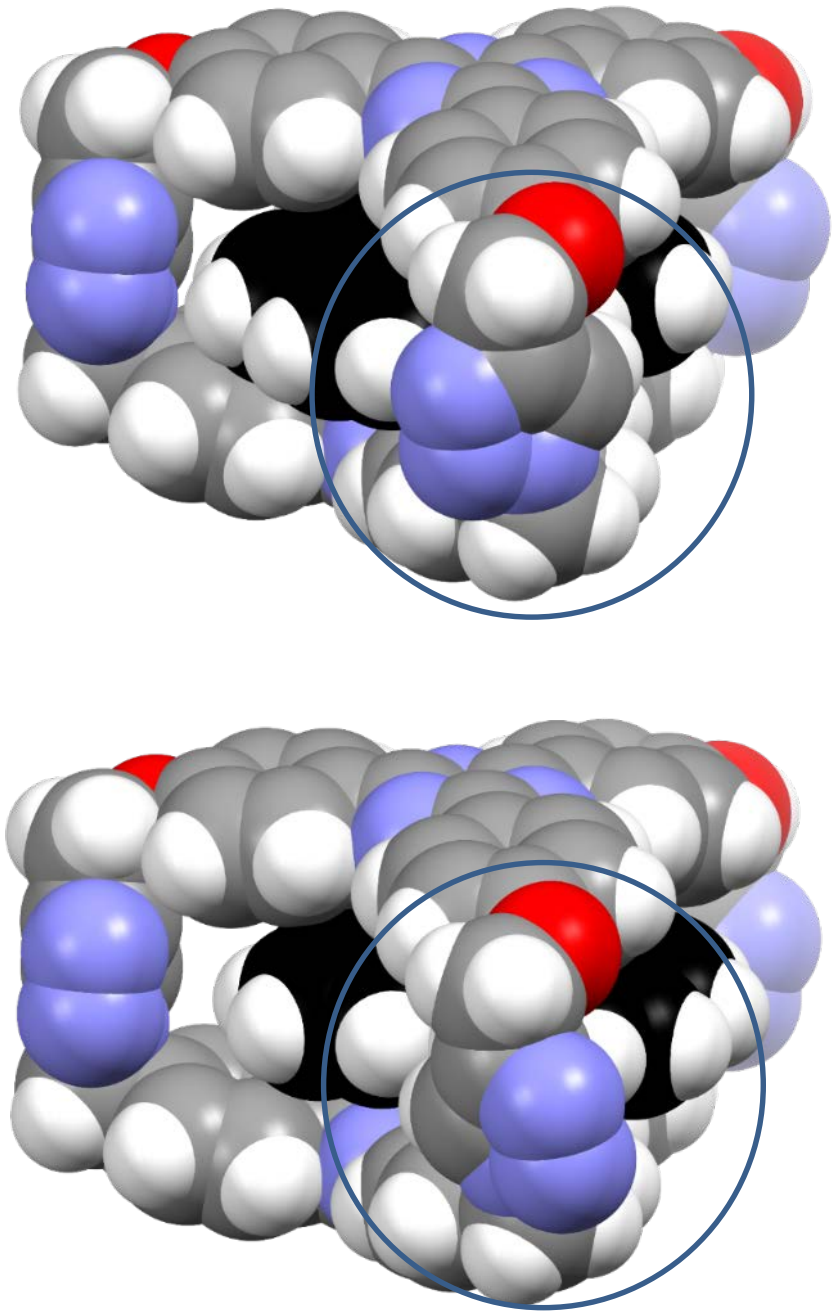

Figure S75. The two models of benzo(*ghi*)perylene(**11**) ⊂ **1** is shown in space filling mode. The disordered triazole is pointing towards the viewer. Also note the guest molecule in two different orientation to reach the best fit.

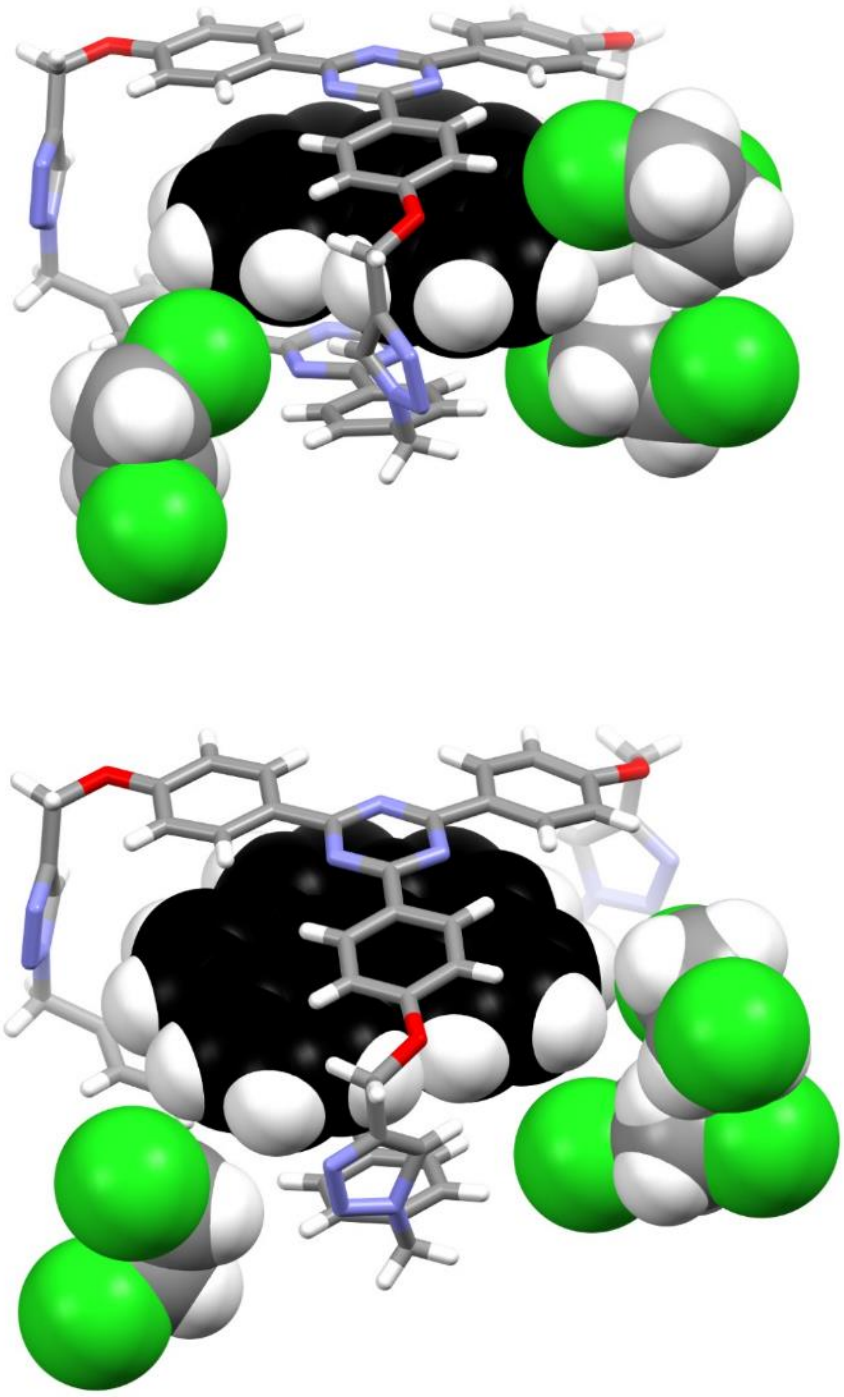

Figure S76. The figure illustrating the close contacts between $C_2H_4Cl_2$ and benzo(*ghi*)perylene molecules bound inside **1**. The shortest distance observed between chlorine and benzo(*ghi*)perylene hydrogen ($d_{C\text{-}Cl\cdots C}$) is 3.2 Å.

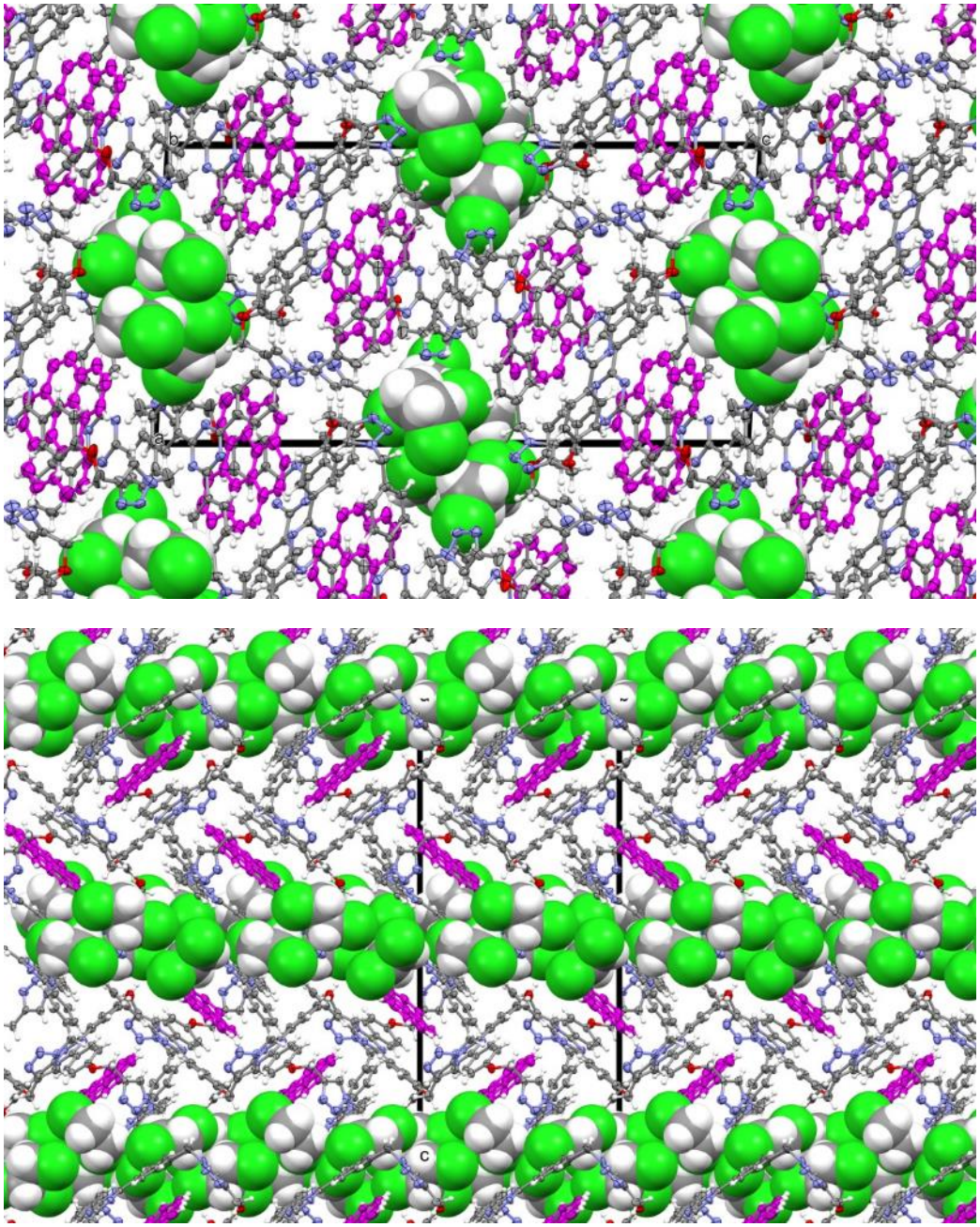

Figure S77. Crystal structure of benzo(*ghi*)perylene(**11**) ⊂ **1**.$(C_2H_4Cl_2)_3$ viewed along viewed along *b*-axis in top and *a*-axis in the bottom. The solvent molecules are shown in the space filling mode.

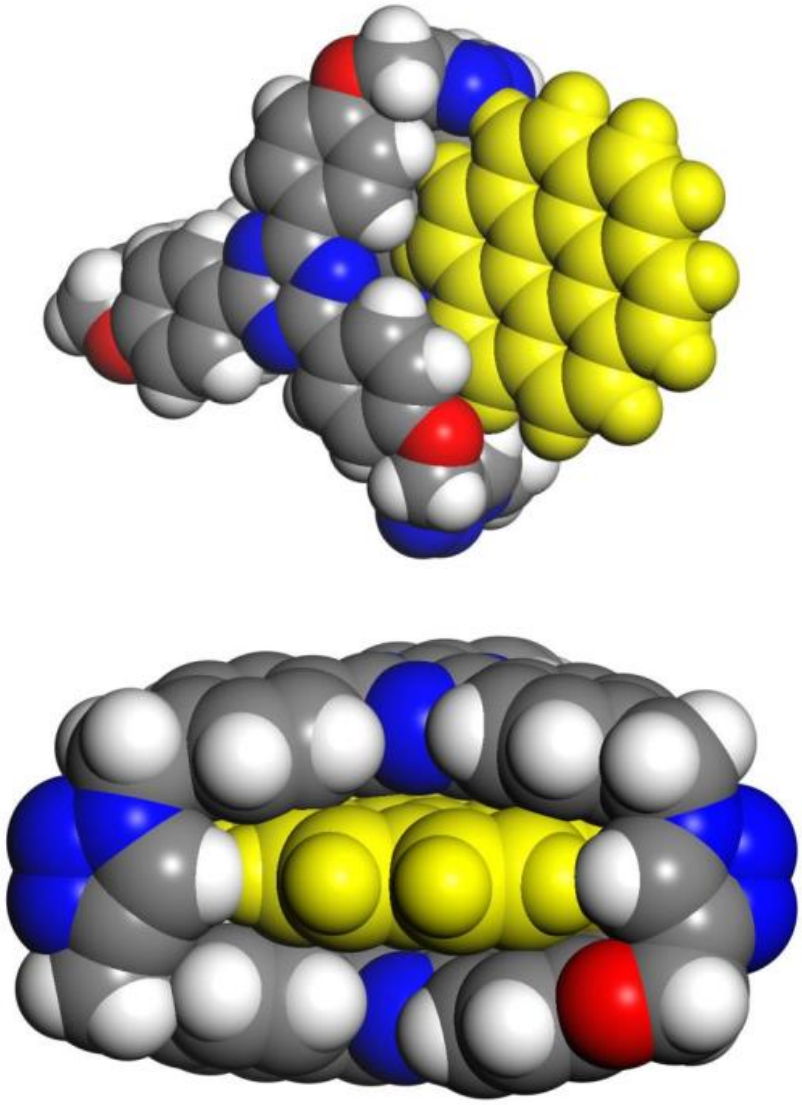

Figure S78. The figures obtained though force field based molecular modelling to explain the entry and positioning of coronene(**12**) into and inside **1** might not be feasible.

7. References:

1. Woiczechowski-Pop, A.; Dobra, I. L.; Roiban, G. D.; Terec, A..; Grosu, I. *Synth. Commun*. **2012**, *42*, 3579–3588.
2. Thordarson, P *Chem. Soc. Rev*. **2011**, *40*, 1305–1323.
3. APEXII, Program for Bruker CCD X-ray Diffractometer Control; Bruker AXS, Inc.: Madison, WI, 2006.
4. SAINT+, Program for reduction of data collected on a Bruker CCD area detector diffractometer; Bruker AXS, Inc.:Madison, WI, 2006
5. Sheldrick, G. M. SADABS, Program for empirical absorption correction of area-detector data; Universität Göttingen: Göttingen, Germany, 2008
6. Sheldrick, G. M. *Acta Cryst.*, **2015**, ***A****71*, 3-8.
7. Sheldrick, G. M. *Acta Cryst.* **2015**, ***C****71*, 3-8.
8. Dolomanov, O. V.; Bourhis, L. J.; Gildea, R. J.; Howard, J. A. K.; Puschmann, H. *J. Appl. Cryst.*, 42, 3 39-341.